SAHC

Assessment and rehabilitation of historic concrete structures
Case study 1-Citta' della musica in Marghera-

Yohei Endo

Italy | 2009

ADVANCED MASTERS IN STRUCTURAL ANALYSIS
OF MONUMENTS AND HISTORICAL CONSTRUCTIONS

Master's Thesis

Yohei Endo

Assessment and rehabilitation of historic concrete structures

Case study 1

-Citta' della musica in Marghera-

Universita' Degli Studi di Padova

UNIVERSITAT POLITÈCNICA DE CATALUNYA

Education and Culture

Erasmus Mundus

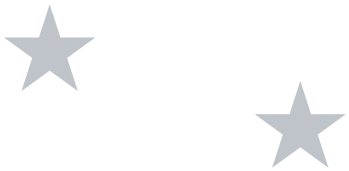

ADVANCED MASTERS IN STRUCTURAL ANALYSIS
OF MONUMENTS AND HISTORICAL CONSTRUCTIONS

Master's Thesis

Yohei Endo

Assessment and rehabilitation of historic concrete structures

Case study1

-Citta' della musica in Marghera-

This Masters Course has been funded with support from the European Commission. This publication reflects the views only of the author, and the Commission cannot be held responsible for any use which may be made of the information contained therein.

Italy I 2009

DECLARATION

Name: Yohei Endo

Email: odensanz@yahoo.co.jp

Title of the Msc Dissertation: Assessment and rehabilitation of historic concrete structures Case study1-Citta' della musica in Marghera-

Supervisor(s): Francesca da Porto

Year: 2009

I hereby declare that all information in this document has been obtained and presented in accordance with academic rules and ethical conduct. I also declare that, as required by these rules and conduct, I have fully cited and referenced all material and results that are not original to this work.

I hereby declare that the MSc Consortium responsible for the Advanced Masters in Structural Analysis of Monuments and Historical Constructions is allowed to store and make available electronically the present MSc Dissertation.

University: University of Padua

Date: 21.07.2009

Signature: _____

This page is left blank on purpose.

This page is left blank on purpose.

ACKNOWLEDGEMENTS

First of all, I am grateful to my supervisor Ing. Francesca da Porto for her four-months' guidance for this small report. I would also like to thank Elena Stievanin for providing me abundant information on the regarding structure. I also cannot but appreciate the European Commission for the huge financial support.
I also have to thank HSH –Hardware Software House- for providing us the temporary licence of Straus, which was employed for the structural analysis. In the end, I am thankful to all of this master's colleagues for the countless and priceless good memories with them, honestly. We really really had good time in Barcelona and in Padova. Thank you :))

This page is left blank on purpose.

ABSTRACT

This dissertation deals with the application of the methodology of preservation on historic concrete constructions. The early concrete structure will be analysed from several points of view: artistic or architectonic value, construction history, structural behaviour, procedures historically followed for the design, on-site and laboratory testing of constitutive materials, modelling and seismic analyses.
The past industrial building in Marghera is taken as a case study here. It was built in the 50s and is going through the conversion into the commercial and business complex.

This page is left blank on purpose.

Estratto

Il titolo e' "Valutazione e riabilitazione delle strutture di calcestruzzo storico Caso di studio 1-Citta 'della musica a Marghera".

L'astratto e' che:

Questa tesi si occupa dell'applicazione di una metodologia di studio per il recupero di edifici storici in cemento armato. Le prime strutture in cemento armato vengono analizzate da diversi punti di vista:

- il valore artistico e architettonico
- la storia della struttura
- il comportamento strutturale
- le normative vigenti all'epoca della costruzione
- prove sperimentali in situ e in laboratorio
- modellazione per analisi sismica (con l'ausilio del software ad elementi finiti Straus 7)

Il caso studio affrontato è un edificio storico industriale ubicato a Marghera (VE). E' stato costruito negli anni Cinquanta ed è previsto un suo riuso come complesso "Città della Musica".

This page is left blank on purpose.

This page is left blank on purpose.

TABLE OF CONTENTS

TABLE OF FIGURES

LIST OF TABLES

1. THE HISTORY OF REINFORCED-CONCRETE STRUCTURE

1.1.1. The overview of the history of RC structures

The history of the modern historic-concrete structure began around at the end of the 19th century. The primitive plain concrete itself had been known since the ancient time and in fact is known to have been employed in ancient Egypt. The concrete became the major-construction material in the Roman time. At that time, the concrete was made from lime and small stones and it is also known the pozzolana was also used then (Proc. Instn Civ. Engrs 1996). The lime contributes to the hardening process of concrete by the exposure in the air, The pozzolana is one of the aggregates and improves the strength and the durability of concrete and the pozzolana reacts with lime even in the water. In the past the problem with concrete came from the fact that it had little tensile strength. However this issue was solved by the development of the reinforced concrete at the end of the 19th century. As a result, it is said that the advent of the reinforced concrete changed the scale of the structure drastically.

After the Second World War, the rapid reconstruction of towns was required because of the large-scale destruction of the towns. Nevertheless, the structural materials such as steel and timber were in short supply since most of them was consumed for the war. On the other hand, the technology of the prestressed concrete units was developed during the war. For instance it was used for the bombproof U-boat pens, expressway bridges and so on. In fact, it allowed the span of the prestressed-concrete floor up to 50ft at that moment and it enabled more flexible planning. Thus the industrialised building system such as the precast-concrete floor and wall panel was introduced largely for the multi-storey buildings after the Second World War. Reinforced-concrete construction became more common during and after the war due to the lack of the steel and the technology of reinforced concrete got progress during this period. Many intriguing RC structures were designed in this period. These new features of the concrete were enabled also by the advent of the larger-scale lifting tools like mobile cranes as well.

In general reinforced-concrete structure is said to imitate structurally the principal biological structural material such as bone, since the evolution of biological structure has been based on highly strength-weight ratio efficient structural forms so as to contend with the range of loading conditions which come from the movement. The efficiency is gained by employing internal direct stress as much as it can and decreasing stress diversity owing to bending. Two different approaches have been developed so far: Firstly, jointed skeletal structure which enables the arrangement of the geometry to set up primarily direct stress systems under a given load arrangement and secondly shell form where the external loads is held by means of its own shape -by internal direct stresses. Incidentally, the latter methods was realised only after the advent of reinforced concrete.

The trusses and the prestressed-concrete beams came to be employed with extraordinary spans after the Second World War. For example, in case of London Airport (1951), Secondary roof units built of

precast units with post-tensioned spanned 110 ft. They are underpinned by 150-feet span primary post-tensioned in-situ concrete box beams.

Shell structure was also enabled thanks to the advent of reinforced concrete, which is readily formed and which possesses tensile strength as well as compressive strength. In fact since the end of the last century, theoretical research had been done on the shell structures to some extent, but at that time the practical examples were limited to the spherical domes since they were more simple to solve mathematically. Initially, the shape of shell followed the forms used for masonry construction. A shell roof would consume less steel than other structures such as a steel truss roof, and in addition shell roof provided the roof covering on its own. Consequently after the Second World War, a great number of concrete shell roofs were constructed due to the lack of the steel and shell structures came to be employed for general building more frequently. Around for 20 years after the war, most of the shell roofs were of single curvature in the shape of part of symmetrical cylinder or barrel vault roof (BVR). Many examples are multi-bay structure with constant spans. The span of the shell would be up to 150ft and the width is half the span and as a result it provides a column layout with a ratio of 2:1. The ratio was important to avoid the trend for the shell to buckle under the compressive forces at the crown.

The slope of the upper surface of the shell springing was restricted to around 40 degrees in order to secure the flesh unhardened concrete during the curing process. The 40 degrees also allowed the thin portion of the shell more fluidity which was required for the concrete around the reinforcement to function in the depth available. The total depth of construction from the intrados of the valley beam to the top of the intrados of the shell was normally one-tenth of the span. For spans over 100ft-span structure prestressed concrete was used occasionally. Extra bars were added throughout the span to the essential theoretical number in order to maintain the crucial full tensile strength could be maintained throughout the beam length. Two layers of roofing felt were in use on the top surface of the roof. This gave waterproofing and also some elasticity against shrinkage movement. Cracking in service was not usually a problem, and though concrete carbonation was not an issue in 1960 apparently, the finished surface effectively avoided it or made deterioration slow.

As time passed, the design of shell structure became more and more common task for architects. Yet, at first stage, due to the lack of the knowledge on the shell construction, the collaboration of architects and engineers was required in many ways. However, today still many shell structures still survive in good condition without need of the excessive maintenance. Incidentally, the boom of the shell structure was gone around in 1965 in the UK for the three reasons: first the steel became available by that time, the architectural trend changed and then the cost of the formwork became more costly than before.

*Table 1. Typical layout dimensions of barrel vault roof**

Span (ft)	Breadth (ft)	Rise (ft)	Radius (ft)	Thickness (in)
180	50	18	40	3·0
140	40	14	35	3·0
100	50	10·5	35	3·0
80	40	8·25	35	3·0
60	30	6·0	30	2·5
Span (m)	**Breadth (m)**	**Rise (m)**	**Radius (m)**	**Thickness (mm)**
54·9	15·2	5·5	12·2	76
42·7	12·2	4·3	10·7	76
30·5	15·2	3·2	10·7	76
24·4	12·2	2·5	10·7	76
18·3	9·1	1·8	9·1	63

* The values given in this table are taken from GKNR;[3] BRC recommended very similar values[2]

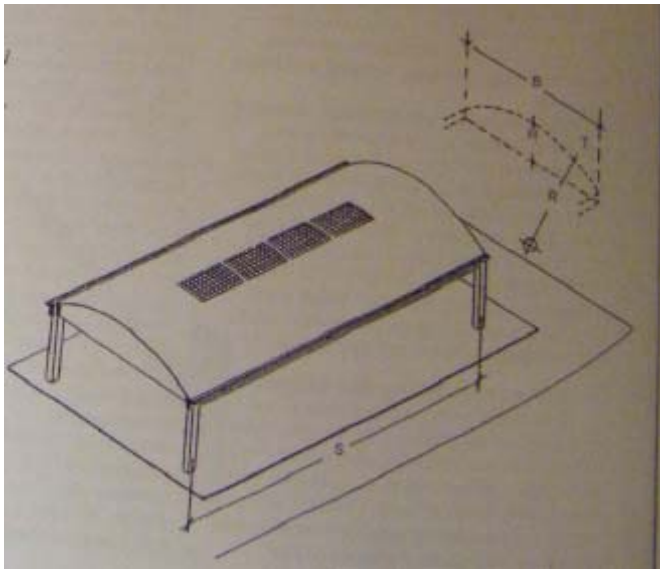

Figure 1: conventional dimension of barrel vault roof

(Proc. Instn Civ. Engrs 1996)

1.1.2. Historical codes for reinforced-concrete structure in Italy

The advent of reinforced concrete in Italy can be dated around at the end of the 19th century. In this period there were no national standards which regulated and specified the measures for the completion of reinforced-concrete works. The practice was limited to the manufacturers which had enough technology and the uniform national standards were not so essential as today.

The extension of the use of reinforced concrete started to be seen at the beginning of 20th century. Moreover, the studies on the RC structures were being carried out and it proved that the concrete structure requires the different calculation from other precedent structures. As a result, the necessity of national standard codes was realized and they were generated one by one from this period.

The optical methods of the standardised test was established at the beginning of the 20th century, and the Italian Association for studies on construction materials held several conferences from 1903 including that in the University of Pisa in 1905 and in Perugia in the following year. The first normative document regarding the construction of cement works in years was developed and proposed in 1904 by engineers and Canevazzi Marro to provincial administrations of Ferrara and Ravenna.

The first decree law was issued with taken into consideration the conclusions of the international congress, which was held in Brussels in advance. As a result the draft legislation was drawn up in 1924, following the administrative decree of 1907 (a.k.a DM 1907) which is thought to be historically very significant as it is one of the earliest normative. The document was accepted and made in force by a decree law on 15 May 1925. It was made up of a series of seven standards which were issued year by year until 1933. Here the code is developed in two approaches: one approach is concerned with the hydraulic binders and their properties, the other with more specific RC construction of concrete. The accuracy of the description of the rules and the degree of precision in providing the resistance values or geometric constitution have to depend on the level of knowledge of the material knowledge acquired through the experiments.

A further evolution of the code occurred in 1939 when two legislative decrees were enacted together with the standards for acceptance of hydraulic binders and regulations for the execution of works in cement and reinforced concrete.
The text remained in force until 1972 and regulated all construction activities occurred during the housing boom of the'50s and'60s and this code is the most relevant to this case study since the structures were built in 1955 and 1960 as discussed in the following chapter. Incidentally this code was called Standards for performance Deüe works in simple concrete or reinforced (RDL No 2229 of 16/11/1939).

Description of the code

This code is made up of 52 articles, which are divided into five chapters. The indicated requirements are much more detailed than the former codes.

The first part is about the general requirements relevant to the importance of the project and the proof of quality of materials issued by laboratories which are approved by the authority.

The next chapter deals with the quality of materials. This part is mostly the same as the earlier ones. As for the mix design, the precise ratio is not indicated any more and only the amount of cement is defined to be equal to 300 kg per m^3 of dry mixture of inactive material (including the sand gravel as the inactive one) or 250 kg per m^3 in the case of aluminous cement. Once concrete is mixed, both samples of concrete (four samples of them for every 500 m^3 of mix) and reinforcement (2 samples for every 1 m long) must be taken in order to examine in laboratories. When the compressive strength of the cubic concrete is examined, specimens of 16 cm high or -20 cm, if the gravel is larger than 3 cm - should be used. The aging should be 28 or 60 days and the result is obtained from the average value of the three highest results. The compressive-strength test is carried out on concrete beams whose section is 70x86 mm and 2.2 m long, and on reinforcement the test is performed with two rods at 12 ~ 6 mm from the bottom edge and at 12 mm from the side. The tests of 28-day-aging samples must show that concrete compressive strength $\sigma_{r,28}$ is at least three times as large as the design loading which is seen in the calculation stage σ_c. At any rate, $\sigma_{r,28}$ always has to be greater than 12MPa for the concrete with portland cement or 16MPa for the one with high-strength cement.
The tensile strength can be determined directly from the reinforcement and it is done with preparing specimens in accordance with the rules where the length must be 10 times as long as the diameter. The value of the strength is defined according to the categories of reinforcement as seen below (table1):

Type of iron	Load at break [MPa]	yield strength [MPa]	Elongation (%)
Wrought iron	450-600	>230	>20
Cast iron	500-600	>270	>16
steel	600-700	>310	>14

Table 1: steel tensile strength in historic code

(Belluco P. 2008)

The third part, which is related to the standards of design, contains two tables (one is about the axial stress, the other about the flexure stress). As a result the below equation is obtained.

$$\sigma_c = 75+(\sigma_{r,\,28}-225)/9 \qquad (1\text{-}1)$$

NB)$\sigma_{r,\,28}$>225 Kg/cm^2=22.5(MPa)
(Belluco P. 2008)

Shear loading should not exceed 0.4 MPa for concrete with Portland cement or 0.6 MPa for the concrete with high-strength cement to be on the safe side. As for the reinforcement the design tensile stress can not exceed 140MPa for wrought iron and 200 MPa for cast-iron and steel. The design tensile stress should not exceed half of the yield strength as well. The weight of the reinforced concrete is same as that of the former code and it is 2500 Kg/m^3.
For the calculation of stresses, the allowable tensile strength method is employed with the assumption of the linear elastic behavior of the material. The difference from the former codes is seen in the ratio of the elastic modules of reinforcement and cement. It should be 10 in the case of concrete with normal concrete, 8 for that with high strength and 6 for that with aluminous cement. It then prescribes the rules for the calculation about the reinforced concrete slabs with ribs and about the minimum size of the slabs according to the type of the roof. It also indicates the amount of reinforcement in line with the stress and the size irons.

The fourth part is concerned with the rules for implementation. As seen below (table2), the type of concrete determines the timing of removal of the formwork.

The part of the formwork to take away	Concrete with normal cement	Other types of Concrete
Sides of the formwork of beams and pillars	After 48 hours	After 36 hours
The slab	After 4 days	After 3 days
The props of beams and the bigger-scale slab	After 8 days	After 5 days

Table 2: the required days for cure of concrete
(Belluco P. 2008)

The last part is related to the execution of testing. According to the type of the concrete, the timing of the test is varied. For instance as for the concrete with normal cement, the testing is carried out after 50 days of aging and as for aluminous cement concrete that of 30 days.
It is required that the testing load is determined from the maximum tensile stress of the structure and it is

given through the tools to detect deformation, such as strain gauges and dual gauges. The stability of the structure also must be judged on the basis of a comparison between the elastic deformation (equal to the difference between maximum and dead-load deformation) and the deformation calculated by applying the appropriate amplification factor to the steel section.

In the end, the summary of the historic codes in Italy is given.

	Presc. FE	Presc. TO	RDL 1906	RDL 1907	RDL 1927	RDL 1933	RDL 1939
Compressive strength (concrete)	evaluated as an average from 5 samples of side 10cm	evaluated as an average from 4 samples of side 14cm	evaluated with the cube of side 10-15cm >15 MPa	evaluated with the cube of side 10-15cm >15 MPa	evaluated as an average from 4 samples of side 16cm	evaluated as an average from 4samples of side 16or 20 cm	evaluated with the cube of side 16-20cm >12 MPa or 16 MPa
Uni-axial Compressive loading for 28-day-aging concrete	1/5 of resistance of concrete at break or 3MPa	1/5 of resistance of concrete at break	1/5 of resistance of concrete at break	1/5 of resistance of concrete at break	1/4 of resistance of concrete at break or precise value depending on the type of concrete	1/4 of resistance of concrete at break or precise value depending on the type of concrete	3.5-4 MPa for the axial stress or 4-5 MPa for flexure stress
Compressive strength of homogeneous iron	>380 MPa	>370 MPa	360-450 MPa	360-450 MPa	380-500 MPa	360-450 MPa	420-500 MPa
Compressive strength of agglomerated iron	>340 MPa	>340 MPa	>340 MPa	>340 MPa	>340 MPa		

Compressive strength of Cast iron							500-600 MPa
Compressive strength of steel							600-700 MPa
Maximum tensile stress of homogeneous iron	100MPa	100 MPa	100 MPa	100 MPa	120 MPa	120 MPa	140 MPa
Maximum shear stress of homogeneous iron	80 MPa	80 MPa	80 MPa	80 MPa	96 MPa	96 MPa	
Max tensile stress of agglomerated iron	4/5 of that of homogeneous iron	4/5 of that of homogeneous iron	4/5 of that of homogeneous iron	4/5 of that of homogeneous iron	80 MPa		-
Max shear stress of agglomerated iron					64 MPa		
Max tensile stress of steel							200 MPa

Table 3: The summary of historic codes in Italy

NB)

Presc. FE:

Prescrizioni da seguire nella progettazione ed esecuzione di opere in ferro-cemento (1904)

Presc. TO:

Prescrizioni speciali per le pere in smalto cementizio armato da eseguirsi per conto della città di Torino (1906)

RDL 1906:

Prescrizioni normali per l'esecuzione delle opere in cemento armato (1906)

RDL 1907:

Decreto ministeriale 10/01/1907 (G.U. D.28 02/02/1907)

RDL 1927:
Nuove norme per l'accettazionedegli agglomeranti idraulici e l'escuzione delle opere in conglomerato cementizio semplice e armato (RDL n. 1981 del 4/09/1927)
RDL 1933:
Norme per l'accettazione dei leganti idraulici e per l'esecuzione delle opere in conglomerato cementizio (RDL 29/07/1933)
RDL 1939:
Norme per l'esecuzione delle opere in conglomerato cementizio semplice o armato (RDL n. 2229 del 16/11/1939)
(Belluco P. 2008)

1.2. The deterioration of reinforced-concrete structure

The issues of reinforced-concrete deterioration mostly come from two causes: concrete deterioration and steel corrosion. Both concrete and steel are deteriorated by the chemical and physical attacks. The deterioration harms RC structure from not only aesthetically but structurally, so it is very significant to identify the cause of the decays. Therefore in this chapter, those deterioration factors are discussed.

1.2.1. Concerning concrete

In case of concrete, physical attacks mean the abrasion and internal stress owing to such reasons as the external loading or the freeze-thaw action. The abrasion results in the loss of the mass. The internal-stress increase causes deformation, cracking and spalling, and also loss of the structural strength. The freeze-thaw action is brought about by the water penetrating into the concrete. This water expands when it is frozen and the frozen water shrinks when it is melted. That circulating action causes the disintegration of the surface layers of the concrete. This action works together with other mechanism quite often.
In general cement is fire-resistant material, as it is sometimes used as a fireproof coating on steel beam, but still it is vulnerable to heat depending on the temperature. Cracks are created on the surface by heat. They are seen along the aggregate surfaces due to the different coefficient of linear expansion between cement paste and aggregate. Then oxidation and dehydration will happen. Thus the phases of aggregate and cement paste are changed. It can be confirmed by the change of the colour. Concrete turns into cream colour around at 300^{o}C and then pink and in the end it becomes whitish grey about at the 600^{o}C.

Chemical attacks are caused by the invasion of outside source such as sulphate and acid products into concrete or the interaction of the constituents in the concrete, for instance alkali-silica reaction. Sulphate attacks create soluble sulphates. It is a result of the reactions between hydrated portland cement and sulphate ions coming from outside. It causes the expansion and cracking in concrete. It also brings

about the reduction of the strength and loss of the volume since cohesiveness of cement hydration products is decreased.

For instance, in case of gypsum formation in the hardened concrete, first it leads to decrease of pH of the concrete and diminution in the stiffness and strength, and then expansion and cracking. In the end, the concrete becomes soft or incoherent mass in case the attack is continued. The sodium sulphate attack forms the sodium hydroxide as seen below (1-2) as a by-product of the reaction and it works in a good manner. It helps to keep the high alkalinity in the concrete. As a result, the stability of C-S-H is kept. On the other hand, the magnesium sulphate action results in the formation of magnesium hydroxide (1-3). As it is soluble, it ends in the reduction of the alkalinity by the chemical action. That is, C-S-H is not stable any more and hence is attacked by the sulphate solution. Therefore it can be said that magnesium sulfate attack is more harmful than that of sodium sulphate (1-4).

$$NaSO_4+Ca(OH)_2+2H_2O\rightarrow Ca\ SO_4+2NaOH \quad (1\text{-}2)$$

$$Mg\ SO_4+Ca(OH)_2+2H_2O\rightarrow CaSO_4\cdot 2H_2O+Mg(OH)_2 \quad (1\text{-}3)$$

$$3MgSO_4+3CaO.2SiO_2\cdot 3H_2O+4H_2O\rightarrow 3(CaSO_4.\ 2H_2O)+3Mg(OH)_2+2SiO_2\cdot H2O \quad (1\text{-}4)$$

Alkali-silica reaction is due to the interaction between alkalis in the concretes and certain kinds of siliceous aggregates. The alkalis come from the cement itself and the pore fluid as well. The reaction generates the alkali-silica gel, which expands by water contacts. Consequently it causes the expansion of mass and cracking in the concrete. It is thought that possibly the deterioration affects the load-carrying capacity, frost resistance and inducing the rebar corrosion. One of the preventions of this reaction is to employ low-alkali cement, and avoid the alkalis to penetrate the concrete from the outside.

There are several other chemical actions. In the concrete both portland cement and high alumina are quite alkaline and hence they are very interactive with acidic solutions. There are two possible acidic sources: inorganic acids such as sulphuric acid, hydrochloric acid and nitric acid, and organic acids such as lactic acids. Generally, the inorganic acids are more aggressive than organic ones. Most of ammonium compounds are harmful to the concrete except for the ammonium carbonate as well. Magnesium chloride is harmful to portland cement concrete, and yet is not as aggressive as ammonium sulphate. This chemical action is due to the hydrated calcium silicates, calcium hydroxide and calcium aluminates.

As a summary, it can be said that these are roughly principle action of the chemical attack: the formation of expansive products, hydrolysis and leaching of components of the cement, the interaction between

the surrounding environment and the components of the cement. They bring about deformation of the concrete, cracking, loss of the strength, loss of the mass and/or loss of alkalinity.

1.2.2. Concerning steel

Steel does not get corroded in case it is covered with the concrete which possesses a pH higher than around 12.5. This high alkalinity can passivate the steel due to the development of the protective layer of the oxidation product like ferric oxide. Hence, the corrosion of the steel- that is, the oxidation- starts when the passivation layer is broken. It is caused by several reasons as follows: physical damage such as impact or abrasion, development of cracks reaching to the steel, high permeability and/or high porosity of the concrete around the steel, insufficient thickness of the cover over the steel and the presence of chlorides. The former four cases in general cause so to speak carbonation which reduces the pH of the concrete up to 9.5. In case of the last one, the corrosion is caused by the chloride attacks.

Chloride is supplied from the concrete mix, aggregates and/or mixing water. It also comes from outside. For instance, sodium chloride in the concrete is dissolved in the water as below (1-5). Thus, the electrically charged negative chloride ions attack the passivate layer of ferric oxide on the surface of the rebar. In fact, the chloride ions are found in the two forms: free chloride ions and combined chloride ions. The combined chloride ions usually exist as tricalcium aluminate and it is thought that the free chloride ions attack the passive layer on the rebars. Consequently they bring about the steel corrosion. The chloride ions mixed during the mixing process usually are not relevant to the chloride attack as they are locked up in the concrete. However, when the chloride reaches the harden concrete, it causes the depassivation, but the chloride ions in the concrete does not start attacking till its concentration gets very high. When the steel gets rusted and expanded, it causes the increase of the volume which breaks the concrete and result in the cracks or spalling.

Sodium chloride action

$$NaCl \rightarrow Na^{+} + Cl^{-} \tag{1-5}$$

Chloride attack

$$Fe + 3Cl^{-} \rightarrow FeCl^{3-} + 3^{e-} \text{ , } O_2 + 2H_2O \rightarrow 4^{e-} + 4OH^{-}: \tag{1-6}$$

Carbonation is another deteriorative process. The chemical action is as below:

$$CO_2 + H_2O \rightarrow H_2CO_3 \tag{1-7}$$

$$H_2CO_3 + Ca(OH)_2 \rightarrow CaCO_3 + 2H_2O \tag{1-8}$$

Carbonation means the process that hydrated products in the concrete is broken up by the air trapped in the concrete to reduce the alkalinity. It causes the neutralisation of the concrete as seen in the second

chemical formula. The pH of concrete gets down to around 8 from the initial pH of 12.5. Therefore, as mentioned above the depassivation of the steel occurs and the steel gets corroded. However, the carbonation itself does not reduce the structural strength of the concrete.

Steel and concrete complete each other in reinforced concrete as steel provides the tensile strength to the concrete and concrete supplies high-alkalinity protective layer to the steel. On the other hand, it means the entire reinforced concrete becomes vulnerable structurally and chemically once either of them is damaged. Therefore, also in this light, the inquiry of the deterioration of reinforced concrete should be regarded as essential issue.

2. HISTORY OF AGRIMONT

2.1. History of Marghera (site)

The industrial zone of Porto Marghera was created in the 1920s and resulted on bringing the railway to Venice. In the 1930s the zone was broadened and brought also automobiles. In the 1960s, a Second Industrial Zone spread southward from Marghera over what until 1953 had been tide-land. By 1970, the industries at Marghera –chemicals, petroleum, plastics, etc.- provided nearly 40.000 jobs. (F.C. Lane, 1973)

Marghera has been one of the principal planning matters under discussion for Venice as indicated in the Revised City Master Plan of 1999 and in preliminary documents of the Strategic Plan (Pugliese, 2003; Barbiani, 2002). The site, along the south-western coastal zone of the lagoon, is composed of about 5000 hectares, divided into three zones. The first one includes surface lands that have been artificially created with waste soil extracted during the maintenance of industrial and urban canals in the period from 1920 to 1960, and then partially occupied by factories of basic industries. The second is connected with an industrial zone where the major part is occupied by commercial port infrastructures of chemical and related industries. The third zone covers a band of near lagoon and port canal water surface. Therefore, the perimeter of the site includes mainland and surrounding waters located between the wonderful historical center of Venice and the post-World War II urban sprawl. The site is further divided into thirteen macro-areas, out of which nine are industrial and four still natural, but with very high soil and water pollution. (D. Patassini et al, 2005)

The companies that were developed in Porto Marghera during the year of 1978 can be presented at Table 4 and Table 5 contains some other data regarding the industrial zone.

sector	number of establishment	number of employees
1. Aliment	9	403
2. Water - Electric energy - Gas	14	1048
3. Ceramics - Fireproof materials - Glass - Building and construction materials	16	2495
4. Chemicals	23	13686
5. Mechanical	57	4445
6. Metallurgic - Iron and Steel	15	6287
7. Petroleum producing	23	1360
8. Transport	43	215
9. Various	36	448
Total	236	30387

Table 4 :Companies of Porto Marghera (1978)

(Stamperia di venezia, 1980)

	1928	1938	1948	1958	1968	1978
surface area occupied (m^2)	3988000	4800000	5280000	5550000	13170000	13170000
number of establishment	81	94	118	195	239	236
number of workers	5270	16500	21200	29000	33000	30387
maritime traffic (tons)	513048	2291000	1459179	6002044	15866799	21628707
rail traffic (tons)	521356	936467	942440	1425000	1413320	1137738

Table 5: Data on Porto Marghera

(Stamperia di venezia, 1980)

2.2. History of Agrimont

Due to the lack of sufficient document, this section is mostly made up of hearing -with the geotechnical manager of the rehabilitation work-, which was carried out on 12th of May, 2009 in Marghera (site).

The building consists of two parts (Figure 2): Principle body and Secondary body (Corpo Principale and Corpo Secandario). Incidentally in this report, they are mentioned as Principle body and Secondary body for each. Secondary body was built in 1955 and Principle body was built in 1960. Interestingly enough, they are next to each other, but they do not share any structural member each other. Marghera is industrial area, and this building was used as storage for the industrial activity. Now this site is being converted into the commercial and business complex –citta' della musica.

Presumably the architectural and structural importance of this building derives from the employment of continuous arches built of reinforced concrete, not of steel. This is presumably due to the lack of the steel then due to the WW II. These arches carry only the roof weight and give the impressive architectural appearance and characteristic structural behaviour which is going to be dealt with in this report.

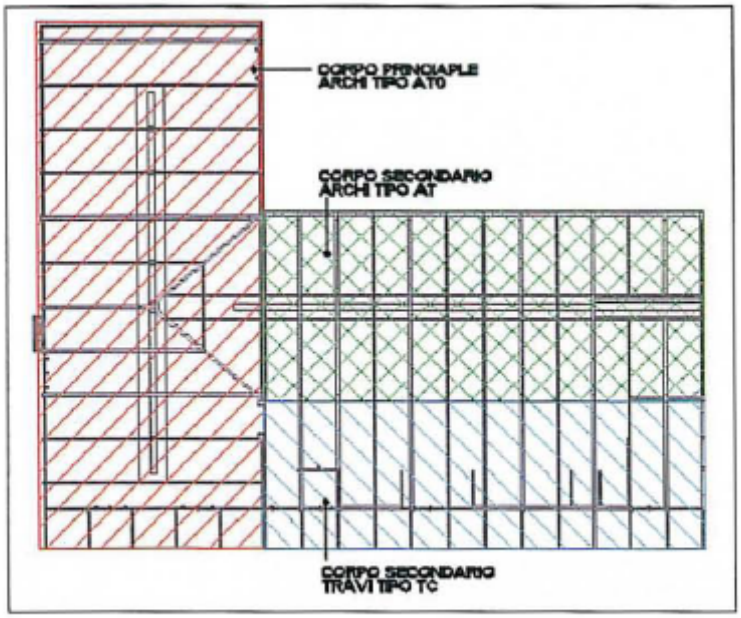

Fig. 1: pianta del complesso

Figure 2 : The plan of Agrimont (right Principle body, left Secondary body)

Figure 3: Agrimont, the picture taken on 12th of May, 2009

3. REPORT OF THE MATERIAL-PROPERTY TESTING

3.1. Overview

This chapter consists of the summary of the report done by ENCO (Engineering Concrete SRL). The report was issued on 21st of March, 2008. In the report they are dealt with: the quality and condition of deterioration of concrete, and estimation of the reinforcement -the diameter and position- including the steel mechanical properties. Testing was carried out on site and in laboratory both. On site the following tests were conducted: coring, calorimetric test, pacometric investigation, sclerometry and ultrasonic assessment. Then in the laboratory: the physical and chemical characterization of concrete and of reinforcement.

The report consists of three chapters in addition to introduction:
Annex 1 (allegato 1) includes plan and sections for the identification of sampling points. Annex 2 (allegato 2) contains the main part of this report and contains all the collection of cards mentioning the results of on-site tests (coring, calorimetric test, pacometric investigation, sclerometry and ultrasonic assessment). Annex 3 (allegato 3) consists of the tables of laboratory tests (the physical and chemical characterisation of concrete and of reinforcement).

3.2. Report regarding concrete

22 cores were extracted from the structure: 11 cores from Principle body and the other 11 cores from Secondary body (Figure 4).
For all the samples, the tests were carried out so as to examine following aspects:
penetration of carbon dioxide, dry density, density in s.s.a. (saturated surface dry), water absorption, measurement of the speed of ultrasonic transmission and compressive strength. Then for 16 cores, corresponding to 10 points, the following tests were carried out: measurement of the speed of ultrasonic transmission, measurement of the indication of the rebound. Moreover, for samples taken from cores taken in position 4 (Figure 5), the following tests were conducted: diffractometric analysis for mineralogical characterisation of the material and the detection of possible forms of degradation and ion chromatography.

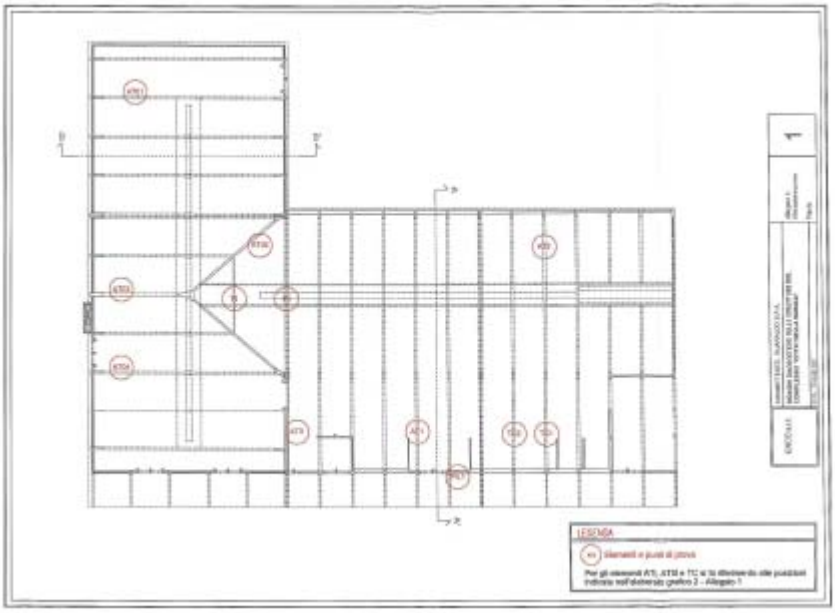

Figure 4: indication of coring in plan

(ENCO, 2008)

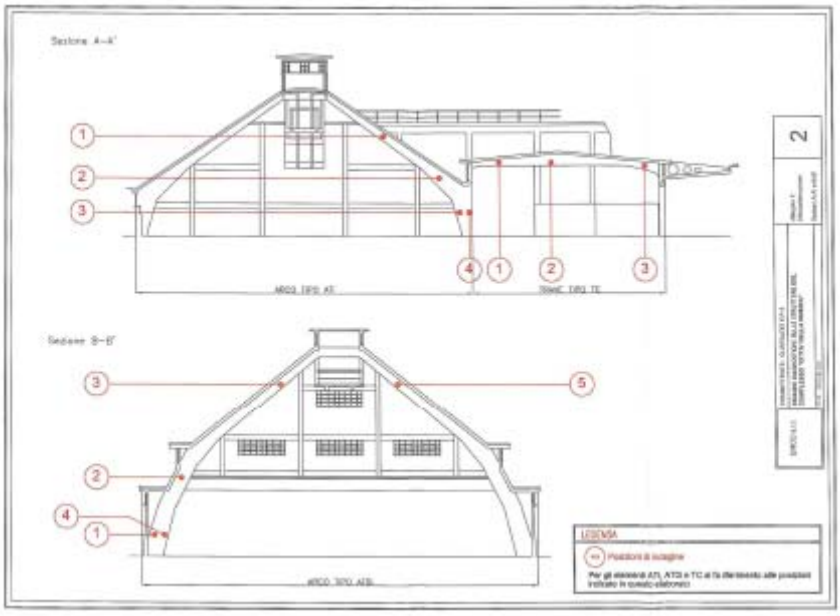

Figure 5: indication of coring in elevation

(ENCO, 2008)

3.2.1. Physical property

Compressive strength

The compressive strength of cylinder core was turned out to be about 30 MPa (average value 32.5 MPa). However those values were fairly scattered, and the standard deviation was equal to 9.5 MPa. The minimum value is 18.7 MPa obtained from core TC1-C1 (extracted position 1, which was extracted from the beam TC1). The scattering of the values becomes much smaller when the cores from Principal body

and Secondary body are seen individually (Table 6). Moreover Secondary body can be divided into arch part (area AT elements) and beam part (area TC elements) (Table 7).

	The average compressive strength, $f_{c(strutt)}$ [MPa]	Standard deviation, s	Min. compressive strength $f_{c(strutt)min}$ [MPa]
Principal body (element AT0)	39.2	7.77	25 (AT03-C1)
Secondary body (element AT and TC)	25.9	5.67	18.7 (TC1-C1)

Table 6: compressive strength of concrete in Principle body and Secondary body

	The average compressive strength, $f_{c(strutt)}$ [MPa]	Standard deviation, s	Min. compressive strength $f_{c(strutt)min}$ [MPa]
Secondary body (element AT)	28.0	5.16	20.3 (AT2-C1)
Secondary body (element TC)	20.2	1.38	18.7 (TC1-C1)

Table 7: compressive strength of concrete in arch part and beam part in Secondary body

Incidentally, it was assumed that only one type of aggregate exists in each body of the building. The cylindrical characteristic strength was calculated under the Technical Standards for Construction and Guidelines for the implementation of concrete and structural evaluation the mechanical characteristics of hardened concrete through non-destructive test. According to them, the lower value among the following two values should be adopted for the structural analysis. The equations and results are shown below (3-1 and 3-2):

$$f_{ck1}=f_{c(strutt)}-k \quad (3\text{-}1)$$

$$f_{ck2}=f_{c(strutt)min}+4 \quad (3\text{-}2)$$

where:

$f_{m\,(n).\,is}$: average of the values obtained from the cores taken from n number of elements;

k: coefficient depending on the number of cores extracted;

$f_{is,\,rnln}$: smaller value obtained from cores;

	The average compressive strength, $f_{c(strutt)}$ [MPa]	K	Min. compressive strength $f_{c(strutt)min}$ [MPa]	f_{ck} [MPa]
Principal body (element AT0)	39.2	4	25 (AT03-C1)	29.0
Secondary body (element AT and TC)	25.9	4	18.7 (TC1-C1)	21.9

Table 8: characteristic value of compressive strength in Principle body and Secondary body

	The average compressive strength, $f_{c(strutt)}$ [MPa]	K	Min. compressive strength $f_{c(strutt)min}$ [MPa]	f_{ck} [MPa]
Secondary body (element AT)	28.0	4	20.3	24.0
Secondary body (element TC)	20.3 (average value)			

Table 9: characteristic value of compressive strength in arch part and beam part in Secondary body

It is noted that, according to the rules cited above, the equivalent characteristic strength $f_{ck,eq,ie,}$ or the resistance characteristic was obtained through crushing tests. It was performed on samples drawn at the timing of being casted, compacted and dried under standard conditions. In the end the value was obtained by dividing the corresponding strength by 0.85. As a result the above assumptions made turn out as follows (Table 10):

	f_{ck1} [MPa]	f_{ck2} [MPa]
Principal body (element AT0)	29.0	34.1
Secondary body (element AT and TC)	21.9	25.8
Secondary body (element AT)	24.0	28.2
Secondary body (element TC)	20.3 (average value)	23.8 (average value)

Table 10: the list of characteristic value of compressive strength of concrete in each part

Measures of water absorption, mass density and carbonation

Mass density and water absorption at atmospheric pressure were confirmed from the results which were obtained from the crushing tests. After all, average porosity values is revealed in line with the type of concrete, which is revealed through the mechanical tests,

For all cores, the depth of penetration of carbon dioxide was carried out by means of the phenolphthalein colorimetric test. The result indicates that the penetration of carbon dioxide is quite homogeneous and the average depth of penetration is 24 mm along with the characteristics of aggregates which has been determined from other surveys.

Carota N°	Penetrazione CO_2 (mm)	d mm	h mm	Assorbimento	0g	5gg	Volume cm^3	$M_v$sec. kg/m^3	$M_v$ssa kg/m^3	E_d secca µs	E_d secca mm/µs	E_d secca MPa	E_d ssa µs	E_d ssa mm/µs	E_d ssa MPa	$f_{c\lambda}$ carota λ=h\d	$f_{c\lambda}$ carota kN	$f_{c\lambda}$ carota MPa	$f_{c(strutt)}$
AT01/C1	15	94,0	188,2	peso	3077,3	3217,2	1305,5	2357	2464	43,1	4,367	38065	42,5	4,428	40927	2,00	304	43,8	45,5
				Δpeso		139,9													
				%		4,5													
AT01/C2	30	94,0	191,9	peso	3174,5	3309,4	1328,9	2389	2490	45,4	4,227	36147	44,1	4,351	39938	2,04	236	34,0	35,5
				Δpeso		134,9													
				%		4,2													
AT01/C3	50	94,0	187,6	peso	2914,7	3078,9	1266,0	2302	2432	46,7	4,017	31466	46,7	4,017	33239	2,00	201	29,0	30,0
				Δpeso		164,2													
				%		5,6													
AT02/C1	15	94,0	189,3	peso	3162,2	3201,1	1310,1	2414	2443	46,3	4,089	34172	46,7	4,054	34003	2,01	302	43,5	45,2
				Δpeso		38,9													
				%		1,2													
AT02/C2	30	94,0	189,6	peso	3074,9	3223,7	1314,1	2340	2453	46,7	4,060	32666	45,7	4,149	35762	2,02	262	37,8	39,3
				Δpeso		148,8													
				%		4,8													
AT02/C3	30	94,0	188,2	peso	3061,2	3203,1	1303,1	2349	2458	45,7	4,118	33742	44,1	4,268	37915	2,00	264	38,1	39,5
				Δpeso		141,9													
				%		4,6													
AT02/C4	-	94,0	94,3	peso	1588,7	1645,6	652,2	2436	2523	21,3	4,427	40437	20,7	4,556	44348	1,00	372	53,6	44,6
				Δpeso		56,9													
				%		3,6													
AT03/C1	35	94,0	188,3	peso	3039,3	3116,6	1301,8	2335	2394	47,2	3,989	31470	52,2	3,607	26384	2,00	167	24,1	25,0
				Δpeso		77,3													
				%		2,5													
AT03/C2	25	94,0	164,8	peso	2699,4	2815,7	1135,1	2378	2481	40,2	4,100	33849	38,6	4,269	38295	1,75	225	32,4	32,5
				Δpeso		116,3													
				%		4,3													
AT03/C3	70	94,0	188,6	peso	3112,5	3246,6	1307,8	2380	2482	45,1	4,182	35249	43,8	4,306	38983	2,01	287	41,4	43,0
				Δpeso		134,1													
				%		4,3													
AT03/C4	-	94,0	96,0	peso	1552,5	1625,6	664,6	2336	2446	21,6	4,444	39080	20,6	4,660	44990	1,02	423	61,0	51,0
				Δpeso		73,1													
				%		4,7													

Carota N°	Penetrazione CO_2 (mm)	d mm	h mm	Assorbimento	0g	5gg	Volume cm^3	$M_v$sec. kg/m^3	$M_v$ssa kg/m^3	E_d secca µs	E_d secca mm/µs	E_d secca MPa	E_d ssa µs	E_d ssa mm/µs	E_d ssa MPa	$f_{c\lambda}$ carota λ=h\d	$f_{c\lambda}$ carota kN	$f_{c\lambda}$ carota MPa	$f_{c(strutt)}$
AT1/C1	10	94,0	188,1	peso	3058,2	3202,4	1307,0	2340	2450	50,3	3,740	27713	47,7	3,943	32270	2,00	195	28,1	29,2
				Δpeso		144,2													
				%		4,7													
AT1/C2	15	94,0	192,9	peso	3103,1	3261,0	1330,6	2332	2451	52,6	3,667	26564	50,0	3,858	30894	2,05	185	26,7	27,8
				Δpeso		157,9													
				%		5,1													
AT1/C3	10	94,0	189,9	peso	3094,3	3234,3	1318,0	2348	2454	48,8	3,891	30110	46,7	4,066	34366	2,02	206	29,7	30,9
				Δpeso		140,0													
				%		4,5													
AT1/C4	-	94,0	95,9	peso	1529,9	1605,3	661,9	2311	2425	23,9	4,013	31518	21,7	4,419	40117	1,02	267	38,5	32,2
				Δpeso		75,4													
				%		4,9													
AT2/C1	5	94,0	170,6	peso	2751,3	2880,4	1177,9	2336	2445	52,6	3,243	20810	48,3	3,532	25838	1,81	139	20,0	20,3
				Δpeso		129,1													
				%		4,7													
AT2/C2	10	94,0	188,6	peso	3078,1	3219,9	1306,8	2355	2464	51,9	3,634	26344	50,3	3,750	29338	2,01	137	19,8	20,5
				Δpeso		141,8													
				%		4,6													
AT2/C3	5	94,0	188,9	peso	3010,2	3136,1	1268,3	2373	2473	46,7	4,045	32889	45,1	4,188	36739	2,01	192	27,7	28,8
				Δpeso		125,9													
				%		4,2													
AT2/C4	-	94,0	92,1	peso	1420,8	1490,0	608,6	2335	2448	21,3	4,324	36967	19,6	4,699	45784	0,98	291	42,0	34,5
				Δpeso		69,2													
				%		4,9													
TC1/C1	20	94,0	188,1	peso	2845,7	2993,5	1230,8	2312	2432	51,3	3,667	26327	49,0	3,839	30355	2,00	125	18,0	18,7
				Δpeso		147,8													
				%		5,2													
TC1/C2	15	94,0	194,3	peso	2984,4	3125,6	1281,8	2328	2438	53,5	3,632	26009	49,6	3,917	31692	2,07	142	20,5	21,4
				Δpeso		141,2													
				%		4,7													
TC1/C3	15	94,0	189,3	peso	3060,9	3214,0	1311,7	2334	2450	49,0	3,863	29497	47,8	3,960	32547	2,01	137	19,8	20,5
				Δpeso		153,1													
				%		5,0													

Table 11: water absorption, density, carbonation and compressive strength
(ENCO, 2008)

3.2.2. Chemical property

X-ray diffraction (XRD)

The diffractive analysis is a fundamental technique in the study of qualitative mineralogical composition and the recognition of secondary chemical materials which could be the cause of any degradation of the investigation object. An analysis called X-ray diffraction, also known as XRD (X-Ray Diffraction) was performed. 5 samples were taken from cores AT1 -C4, AT2-C4, AT01-C4, AT02-C4 and AT03-C4. They were crushed into pieces for the analysis. Consequently, specific variation was not seen.

ion chromatography

Ion chromatography was carried out on the above-mentioned 5 samples and as a result the amount of chlorides and nitrates was determined. The content of chlorides in the aggregates is far more than usual concrete. This fact could be relevant to the cause of the capillary rise.

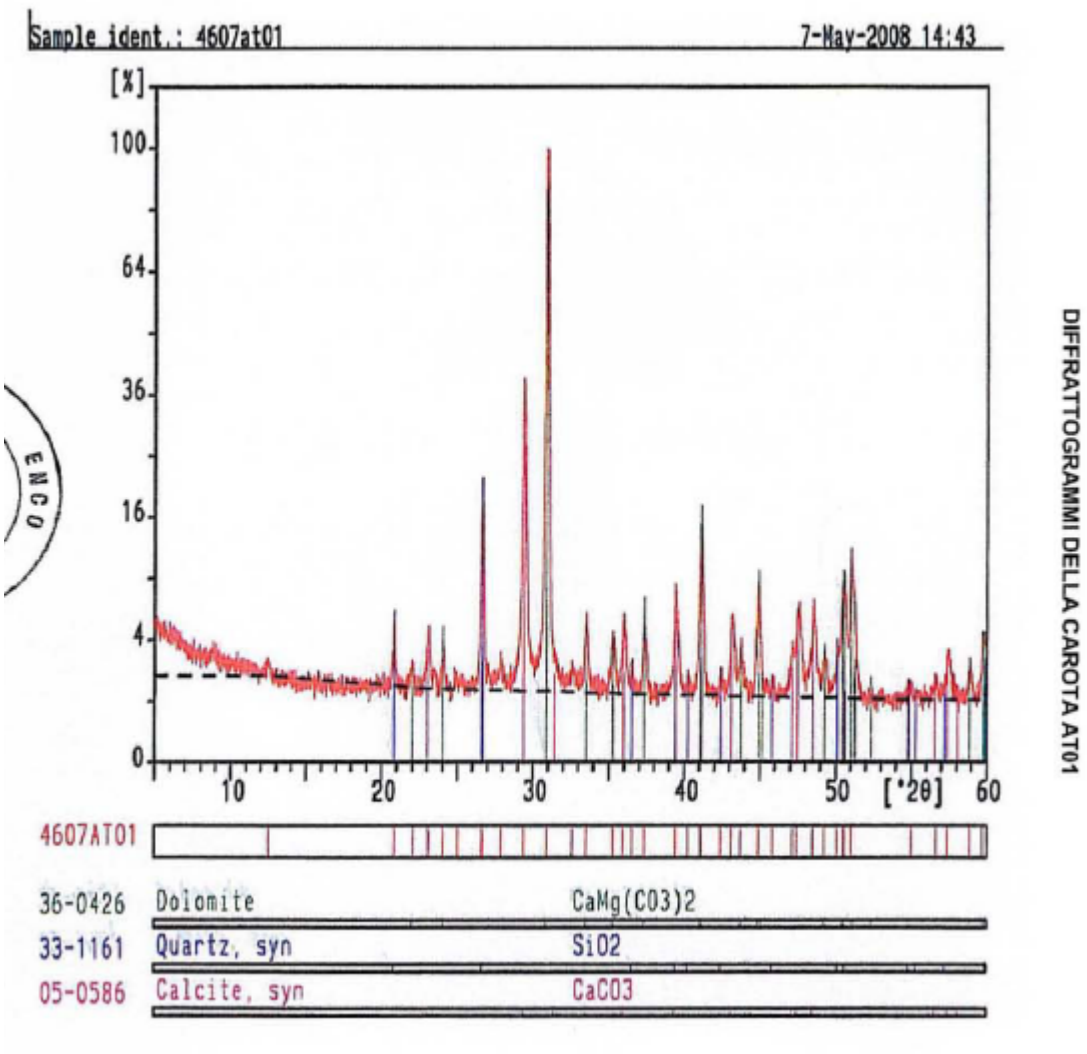

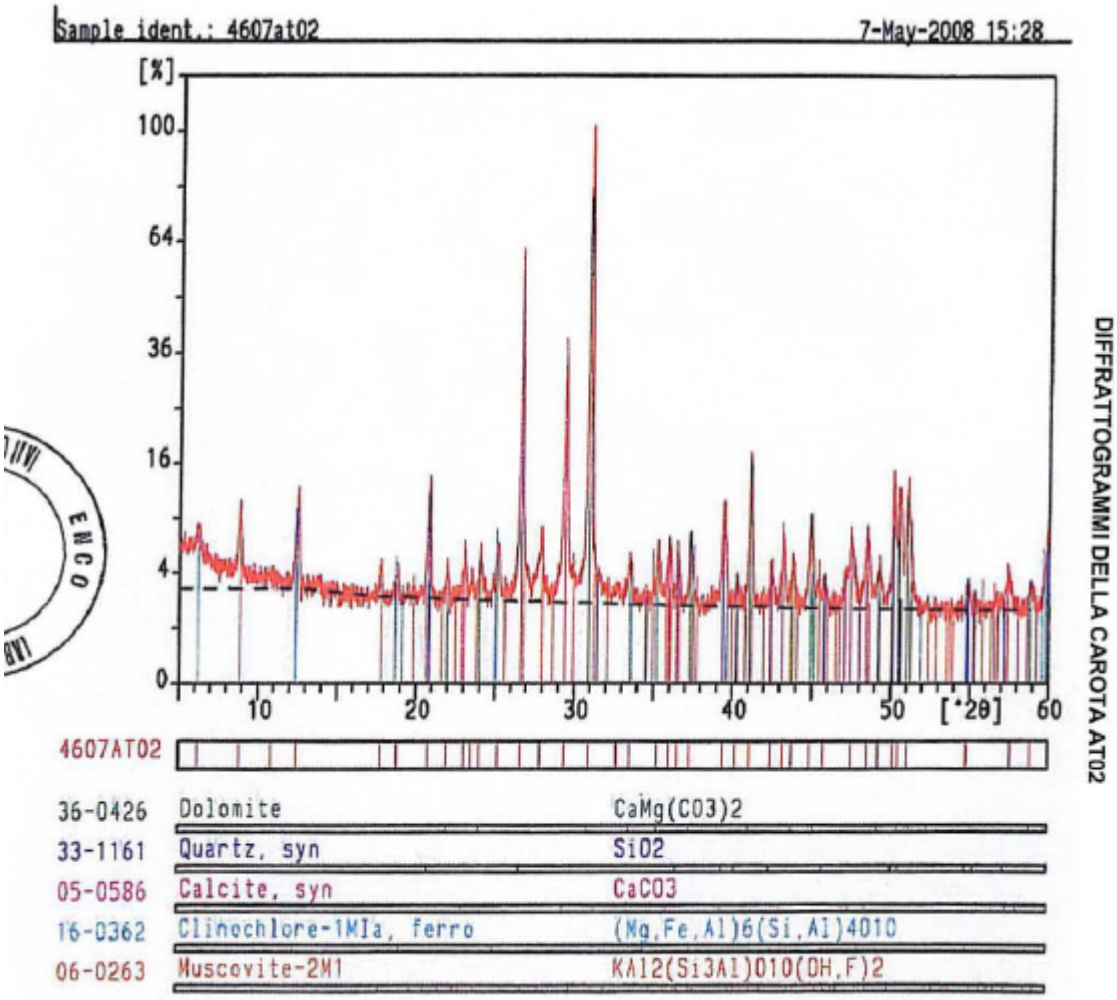

DIFFRATTOGRAMMI DELLA CAROTA AT02

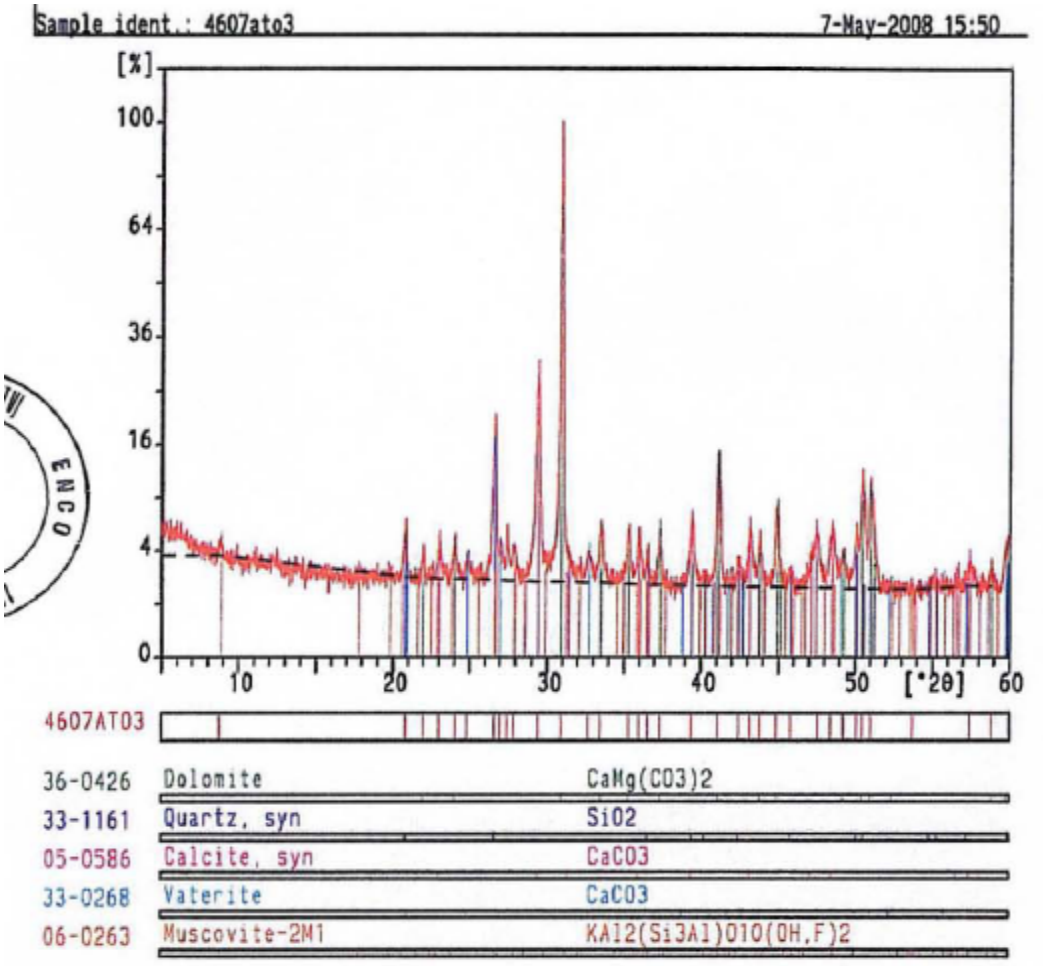

DIFFRATTOGRAMMI DELLA CAROTA AT03

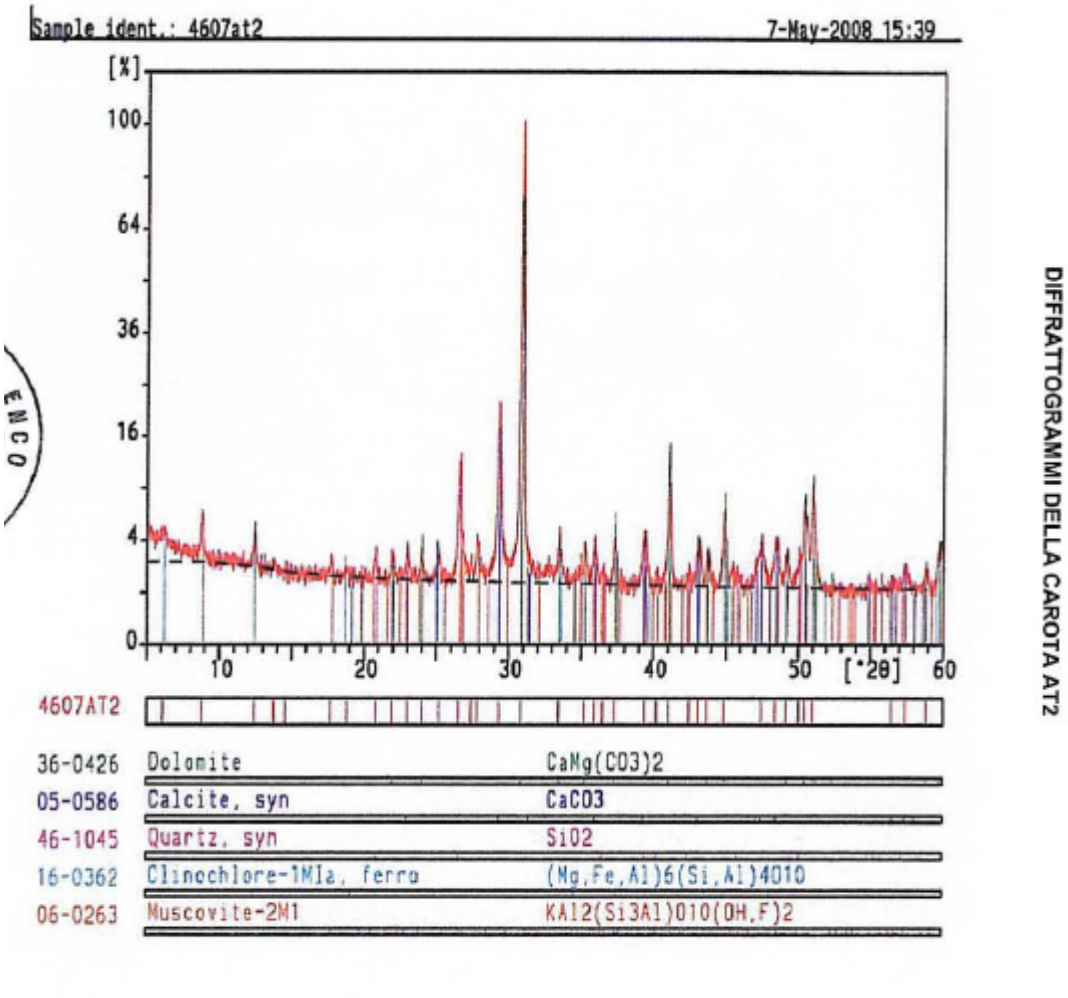

Figure 6: the result of X-ray diffraction (AT01, AT02, AT03, AT1 from the top)
(ENCO, 2008)

3.3. Report regarding reinforcement

Pacometric investigation was also carried out in order to assess the position of steel reinforcement, the estimation of the cover and the assessment of diameter of the bars on all measured areas on site. Tensile-strength tests were performed on 10 pieces of reinforcement in the laboratory.

RISULTATI DELLE PROVE

SIGLA provino	DATA Prelievo o Rif. Colata	POSIZIONE PRELIEVO dichiarata	MARCHIO (Scheda n° C.A. Allegata)	TIPO DI ACCIAIO dichiarato	TIPO DI PROVINO	Ø nomin. (mm)	Peso provino (gr)	L barra (mm)	S_o barra liscia equipes. (mm^2)	L_o (mm)	Ø reale (mm)
7	29/04/08	AT01	/	/	barra a.m.	20x20	1625,0	657	315,08	100	20,0
8	29/04/08	AT02	/	/	barra liscia	28	2462,0	514	610,18	140	27,9
9	29/04/08	AT03	/	/	barra a.m.	22x22	1552,0	514	384,65	110	22,1
10	29/04/08	AT04	/	/	barra a.m.	20x20	1374,7	563	311,05	100	19,9

SIGLA provino	DATA PROVA	PROVA TRAZIONE (UNI EN 15630/1-'04 e UNI EN 10002/1:2004)								PIEGA (UNI EN 15630/1-'04 UNI EN ISO 7438:2005)		
		Snervam. F_y (KN)	Snervam. f_y (N/mm^2)	Rottura F_t (kN)	Rottura f_t (N/mm^2)	f_t/f_y	f_y/f_{yk}	Allung. su L_o (%)	Diagr σ–ε (si-no)	180°a freddo	90°a caldo	Ø mandrino (mm)
7	15/05/08	141,0	447,5	211,2	670,3	1,50		16,0	no	/	/	/
8	15/05/08	215,9	353,8	324,8	532,3	1,50		26,2	no	/	/	/
9	15/05/08	167,8	436,2	253,4	658,8	1,51		14,8	no	/	/	/
10	15/05/08	140,2	450,7	210,4	676,4	1,50		16,3	no	/	/	/

In accordo alla UNI EN ISO 10002/l, il calcolo di f_y e f_t viene fatto rispetto all'area reale So

RISULTATI DELLE PROVE

SIGLA provino	DATA Prelievo o Rif. Colata	POSIZIONE PRELIEVO dichiarata	MARCHIO (Scheda n° C.A. Allegata)	TIPO DI ACCIAIO dichiarato	TIPO DI PROVINO	Ø nomin. (mm)	Peso provino (gr)	L barra (mm)	S_o barra liscia equipes. (mm^2)	L_o (mm)	Ø reale (mm)
1	29/04/08	AT1	/	/	barra liscia	16	754,9	475	202,46	80	16,1
2	29/04/08	AT2	/	/	barra liscia	16	766,7	500	195,34	80	15,8
3	29/04/08	AT3	/	/	barra liscia	14	592,1	492	153,31	70	14,0
4	29/04/08	MURO	/	/	barra a.m.	17x17	1050,2	600	222,97	85	16,9
5	29/04/08	MURO	/	/	barra a.m.	17x17	1053,0	601	223,20	85	16,9
6	29/04/08	MURO	/	/	barra a.m.	17x17	1049,4	600	222,81	85	16,8

SIGLA provino	DATA PROVA	PROVA TRAZIONE (UNI EN 15630/1-'04 e UNI EN 10002/1:2004)								PIEGA (UNI EN 15630/1-'04 UNI EN ISO 7438:2005)		
		Snervam. F_y (KN)	Snervam. f_y (N/mm^2)	Rottura F_t (kN)	Rottura f_t (N/mm^2)	f_t/f_y	f_y/f_{yk}	Allung. su L_o (%)	Diagr σ ε (si-no)	180°a freddo	90°a caldo	Ø mandrino (mm)
1	15/05/08	60,3	297,8	80,9	399,6	1,34		31,2	no	/	/	/
2	15/05/08	63,8	326,6	91,8	470,0	1,44		25,8	no	/	/	/
3	15/05/08	50,7	330,7	63,5	414,2	1,25		29,8	no	/	/	/
4	15/05/08	100,5	450,7	143,2	642,2	1,42		17,7	no	/	/	/
5	15/05/08	98,7	442,2	141,3	633,1	1,43		16,3	no	/	/	/
6	15/05/08	99,4	446,1	141,7	636,0	1,43		17,0	no	/	/	/

In accordo alla UNI EN ISO 10002/l, il calcolo di f_y e f_t viene fatto rispetto all'area reale So

Table 12: the physical property of the steel, Principle body and Secondary body (below) (ENCO, 2008)

4. STRUCTURAL ANALYSIS

4.1. Introduction

In this thesis, the structural analysis is carried out with numerical method. The purpose of the analysis is to examine the global behaviour with static and dynamic load and also the verification of the member. This chapter especially deals with the former purpose, and the verification is carried out in the following chapter. Here the following analyses are carried out: modal analysis, linear static analysis and response spectral analysis. Incidentally, for the convenience of the discussion, the arches are numbered as below (Figure 7). Incidentally the unit of equation and the value in table is "m, kN, kNm", unless it is not defined particularly.

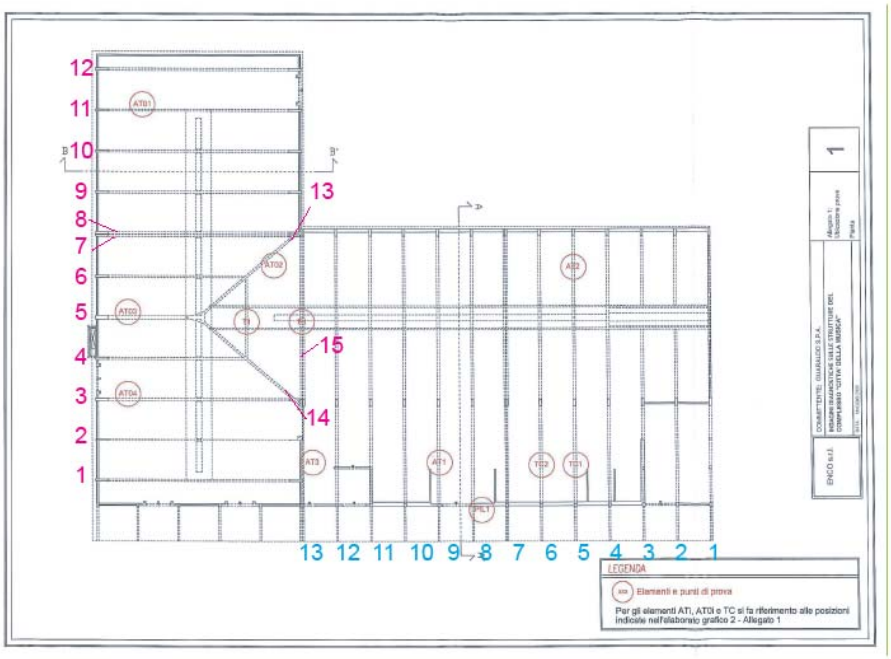

Figure 7: the numbering of the arches

(ENCO, 2008 modified by author)

4.2. Preparation of model

The numerical model is built with Straus 7. As this is simple continuous-arch structure, the beam element is employed-but not brick. Two buildings (Principle body and Secondary body) stand very close to each other, and yet they are independent structurally and do not share any structural element. Therefore they are modelled individually in this analysis (Figure 8).
Principle body is composed of 334 nodes and 452 beams, and Secondary body is of 778 nodes and 891 beams.

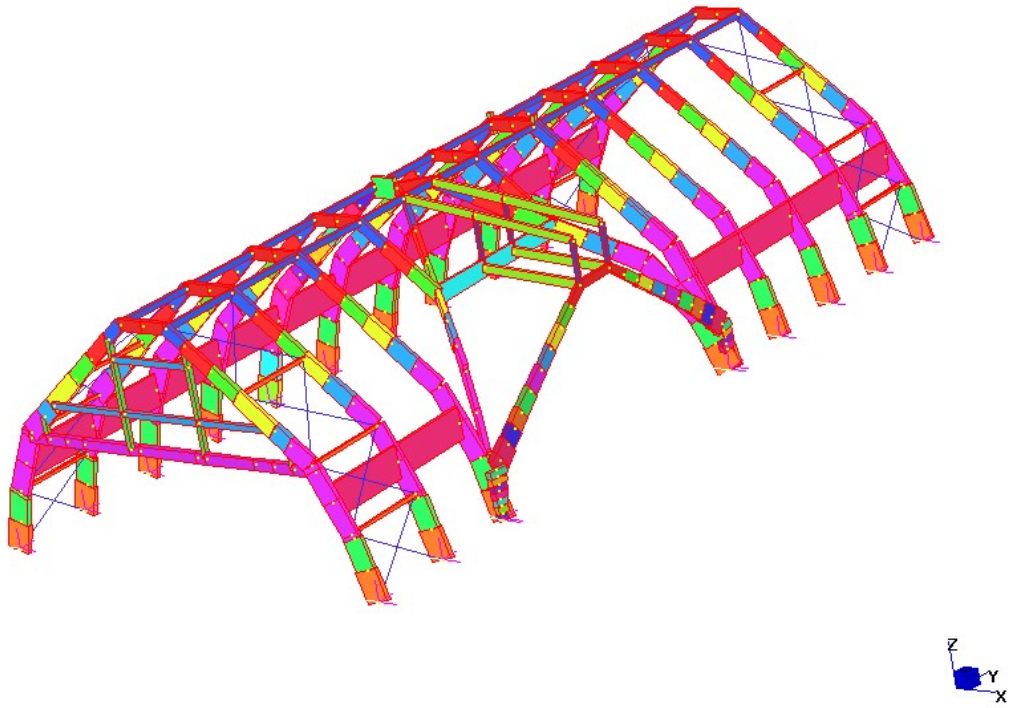

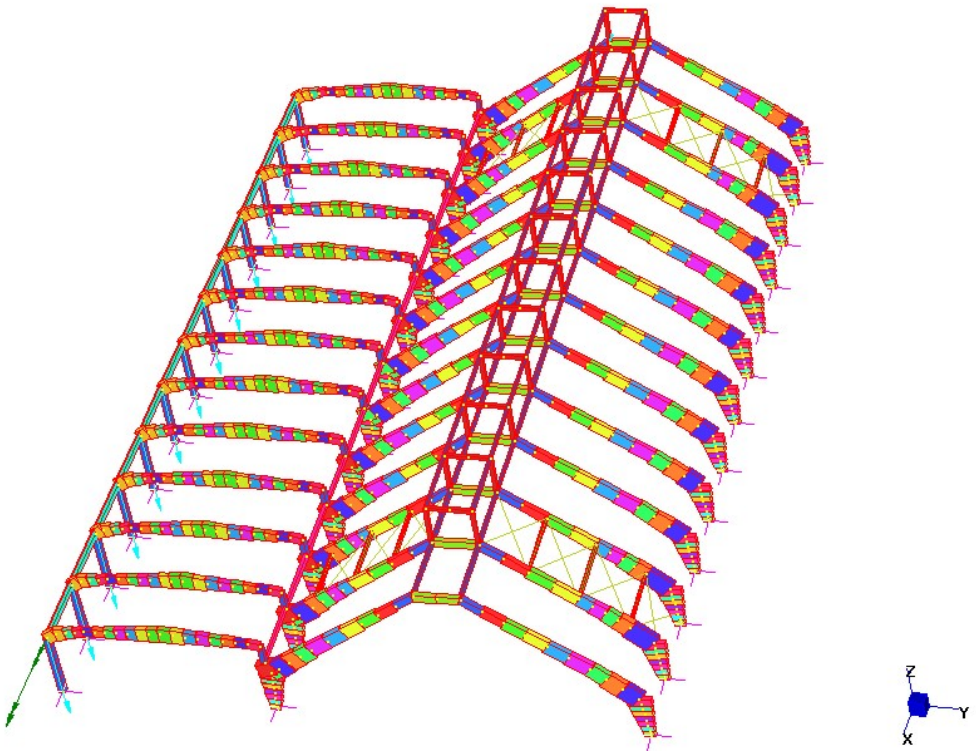

Figure 8: The numerical model, Principle Body and Secondary body (below)

Material

The material properties are assigned as follows. The values are taken from ENCO (2008) as discussed above. As for the Young modulus, the mean value is taken, and with regard to compressive the characteristic value which is discussed in ENCO (2008) is adopted. The density is determined from the usual concrete density (usually, 2400 [kg/m^3])+100([kg/m^3) which comes from the consideration of reinforcement, as in Straus it is not possible to place reinforcement in concrete. Steel beams and steel cables are placed between the arches. However, in linear static analysis, cables cannot be located and hence instead trusses are placed there.

	Young's modulus (MPa)	compressive strength (MPa)	density (kg/m^3)
principle body	29114	29	2500
secondary body (arch)	27227	24	2500
secondary body (beam)	35112	20.3	2500

Table 13: material property of each structure

Plan of structural analysis

First, the modal analysis is performed. Then, linear static analysis is carried out with gravity, snow load and wind load. The value and direction of each load are determined according to Euocode. In the end, the spectral response analysis is done. The spectrum employed in the analysis is obtained from the Italian code (Norme tecniche per le costruzioni NB: from this point it is called the Italian code). At any rate, the load assignment is discussed in detail below.

4.3. Linear analysis

4.3.1. Modal analysis

The modal analysis is conducted in the first place. The result is as below.
Here, the frequency of first 10 modes is shown. However, it is found that most of them show the local behaviour when the modal shapes are seen. Seemingly the 1^{st} mode and 4^{th} mode show the global behaviour relatively for Principle body and the 1^{st} mode and 2^{nd} mode as for Secondary body. This fact is confirmed below again in the spectral response analysis.

Principle body		
Mode	Eigenvalue	Frequency (Hz)
1	1.85E+02	2.17
2	2.37E+02	2.45
3	2.59E+02	2.56
4	3.54E+02	3.00
5	4.74E+02	3.47
6	4.84E+02	3.50
7	5.77E+02	3.82
8	5.96E+02	3.88
9	6.11E+02	3.93
10	7.77E+02	4.44

Table 14: The natural frequency and eigenvalue for first 10 modes (Principle body)

Secondary Body		
Mode	Eigenvalue	Frequency (Hz)
1	1.64E+02	2.04
2	2.78E+02	2.65
3	3.78E+02	3.09
4	3.85E+02	3.12
5	3.92E+02	3.15
6	3.93E+02	3.16
7	3.95E+02	3.16
8	3.99E+02	3.18
9	4.02E+02	3.19
10	4.05E+02	3.20

Table 15: The natural frequency and eigenvalue for first 10 modes (Secondary body)

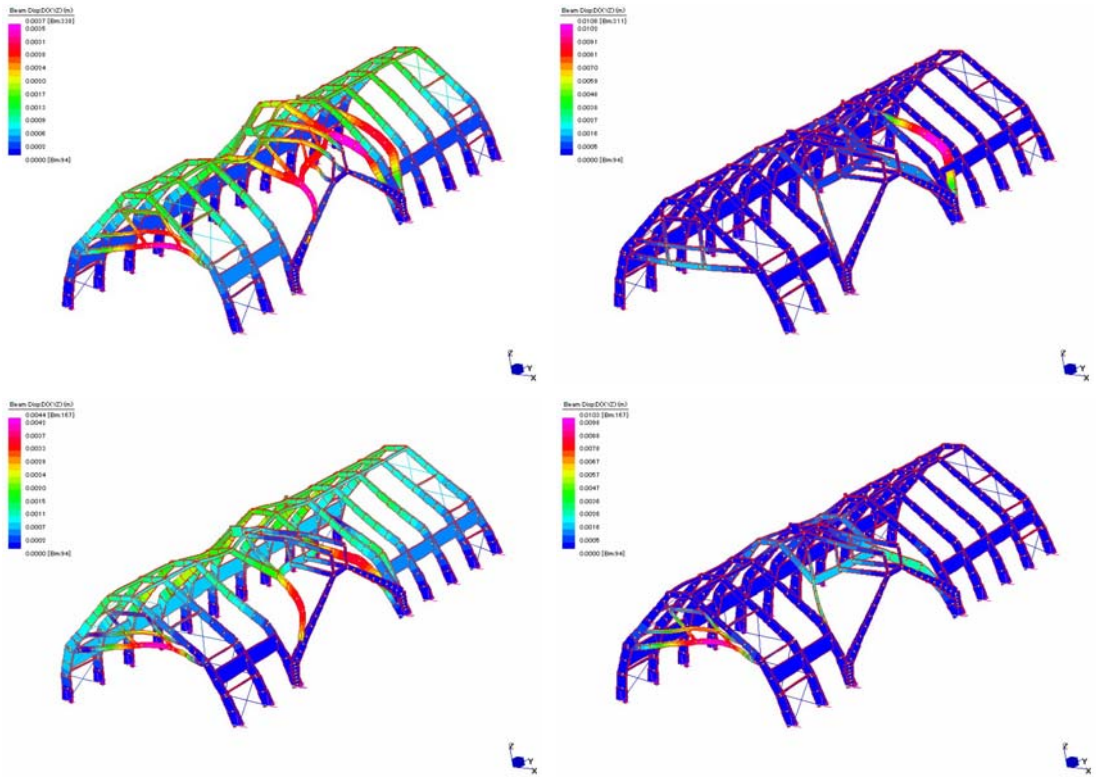

Figure 9: Mode1, Mode2, Mode3, Mode4 (clockwise, from the left top) Principle body: displacement scale 10% (XYZ)

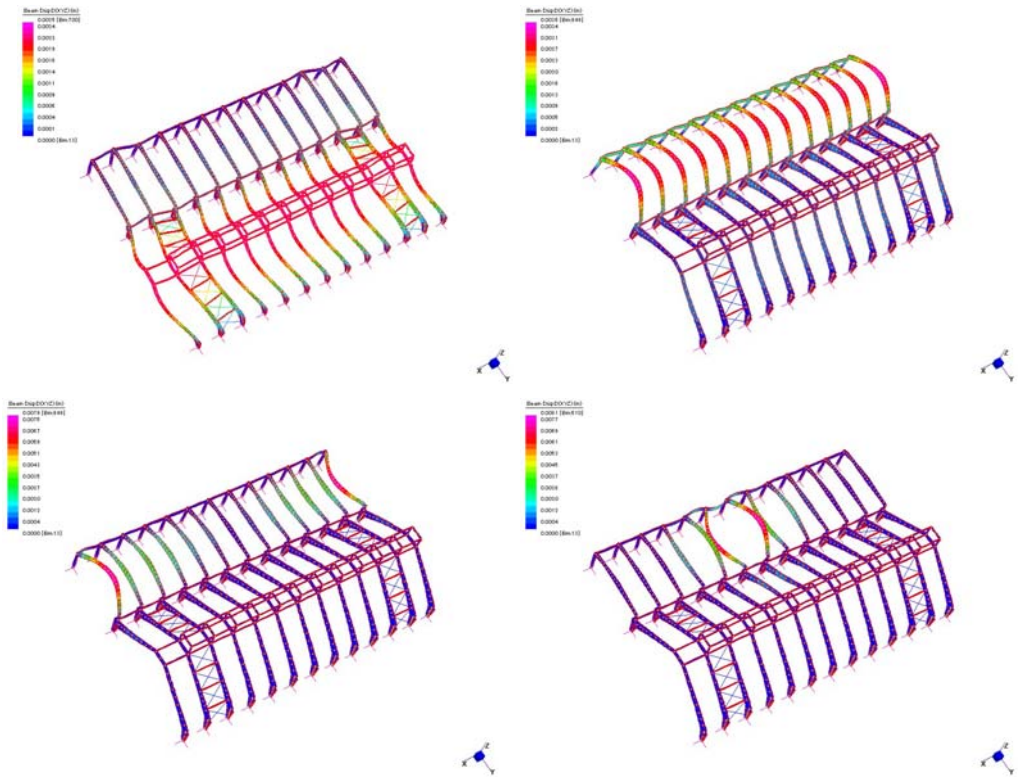

Figure 10: Mode1, Mode2, Mode3, Mode4(clockwise, from the left top), Secondary body

4.3.2. Linear Static Analysis (gravity, snow load and wind load)

Assignment of the Load

For the linear static analysis, the gravity, snow load and wind load should be assigned on the structure. Therefore, here the determination each load is discussed in accordance with the regarding Eurocode.

Gravity load

9.8m/s^2 ,in the global z-direction, is assigned to the structure as gravity load.

Snow load

Snow load is determined in accordance with EN1991-1-3:2003. In Marghera the characteristic value of snow load on the ground: $s_{k,}$ is determined to be 0.3kN/m^3 (Figure 11). Then depending on the angle of the roof, the snow loads on the roof is assigned to each structure as seen below.

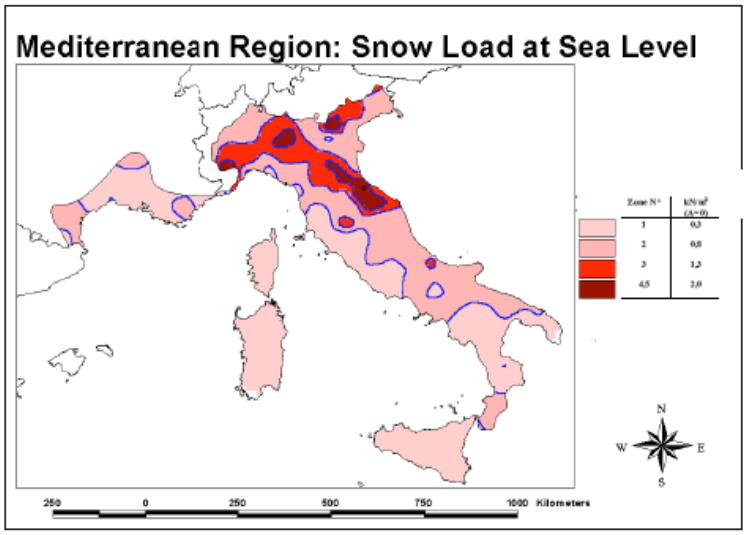

Figure C.6

Figure 11: Snow Load at Sea Level, Italy

(EN1991-1-3-2003, p45)

$$s=\mu_i*C_e*Ct*s_k \qquad (4\text{-}2)$$

(EN1991-1-3-2003, p18)

where:

s is snow load on the roof

μ_l is the snow load shape coefficient-see 5.3

C_e is the exposure coefficient

Ct is the thermal coefficient

s_k is the characteristic value of snow load on the ground

S_k=0.3 kN/m^2
C_e=1
C_t=1

Table 16: the characteristic value of snow load on the ground, the exposure coefficient, the thermal coefficient on site (Marghera)

Table 5.2: Snow load shape coefficients

Angle of pitch of roof α	$0° \le \alpha \le 30°$	$30° < \alpha < 60°$	$\alpha \ge 60°$
μ_1	0,8	0,8(60 - α)/30	0,0
μ_2	0,8 + 0,8 α/30	1,6	--

Table 17: Snow Load shape coefficient

(EN1991-1-3-2003, p21)

a	$\mu_{1,0}$=0.8	$s_{1,0}$=	0.24	kN/m^2
b	$\mu_{1,1}$=0.56	$s_{1,1}$=	0.168	kN/m^2
c	$\mu_{1,2}$=0	$s_{1,2}$=	0	kN/m^2

Table 18: The snow load shape coefficient and the characteristic value of snow load on roof for Principle body

d	$\mu_{2,0}$=0.8	$s_{2,0}$=	0.24	kN/m^2
e	$\mu_{2,1}$=0.7	$s_{2,1}$=	0.21	kN/m^2
f	$\mu_{2,2}$=0.8	$s_{2,2}$=	0.24	kN/m^2

Table 19: The snow load shape coefficient and the characteristic value of snow load on roof for Secondary body

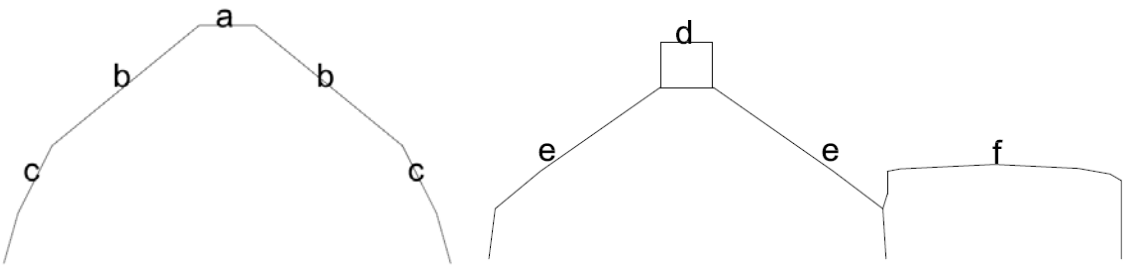

Figure 12: the distribution of the snow load, Principle body and Secondary body (right)

Wind load

Wind load is discussed in EN 1991-1-4:2005. In this analysis, the wind is assumed to come from east-in case of Principle body, and north as for Secondary body. As Principle body has almost the symmetrical shape, the case where wind comes from west is skipped-for the same reason, the case where wind comes from south is ignored in Secondary body. The structure of Principle body has several angles of roof but here it is simplified and thus it is considered that it has single angle of roof (blue line, 52 degrees, Figure 18). With regard to the Secondary body two structures are aligned-arch part and beam part- and another simplification is applied here. That is, two parts are considered to stand individually, and the wind is assumed to work on them separately.

According to EN 1991-1-4:2005, first the basic wind velocity should be obtained for the computation of wind load.

$$v_b = C_{cr} * C_{season} * v_{b,0} \quad (4\text{-}2)$$

(EN 1991-1-4:2005, p18)

where:

v_b is the basic wind velocity, defined as a function of wind direction and time of year at above ground of terrain category II

$v_{b,0}$ is the fundamental value of the basic wind velocity

C_{cr} is the directional factor

C_{season} is the season factor

$v_{b,0(m/s)}$	25
$v_{b\ (m/s)}$	25
C_{cr}	1
C_{season}	1

Table 20: basic wind velocity and other relevant factors

NB), The fundamental value of the basic wind velocity $v_{b,0}$ is taken from the Italian code in line with Eurocode.

Then from the basic wind velocity, the peak velocity pressure is to be obtained. With the peak velocity pressure, the value of the wind pressure working on the structure can be indicated by the multiplication with other several factors as shown below. First, it is necessary to determine the height of the structure. Here the reference height is the same as the height of the building as it is seen that the h<b is satisfied (Figure 13). Then once the peak velocity pressure is acquired, it needs to be multiplied by the external pressure coefficient which depends on the angle and position of the regarding wall or roof. The result is seen in Table 23. There are 10 cases in total. The case 3-6 correspond to the case 7-10 with regard to the Secondary body. That is, when the case 3 is chosen for the arch part of Secondary body, case 7

follows automatically for its beam part. In the Table 23, the values are multiplied also by the span of the arch-that is, 6.1(m) for Principle body and 5(m) for Secondary body-, as the force is assumed to be assigned on the arch, not directly on the roof.

$$q_p(z)=C_e(z)*q_b \quad (4\text{-}3)$$

(EN1991-1-4-2005 p22)

$$q_b = 0.5*\rho*v_b^2 \quad (4\text{-}4)$$

(EN1991-1-4-2005 p23)

where:

$q_p(z)$ is the peak velocity pressure, at height z

$C_e(z)$ is the exposure factor given in Figure 14

ρ is the air density, which depends on the altitude, temperature and barometric pressure to be expected in the region during wind storms, 1.25kg/m^3 (from the Italian code)

q_b is the basic velocity pressure

m	h	b	d	e
principle body	15.5	65	30	31
secondary body (arch)	10	60	26	20
secondary body (body)	6.4	60	15	12.8

Table 21: height (h), width (b), depth (d) and edge distance (e) of each structure

	$q_p(z_e)_{(kN/m2)}$	$z_{e\ (m)}$	$c_e(z)$	$q_{b(kN/m2)}$	$q_b(z)_{(kN/m2)}$
principle body	1.02	15.5	2.6	391	1016
secondary body (arch)	0.92	10	2.35	391	918
secondary body (beam)	0.8	6.4	2.05	391	801

Table 22: the peak velocity at the reference height for external wind action

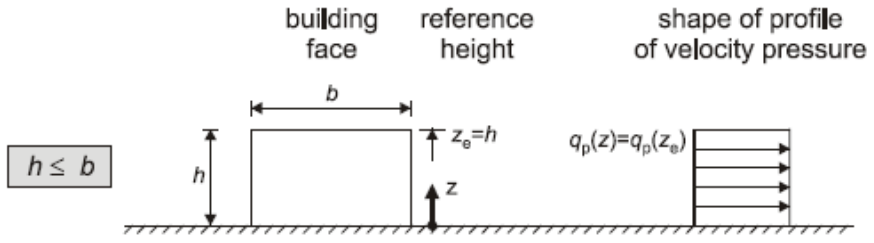

Figure 13: Reference height z_e, depending on h and b, and corresponding velocity pressure profile

(EN1991-1-4-2005 p35)

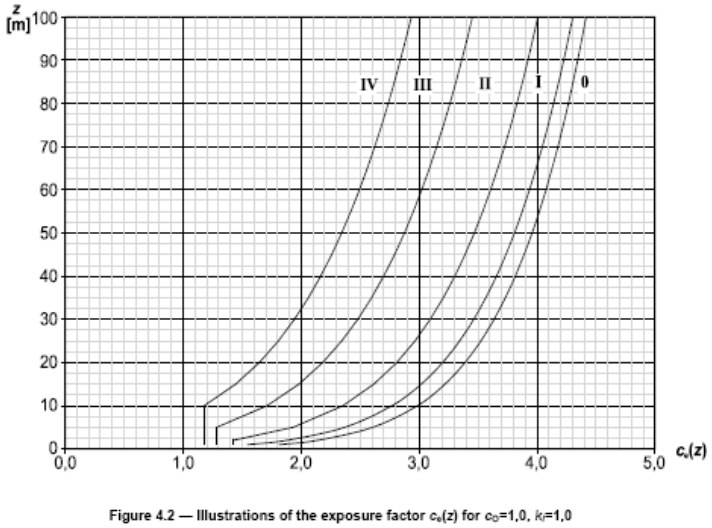

Figure 4.2 — Illustrations of the exposure factor $c_e(z)$ for c_0=1,0, k_l=1,0

Figure 14: the graph of the exposure factor $C_e(z)$ c_c=1, k_r=1

(EN1991-1-4-2005 p23)

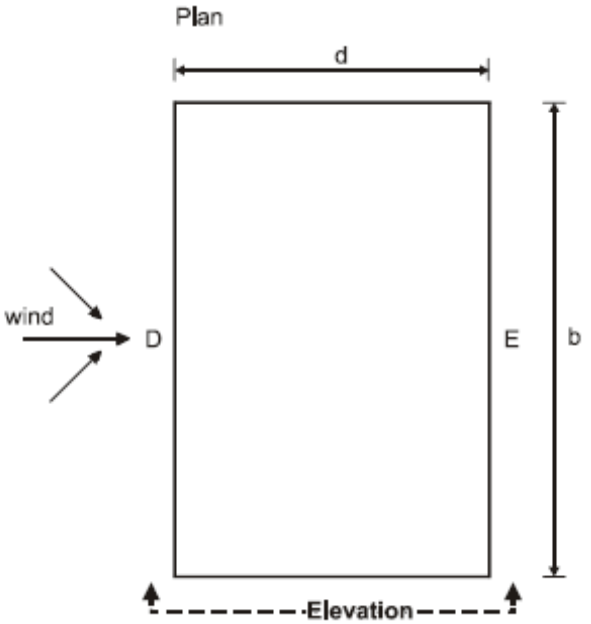

Figure 15: Wind pressure on the vertical wall

(EN1991-1-4-2005 p36)

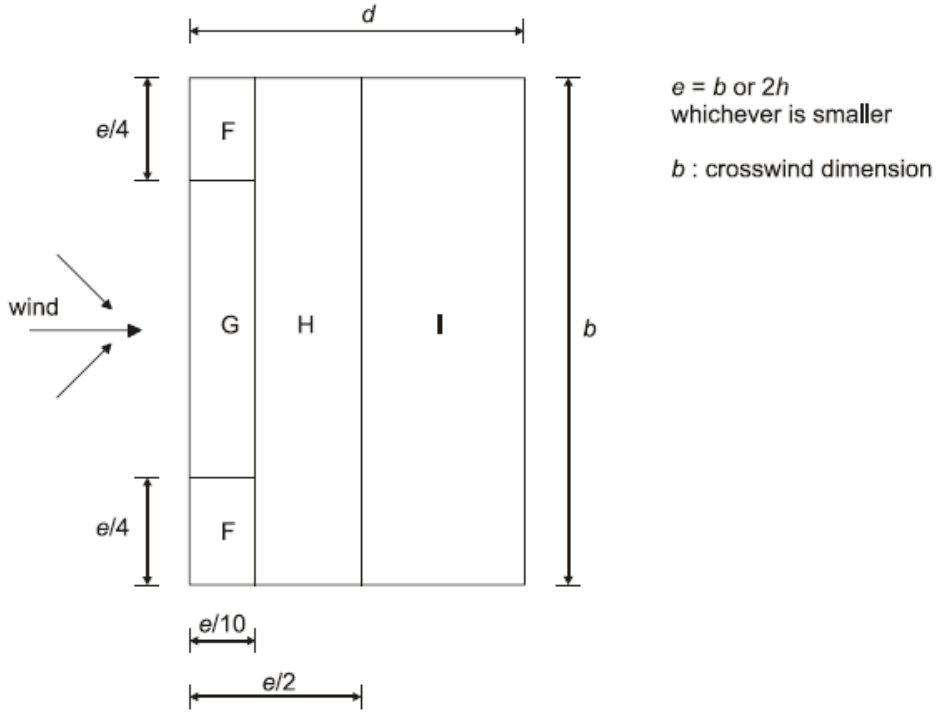

Figure 7.6 — Key for flat roofs

Figure 16: Wind pressure on flat roof

(EN1991-1-4-2005 P42)

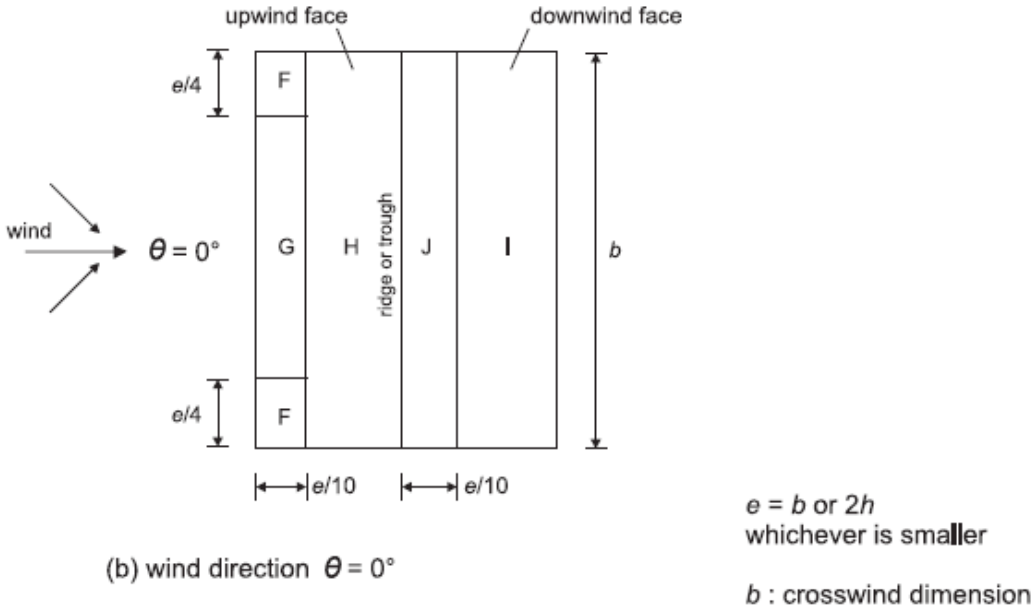

(b) wind direction $\theta = 0°$

Figure 17: Wind pressure on duopitch roof

(EN1991-1-4-2005 P48)

kN/m	front				back				
case1	F	G	H	H (flat)	I(flat)	I	J	D	E
	2.6	2.6	2.4	−1.3	0.75	0.75	−1.1		
case2	F	G	H	H (flat)	I(flat)	I	J	D	E
	2.6	2.6	2.4	−1.3	0.75	−0.75	−1.1		

kN/m	front				back				
case3	F	G	H	H (flat)	I(flat)	I	J	D	E
	−0.92	−0.92	−0.37	−2	0.92	−1.3	−1.7	2.8	−1.3
case4	F	G	H	H (flat)	I(flat)	I	J	D	E
	−0.92	−0.92	−0.37	−2	−0.92	0	0	2.8	−1.3
	0	0							
case5	F	G	H	H (flat)	I(flat)	I	J	D	E
	3.2	3.2	2.4	−2	0.92	−1.3	−1.7	2.8	−1.3
case6	F	G	H	H (flat)	I(flat)	I	J	D	E
	3.22		2.4	−2	−0.92	0	0	2.8	−1.3

kN/m	front				Back				
case7	F	G	H	H (flat)	I(flat)	I	J	D	E
	−6.8	−4.8	−2.4			−2.4	0.8		−1.2
case8	F	G	H	H (flat)	I(flat)	I	J	D	E
	−6.8	−4.8	−2.4			−2.4	−2.4		−1.2
case9	F	G	H	H (flat)	I(flat)	I	J	D	E
	0	0	0		−2.4	−2.4	0.8		−1.2
case10	F	G	H	H (flat)	I(flat)	I	J	D	E
	0	0	0			−2.4	−2.4		−1.2

Table 23: The surface pressure, Principle body, Secondary body (arch part) and Secondary body (beam part) (from the top)

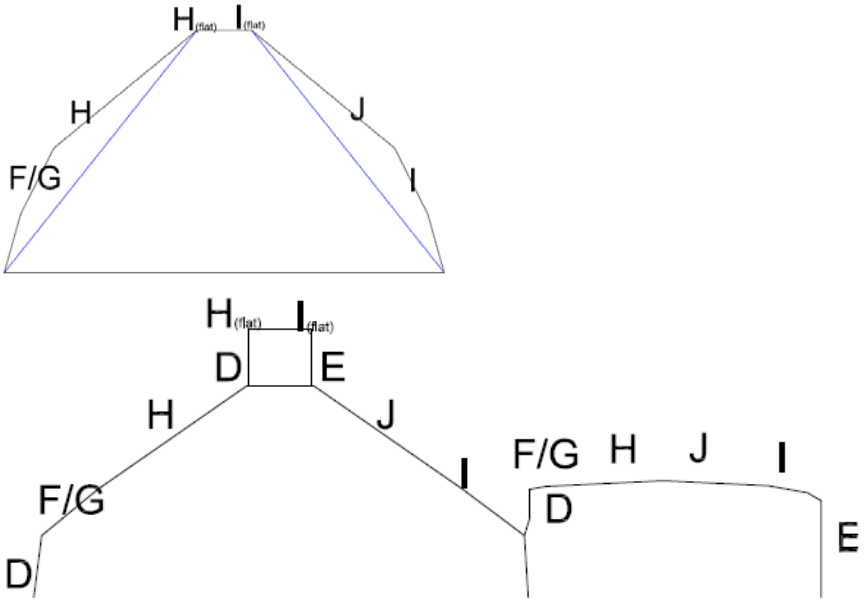

Figure 18: The distribution of the wind load, Principle body and Secondary body (below)

4.3.3. Spectral Response Analysis (Seismic Analysis)

The adoption of Elastic Spectrum

The input response spectrum is given according to the Italian code. As for the spectral response analysis according to Italian code, for the Serviceability Limit States (SLE: Stati Limiti di Esercizio in the Italian code) SLD and SLV for the Ultimate Limit States (SLU: Stati Limiti Ultimi in the Italian code) are chosen as mentioned below, considering the usage and the scale of the building which is going to be used as commercial purpose.

Tabella 3.2.I – *Probabilità di superamento* P_{V_R} *al variare dello stato limite considerato*

Stati Limite		P_{V_R} : Probabilità di superamento nel periodo di riferimento V_R
Stati limite di esercizio	SLO	81%
	SLD	63%
Stati limite ultimi	SLV	10%
	SLC	5%

Table 24: exceedance probability P_{VR} and reference life period V_R

(The Italian code, p16)

According to the Italian code, first the nominal life of the building (V_n) should be determined. V_n depends on the construction type (tipo di costruzione). Then it should be multiplied by the coefficient factor (C_u). C_u is given by the class of the usage (classe d'uso), which is determined to be III considering the usage. As a result, reference life period (vita di riferimento: V_R) is given as below (4-5).

In addition to above discussion, now the subsoil category (categorie di sottosuolo) and the topographical category (categorie topographiche) are to be determined. The site (Marghera) should be C and T1 for each. From above all the information, the response spectrum is acquired. First a_g, F_0, T_C* should be obtained in order to calculate each period T_B, T_C, T_D. As a result, below two spectrum is acquired. Incidentally, the return period T_R is 75 years for SLD and 712 years for SLV. Final outcome is seen in the Figure 19, 20.

$$V_R=C_u*V_n \quad (4\text{-}5)$$

(Italian code, p5)

V_n/Vita nomiale	50
C_u/coefficiente d'uso	1.5
V_R/Vita di riferimento	75
Categoria topografica	T1
Categoria di sottosuolo	C
Classe d'uso	III
tipo di costruzione	2

Table 25: the list of the values relevant to determination of the elastic spectrum I

Tabella 2.4.I – *Vita nominale* V_N *per diversi tipi di opere*

	TIPI DI COSTRUZIONE	Vita Nominale V_N (in anni)
1	Opere provvisorie – Opere provvisionali - Strutture in fase costruttiva[1]	≤ 10
2	Opere ordinarie, ponti, opere infrastrutturali e dighe di dimensioni contenute o di importanza normale	≥ 50
3	Grandi opere, ponti, opere infrastrutturali e dighe di grandi dimensioni o di importanza strategica	≥ 100

Table 26: the list of the nominal life of buildings

(the Italian code, p4)

Tab. 2.4.II – *Valori del coefficiente d'uso* C_U

CLASSE D'USO	I	II	III	IV
COEFFICIENTE C_U	0,7	1,0	1,5	2,0

Se $V_R \leq 35$ anni si pone comunque $V_R = 35$ anni.

Table 27: the list of the nominal life of buildings

(the Italian code, p5)

	SLD	SLV
a_g	0.3724	0.7938
$\xi(\%)$	5	5
η	1	1
T_C*	0.269	0.38
T_C	0.435636	0.549091
F_0	2.529	2.647
T_B	0.145212	0.18303
T_D	1.752	1.924
S_S	1.5	1.5
S_T	1	1
C_C	1.619	1.445
T_R	75	712

Table 28; the list of the values relevant to determination of the elastic spectrum II and T_R

Tabella 3.2.VI – *Valori massimi del coefficiente di amplificazione topografica* S_T

Categoria topografica	Ubicazione dell'opera o dell'intervento	S_T
T1	-	1,0
T2	In corrispondenza della sommità del pendio	1,2
T3	In corrispondenza della cresta del rilievo	1,2
T4	In corrispondenza della cresta del rilievo	1,4

Table 29: the maximum topographic condition factor

(the Italian code, p18)

Tabella 3.2.V – *Espressioni di* S_S *e di* C_C

Categoria sottosuolo	S_S	C_C
A	1,00	1,00
B	$1,00 \le 1,40 - 0,40 \cdot F_o \cdot \frac{a_g}{g} \le 1,20$	$1,10 \cdot (T_C^*)^{-0,20}$
C	$1,00 \le 1,70 - 0,60 \cdot F_o \cdot \frac{a_g}{g} \le 1,50$	$1,05 \cdot (T_C^*)^{-0,33}$
D	$0,90 \le 2,40 - 1,50 \cdot F_o \cdot \frac{a_g}{g} \le 1,80 \cdot$	$1,25 \cdot (T_C^*)^{-0,50}$
E	$1,00 \le 2,00 - 1,10 \cdot F_o \cdot \frac{a_g}{g} \le 1,60$	$1,15 \cdot (T_C^*)^{-0,40}$

Table 30: the expression of S_S and C_C

(the Italian code, p20)

Tabella C.3.2.I.- Valori di T_R espressi in funzione di V_R

Stati Limite		Valori in anni del periodo di ritorno T_R al variare del periodo di riferimento V_R
Stati Limite di Esercizio (SLE)	SLO	(2) 30 anni $\leq T_R = 0,60 \cdot V_R$
	SLD	$T_R = V_R$
Stati Limite Ultimi (SLU)	SLV	$T_R = 9,50 \cdot V_R$
	SLC	$T_R = 19,50 \cdot V_R \leq$ 2475 anni (1)

Table 31: the value of the return period

(Consiglio Superiore dei Lavori Pubblici 2008, p14)

$$S=S_S*S_T \quad (4\text{-}6)$$

$$\eta=10/(5+\xi)^{0.5} \geq 0.55 \quad (4\text{-}7)$$

$$T_C=C_C*T^*_C \quad (4\text{-}8)$$

$$T_B=T_C/3 \quad (4\text{-}9)$$

$$T_D=4.0*a_g/g+1.6 \quad (4\text{-}10)$$

$0 \leq T < T_B$

$$S_e(T) = a_g * \eta * F_0 [T/T_B + 1/\eta * F_0 * (1 - T/T_B)] \quad (4\text{-}11)$$

$T_B \leq T < T_C$

$$S_e(T) = a_g * S * \eta * F_0 \quad (4\text{-}12)$$

$T_C \leq T < T_D$

$$S_e(T) = a_g * S * \eta * (T_C/T) \quad (4\text{-}13)$$

$T_D \leq T$

$$S_e(T) = a_g * S * \eta * (T_C * T_D / T\text{^}2) \quad (4\text{-}14)$$

(Italian code. p19,20)

Where:

$S_e(T)$ is the elastic response spectrum*

T is the vibration period of a linear single-degree-of-freedom system*

T_B is the lower limit of the period of the constant spectral acceleration branch*

T_C is the upper limit of the period of the constant spectral acceleration branch*

T_D is the value defining the beginning of the constant displacement response range of the spectrum*

S is the soil factor*

S_S is the stratigraphic amplification coefficient

S_T is the topographic condition factor

η is the damping correction factor with a reference value*

ξ is the viscous damping ratio*

C_C is the subsoil category coefficient

T^*_C is the initial period of the constant spectral acceleration branch in the horizontal acceleration

a_g is the maximum horizontal acceleration on site

g is the gravity acceleration

F_0 is the maximum amplification factor of the spectrum in the horizontal acceleration

(* from EN1998-1-1:2004, p37)

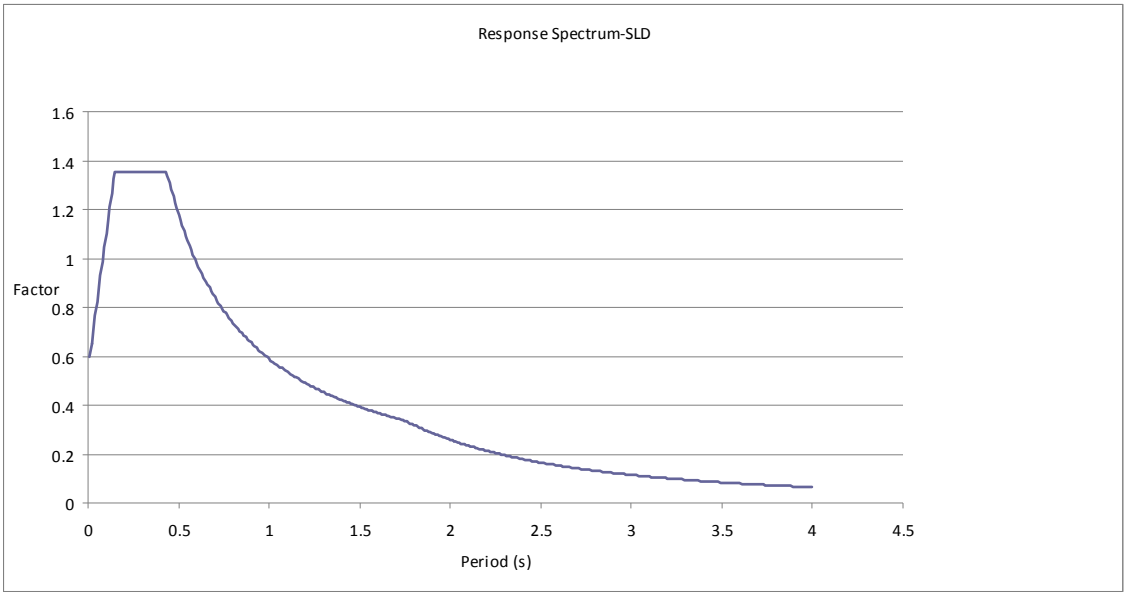

Figure 19: Response Spectrum-SLD

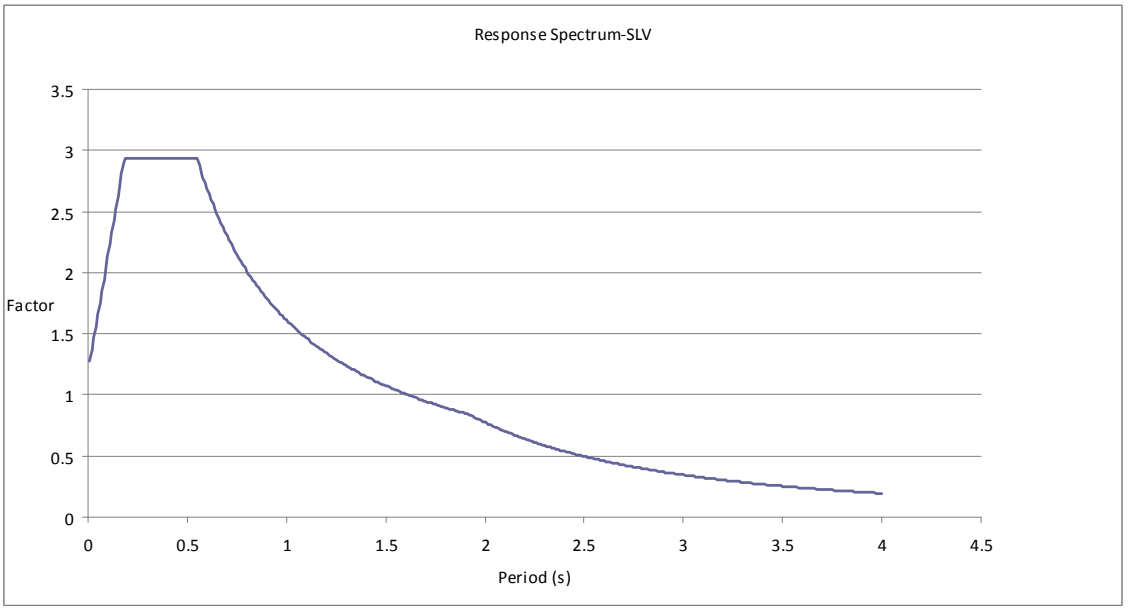

Figure 20: Response Spectrum-SLV

4.3.4. Qualitative overview of the Linear Static Analysis (ULS)

Firstly, Ultimate Limit state is dealt with. In turn, bending moment and displacement, shear force and then axial force is discussed. In shear-force and axial-force discussion, the seismic analysis is also handled for the saving of the space, and there the seismic analysis dealt with is out-of-plane earthquake and the in-plane earthquake discussion is done in 4.3.6.

For Ultimate Limit State, each load case should be combined as below and the procedure of combination of those load cases is defined in EN1990-2002 (p53 and p54). The two patterns should be considered here as shown in the equation (4-15 and 4-16). Thus, there are the case where the wind load is dominant and the case where so is the snow load. Incidentally, the result is discussed for Principle body and Secondary body individually.

Combination of the load cases in Ultimate Limit State

1st case: snow is leading action

$$K_{FI} *\gamma_{Gj,sup} *G+ K_{FI} *\gamma_{Qi} *S+K_{FI} *\gamma_{Qi} *\psi_{0,1}*W \quad (4\text{-}15)$$

2nd case: wind is leading action

$$K_{FI} *\gamma_{Gj,sup} *G+ K_{FI} *\gamma_{Qi} *\psi_{0,2}*S+ K_{FI} *\gamma_{Qi} *W \quad (4\text{-}16)$$

(EN1990-2002 (p53 and p54))

where:

K_{FI}=1.1 (multiplication factor for RC3)

$\gamma_{Gj,sup}$=1.35 (partial factor for gravity, unfavourable)

γ_{Qi}=1.5 (partial factor, unfavourable)

$\psi_{0,1}$=0.6 (reduction factor, wind load)

$\psi_{0,2}$=0.5 (reduction factor, snow load)

Displacement and Bending moment

Principle body

When the snow load (thus, vertical load) is dominant -thus, snow+w1, and snow+w2-, the maximum value (about 0.008m over 12m span) of the displacement is seen in the Beam 367, which positions in the middle of the long beam (12m span) in the entrance part (Figure 21). Probably this fact comes from the structural composition. That is, this part does not have the adequate vertical support underneath so it has become vulnerable to the vertical load. When it comes to the wind-load dominant case-wind1+s and wind2+s-, the maximum displacement (around0.0085m) is seen in the middle of the arch (Beam 257 and 258-span 12.1 m) and hence the max value of deflection -displacement/span- is 0.0007 (=0.0085/12.1) in static analysis. The reason of maximum displacement apparently comes from the direction of the wind-that is, it works as lateral load.

The max value of the bending moment (about 500kNm) is found in the entrance part (beam: 72 and 215) in vertical-load (snow load) dominating case. The min value (around -750kNm) is at the bottom of 14th arch (beam 352). It probably is due to the fact that this part does not have as many structural members as the other parts. In the wind-load dominant case, the max bending-moment value (around 600kNm) is

seen at the bottom of the 3rd arch (beam 356) and the min value (about -900kNm) is found at the bottom of the 13th arch (beam 351). This result looks reasonable as the lateral load works to the structure and the absolute max bending-moment value is found at the bottom.

When the value -displacement or bending moment- from individual loading (gravity, snow and wind) is compared, it turns out that the gravity is the most dominant factor to the structure among them. Thus, the value of bending moment and displacement is the largest in gravity-around 300kNm in absolute bending moment and about 0.006m in displacement. This derives from the fact that this structure is built of concrete whose density is relatively high compared to other structural material such as steel and timber.

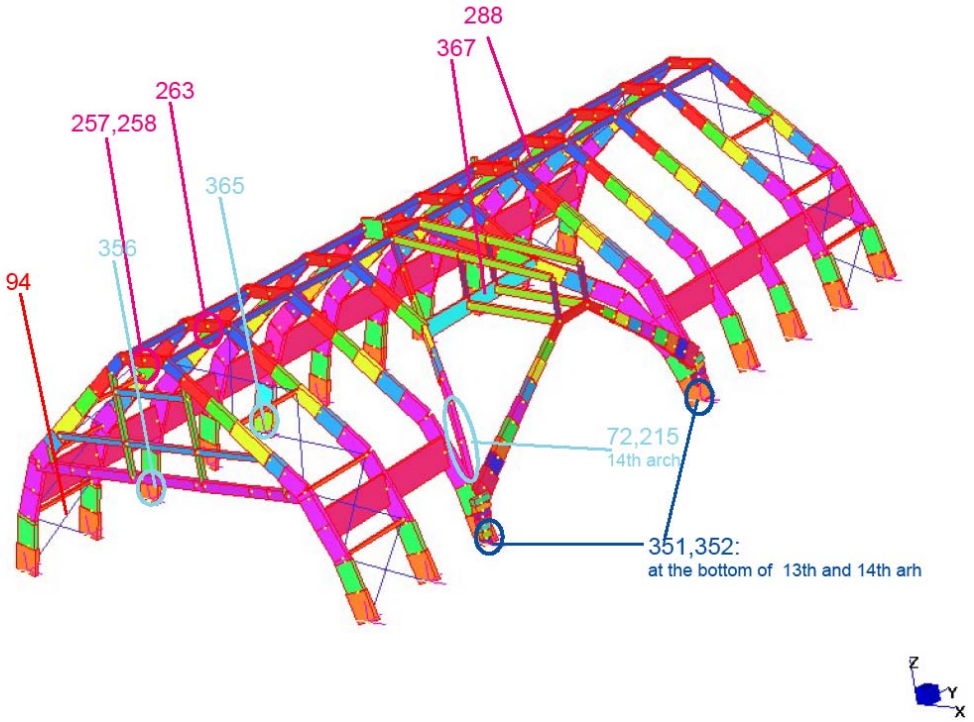

Figure 21: the mapping of the beams for max and min bending moment and those of displacement. Principle body

NB) pink-max. displacement, red-min displacement,

sky blue-max. bending moment, blue-min. bending moment

Principle	max. Dis.	Beam	min. Dis.	Beam	max BM.	Beam	min BM	Beam
gravity	0.0061	367	0	94	282.3	215	−320.3	352
snow	0.0001	367	0	94	12.8	72	−20.4	351
wind1	0.0023	263	0	94	269.6	365	−140.9	352
wind2	0.0023	288	0	94	276.6	365	−132.6	352
snow+w1	0.0081	367	0	94	500.2	215	−775.2	352
snow+w1	0.008	367	0	94	493.3	72	−761.5	352
wind1+s	0.0083	258	0	94	601.5	356	−896.8	352
wind2+s	0.0084	257	0	94	614.6	356	−873.8	352

Table 32: the list of the max and min values of bending moment and displacement, Principle body

(Displacement-m, Bending moment-kNm)
NB) snow+w1 means 1st case (snow load is leading action in the equation-4-15) and wind1+s means 2nd case in the equation 4-16.

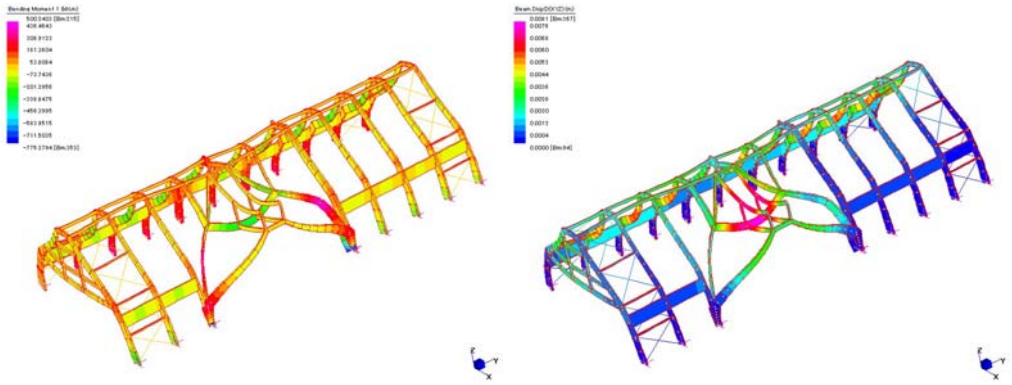

Figure 22: the combination of load, snow leading case, wind case 1 Bending moment and Displacement (right), Principle body

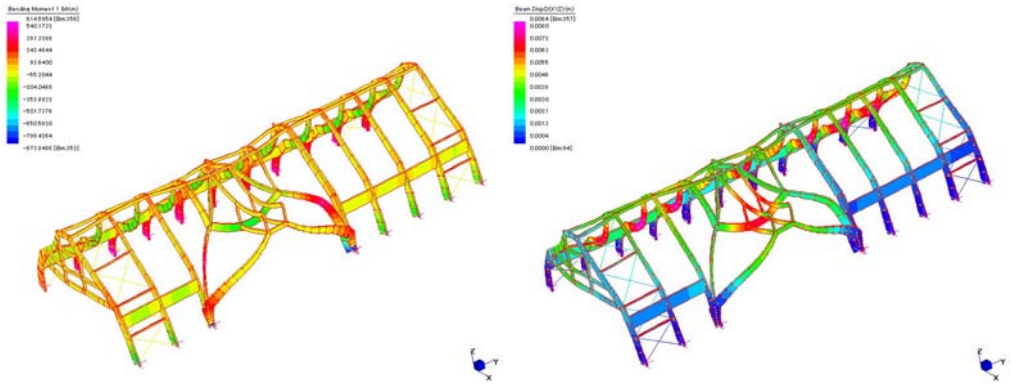

Figure 23: the combination of load, wind load leading case wind case 2 Bending Moment and Displacement (right), Principle body

Secondary body

In snow-load dominant case, the value of maximum displacement is always seen in the middle of the beam (549, 633 and 848) in beam part. The value is from 0.005 to 0.006m over the span of 15m. In wind-load leading case, the maximum displacement is found again at the middle of the arch of beam part (beam 848) or at the middle of the arch in the arch part (beam 680). Apparently, the span of the beam in the beam part, is quite long-15m and hence this part is likely to get the max displacement. On the other hand, when the lateral load-wind load- is large enough, the max displacement is found at the middle of the arch of the arch part. Given that the above discussion of Principle body, these outcomes looks reasonable enough. The max value of deflection in static analysis is found to be 0.00053 (=0.0069/13.1) at the beam 680 in wind5+s.

In snow leading case, the max values of bending moment are found at the corner of the arch (beam 159, 161 and 173), where the arch angle changes. They all are positioned in 12^{th} arch, which are next to steel brace. On the other hand, min value is found again at the middle of the beam of the beam part (beam 16 and 848). When the absolute min and max values are compared, the max value is larger (max value is about 300kNm and min value is around 200kNm). Hence it can be said that max value is more significant to the structure.
In wind dominant case, the max value is found in beam 173 and 684. They are positioned at the arch corner of the 2^{nd} and 12^{th} arch, and hence it shows the steel brace effect again. The min value is found in the middle of the beam of the beam part (beam 718 and 848) other than beam 21 which is at the bottom of the 12^{th} arch.

When the value of bending moment is compared with that of Principle body, they are relatively bigger in Principle body than in Secondary body in any case- especially wind load. The wind-load difference comes from the height of the building-15.5m high, Principle body and 10m high, Secondary body. As for the gravity, the mass of the structural is $7.2*10^5$ (kg) in Principle body and $6.6*10^5$ (kg) in Secondary body, and this difference result in the higher bending moment due to the gravity in Principle body. The values from snow load are more or less the same each other, as the applied load is similar in Principle body and Secondary body. At any rate, even in Secondary body, the gravity is the most dominant factor to the structure.

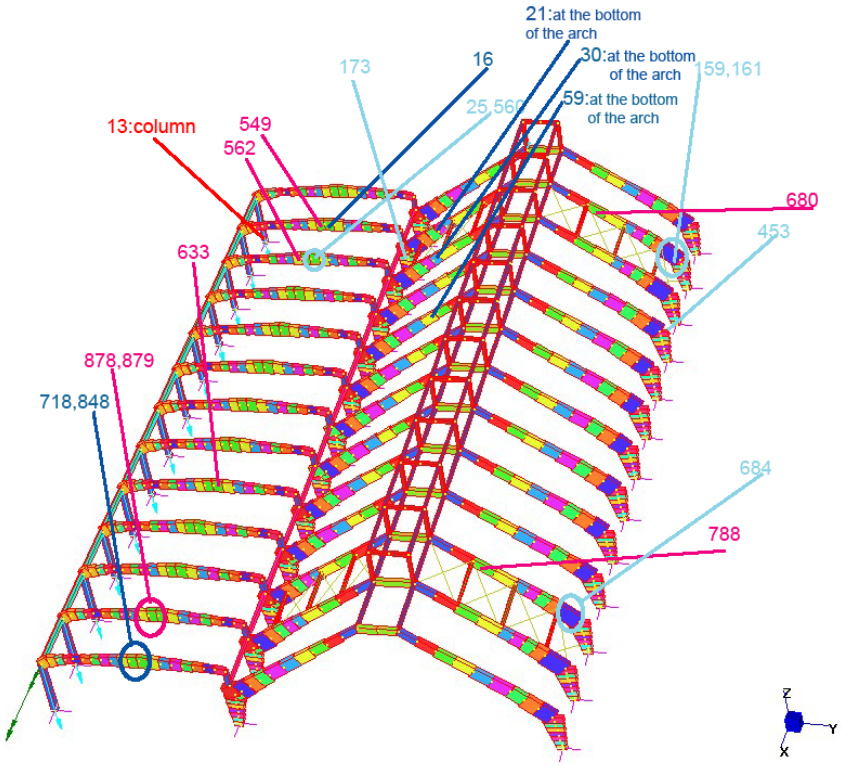

Figure 24: the mapping of the beams for max and min bending moment and those of displacement. Secondary body

Secondary	max. Dis.	Beam	min. Dis.	Beam	Max BM	Beam	min BM	Beam
gravity	0.0038	848	0	13	169.5	173	−129.1	718
snow	0.0007	879	0	13	19.3	159	−20.3	878
wind3	0.0019	562	0	13	56.3	560	−65.3	59
wind4	0.0021	562	0	13	61.2	25	−65.4	59
wind5	0.0032	788	0	13	116	453	−152.4	30
wind6	0.0025	788	0	13	95.6	453	−74.4	30
snow+w3	0.0053	848	0	13	278	173	−180.6	848
snow+w4	0.0052	848	0	13	276.7	173	−177.8	848
snow+w5	0.0062	549	0	13	297	161	−210.2	16
snow+w6	0.0061	633	0	13	292.7	159	−206.3	16
wind3+s	0.0044	848	0	13	261.2	173	−154.2	848
wind4+s	0.0043	848	0	13	258.7	173	−149.4	848
wind5+s	0.0069	680	0	13	302.1	684	−−196.7	21
wind6+s	0.0058	680	0	13	294.2	684	−184.8	718

Table 33: the list of the max and min values of bending moment and displacement, Secondary body

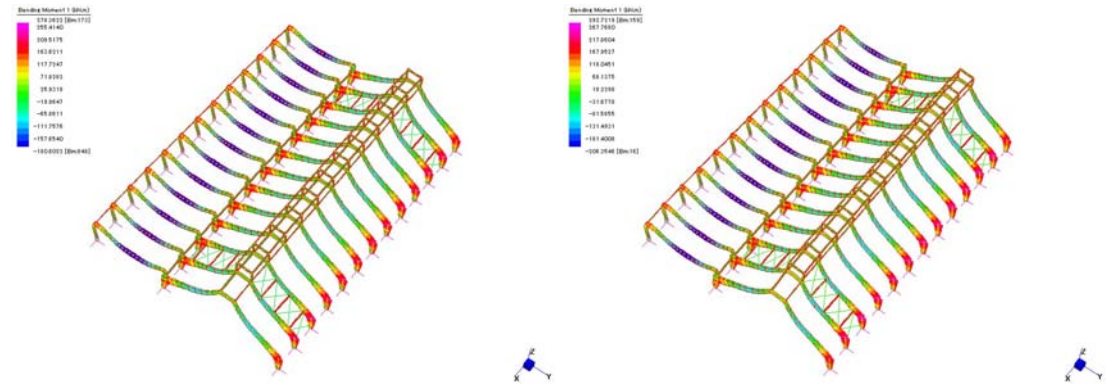

Figure 25: the combination of load, snow load leading case wind case 3, 6, Bending Moment, Secondary body

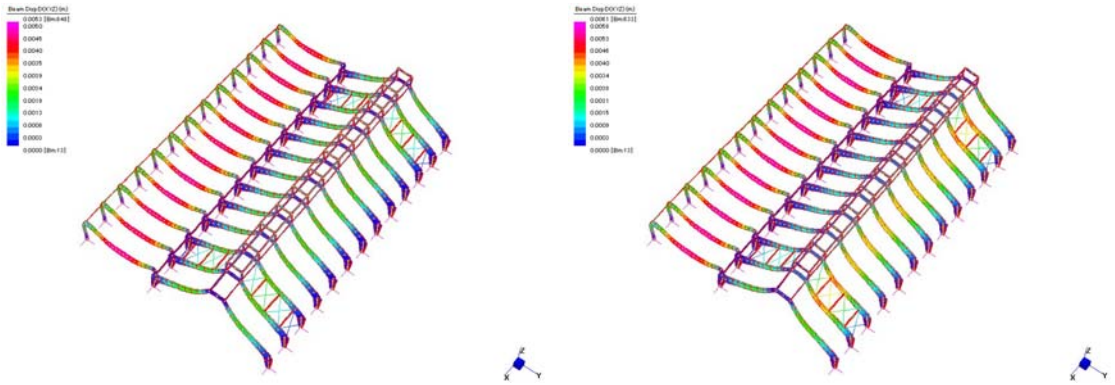

Figure 26: the combination of load, snow load leading case wind case 3,6, Displacement, Secondary body

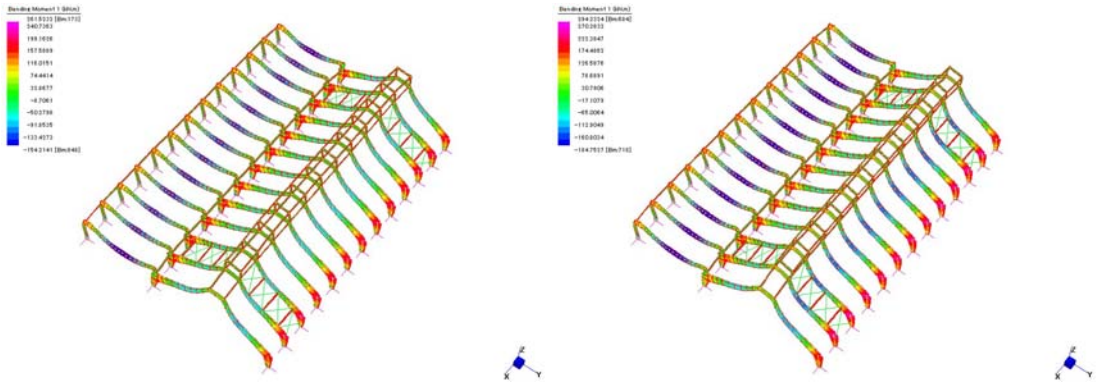

Figure 27: the combination of load, wind load leading case, wind case 3,6, Bending Moment, Secondary body

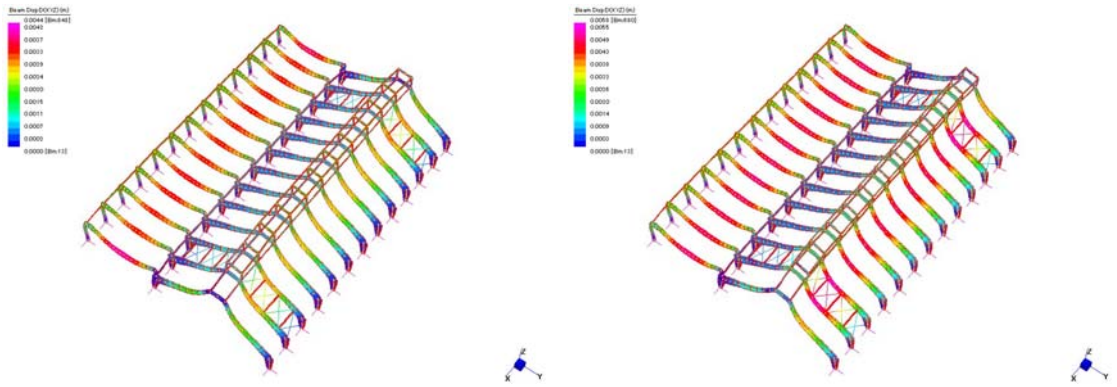

Figure 28: the combination of load, wind load leading case, wind case 3, 6, Displacement, Secondary body

Shear force

For the saving of the space, also the result of the response spectral analysis (out-of-plane earthquake) is put down and discussed here.

Static analysis

As for Principle body, the max value is found at the middle of the 14th arch (beam71) in any combination of load case. Then the min value is always in the 15th arch (beam 407). As these arches go through even higher bending moment including max and min bending-moment values compared to other arches, the shear force is also likely to become larger.

In Secondary body, the max value is seen at the arch corner in 3rd arch and the min value is found at the corner of the arch in 12th arch. So again, the steel-brace effect is confirmed here.

Seismic analysis

In Principle body, the max value is found in the middle of the 14th arch and the reason should be the same as above- thus, due to the lack of sufficient vertical support member. The min value in SLV+ is found at the top of 1st arch, and presumably this is due to the supporting members attached to the 1st arch (Figure 29), which are very flexible as they do not have a lot of supports in any direction. At any rate, even in SLV+ case, absolute min and max value is confirmed in 13th, 14th and 15th arch (Figure 29).

When it comes to Secondary body, the max and min values are a bit scattered. However, when the force distribution (Figure 32) is referred, distribution of the values is pretty much the similar tendency to static analysis is confirmed. Thus, the higher absolute values are found in around the bottom part of 2nd, 3rd, 11th and 12th arch.

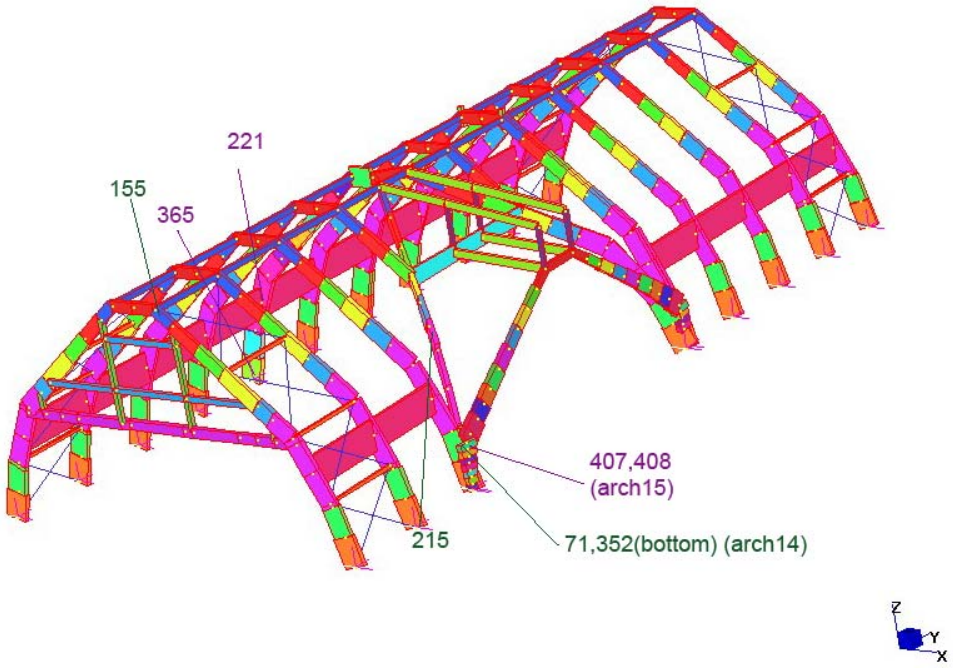

Figure 29: the mapping of the beams for max and min shear force. Principle body
purple-the value from Static Analysis green-those from Dynamic analysis

SH	max	Bm no	min	Bm no
gravity	109	71	−94.3	407
snow	5.4	352	−3.4	408
wind1	37	221	−44.9	365
wind2	37.9	221	−46.2	365
snow+w1	213.4	71	−147.7	407
snow+w2	210.2	71	−147.7	407
wind1+s	225.5	71	−139.6	407
wind2+s	221.5	71	−139.8	407
SLV+	327.4	71	−68.9	155
SLV−	93.2	215	−146.2	407

Table 34: max and min shear-force value, Principle body

Figure 30: shear-force distribution, snow+w1 and SLV+(right), Principle body

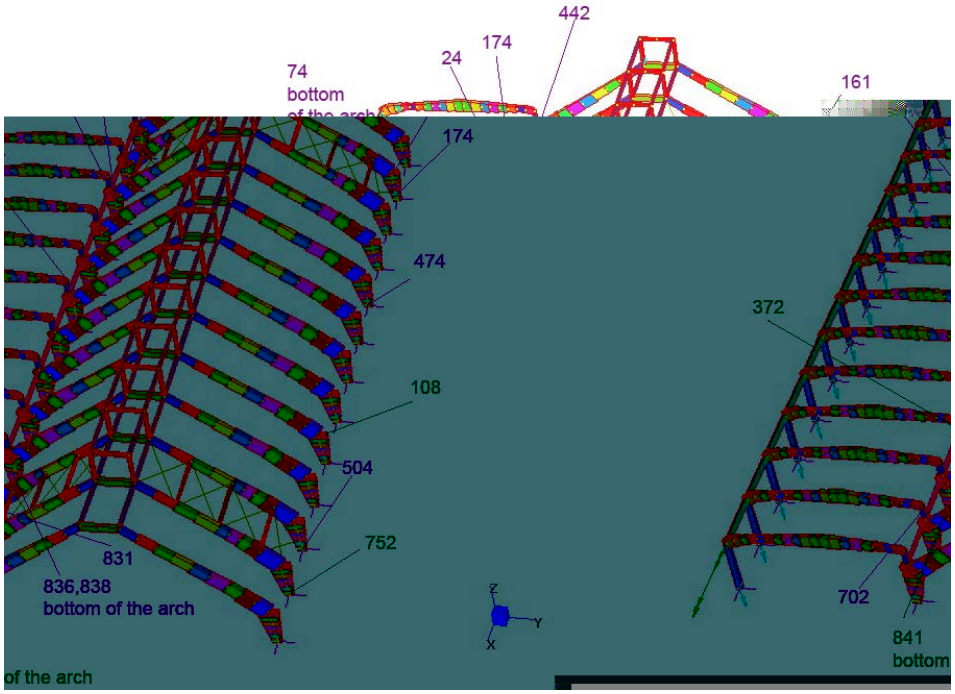

Figure 31: the mapping of the beams for max and min shear force, Secondary body

NB) purple-values for Linear Static Analysis, green-values for Response Spectral Analysis

SH	max	Bm no	min	Bm no
gravity	66.4	161	−54.3	174
snow	8.1	158	−7.7	702
wind3	26.7	24	−21.4	74
wind4	27.6	24	−22.4	474
wind5	26.8	838	−31	452
wind6	23.9	836	−26.1	504
snow+w3	103.5	831	−107.4	442
snow+w4	102.9	831	−106.7	442
snow+w5	111.3	831	−114.2	442
snow+w6	108.4	831	−111.2	442
wind3+s	112.4	831	−117.3	442
wind4+s	111.5	831	−116.2	442
wind5+s	125.4	831	−128.6	442
wind6+s	120.6	831	−123.5	442
SLV+	284	752	−54.3	372
SLV−	64.5	108	−281.8	841

Table 35: max and min shear-force value, Secondary body

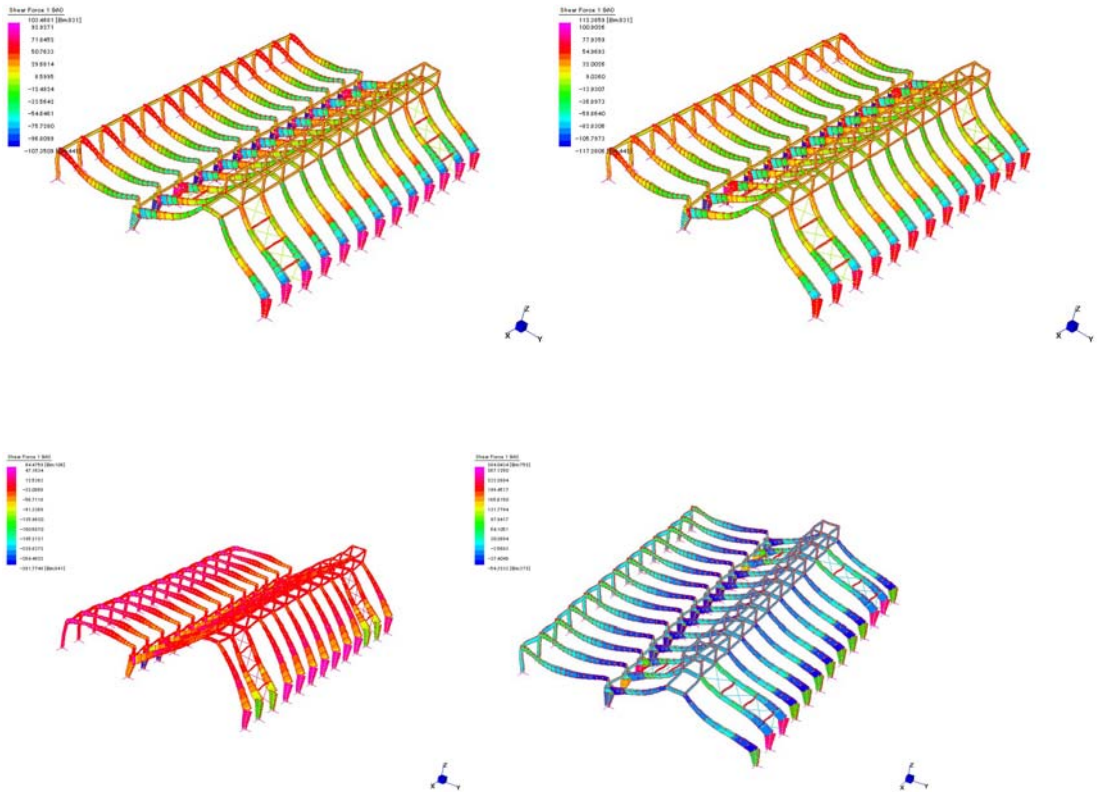

Figure 32: shear-force distribution examples, snow+w3, wind3+s, SLV+ and SLV- (from the top clockwise), Secondary body

Axial force

Here, again static and seismic analysis is discussed together.

Static analysis

In Principle body, the max tensile value is found in beam 174 (Figure 33). This is presumably due to this part does not have many vertical structural support members. The max compressive value is seen at the bottom of the 5th arch (beam 365) in any combination of the load case.

Probably it comes from the size of the cross-section -500(mm)*1600(mm)- which is bigger than the same part of the other arches -300(mm)*1600(mm). Hence, this part is heavier than others. This guess is supported by the fact that beam 365 undergoes max compressive axial force when only the gravity works in Principle body. Moreover, again its absolute value (531kN) is far bigger than that in other load cases-14.8kN in snow and around 20kN in wind, and therefore it can be said the gravity is dominating factor also in case of axial force.

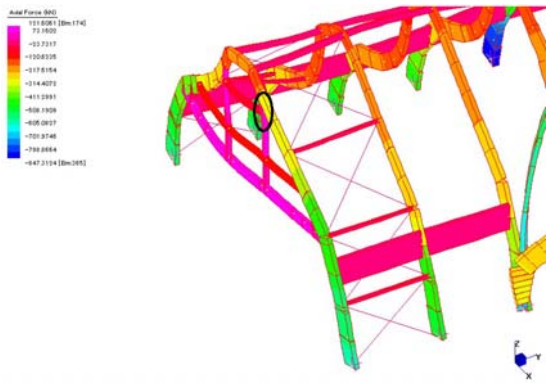

Figure 33: the position of the beam 174

As for Secondary body, the max tensile value is found at the corner of the 12th arch (beam 138) in any load-case combination and the max compressive value is located mostly at the bottom of the 12th arch (beam 21) or at the bottom of the 13th arch in case of wind3+s and wind4+s. However, in any combination of load case, when the distribution of axial force is seen, the similar value distributes and presumably it is not easy to point out the difference.

Seismic analysis

In Principle body, the maximum tensile value is found at the top of the 13th arch (beam 331) or bean 81 (Figure 34). The maximum compressive value is found at the bottom of 4th and 5th arch (beam 341 and 365).

In Secondary body, the max tensile value is found at the bottom of 3rd arch (beam 753) and 11th arch (beam 510) and max compressive value is positioned at the middle of 7th arch (beam 74) and at the bottom of 2nd arch (708). This outcome looks a bit scattered but it turns out that higher tensile and compressive value is focused on in 2nd, 3rd, 11th and 12th arch which are next to the steel-braces when the force distribution is seen (Figure 38).

The results of seismic analysis are somehow similar to that of static analysis in terms of force distribution and the position of max and min value in both bodies. Moreover in any case, the gravity is dominant. Hence, also in case of axial force, in particular, gravity can be said to be dominant factor.

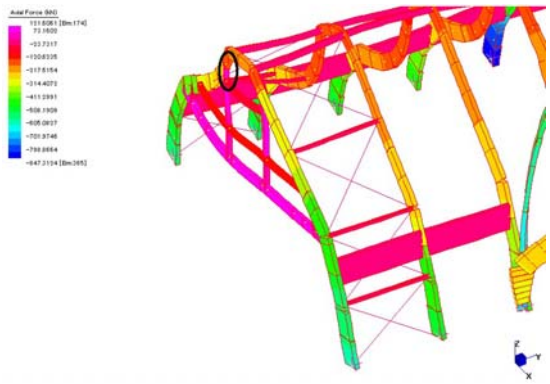

Figure 34: the location of beam81

Principle body

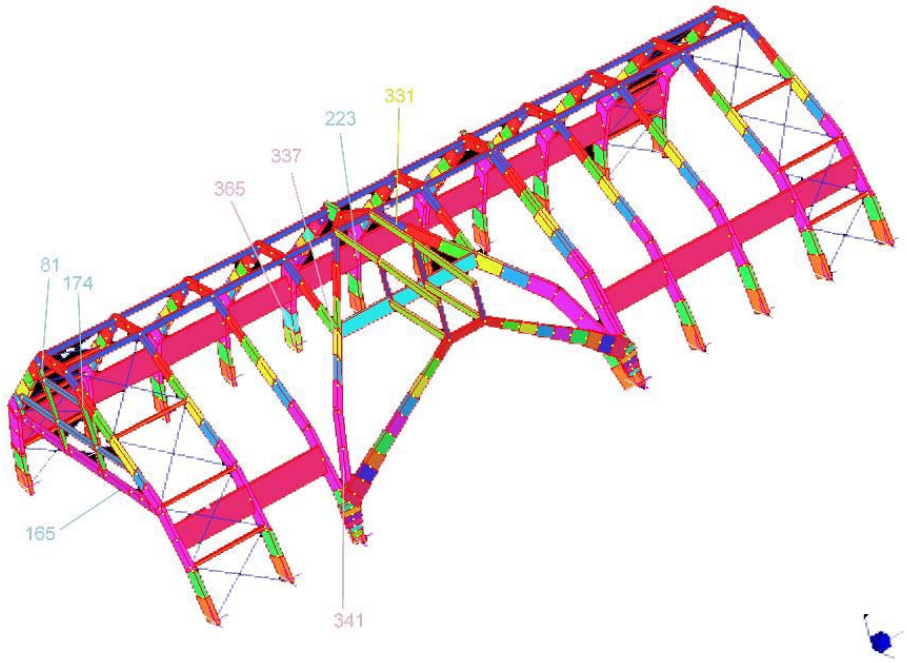

Figure 35: the mapping of the beams for max and min axial force. Principle body

NB) Blue-maximum value (in tension), purple-minimum value, yellow (and purple)-values from Spectral Response Analysis

AX	max	Bm no	min	Bm no
gravity	73.2	81	−531	365
snow	1.6	165	−14.8	341
wind1	12.1	223	−23	337
wind2	14	223	−19.2	337
snow+w1	116.2	174	−852.1	365
snow+w2	116.5	174	−848.9	365
wind1+s	121.3	174	−852.7	365
wind2+s	121.6	174	−847.3	365
SLV+	136.3	331	−562	365
SLV−	74.8	81	−711	341

Table 36: maximum and minimum axial force value and position, Principle body

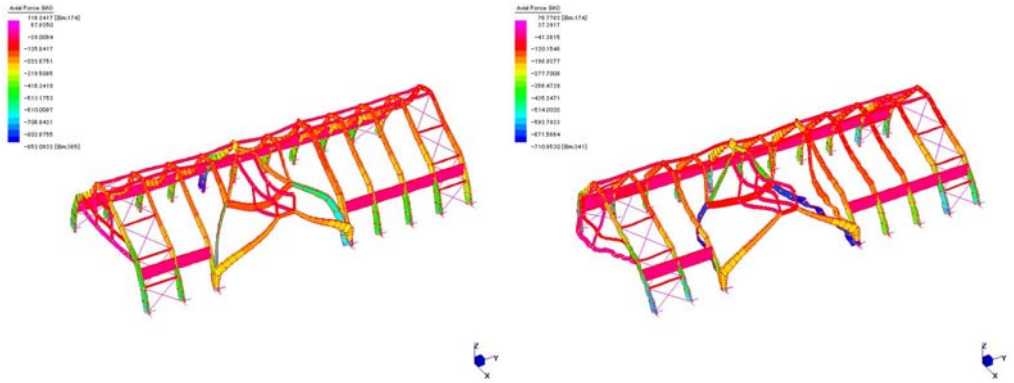

Figure 36: axial force distribution examples, snow+w1 and SLV-(right), Principle body

Secondary body

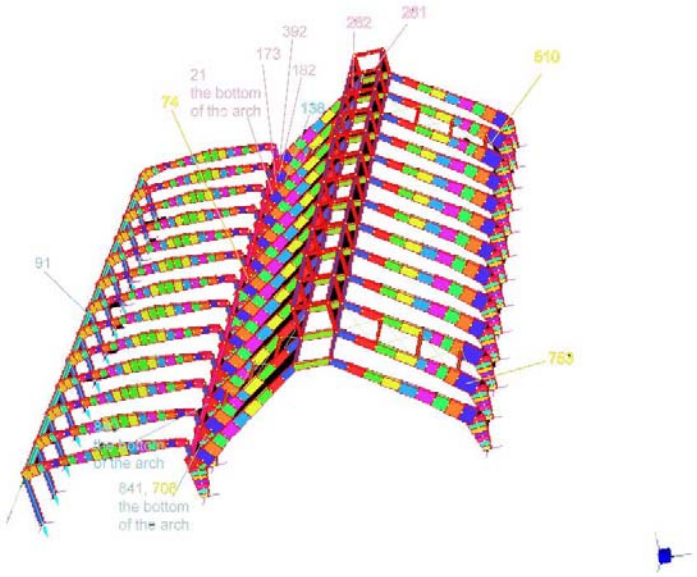

Figure 37: the mapping of the beams for max and min axial force. Secondary body

NB) Blue-maximum value (in tension), red-minimum value , yellow-values from Seismic analysis

AX	max	Bm no	min	Bm no
gravity	2.5	138	−255	21
snow	0.24	138	−24.4	21
wind3	36.6	841	−2	262
wind4	39.1	840	−0.8	261
wind5	12.4	91	−17.3	173
wind6	14	91	−18.5	182
snow+w3	3.9	138	−384.7	21
snow+w4	3.8	138	−382	21
snow+w5	3.7	138	−417	21
snow+w6	4	138	−425.4	21
wind3+s	3.5	138	−343.2	392
wind4+s	3.4	138	−340.9	392
wind5+s	3.3	138	−395.5	21
wind6+s	3.7	138	−409.5	21
SLV+	181.8	753	−272.6	74
SLV−	107.1	510	−558.2	708

Table 37: maximum and minimum axial-force value and position, Secondary body

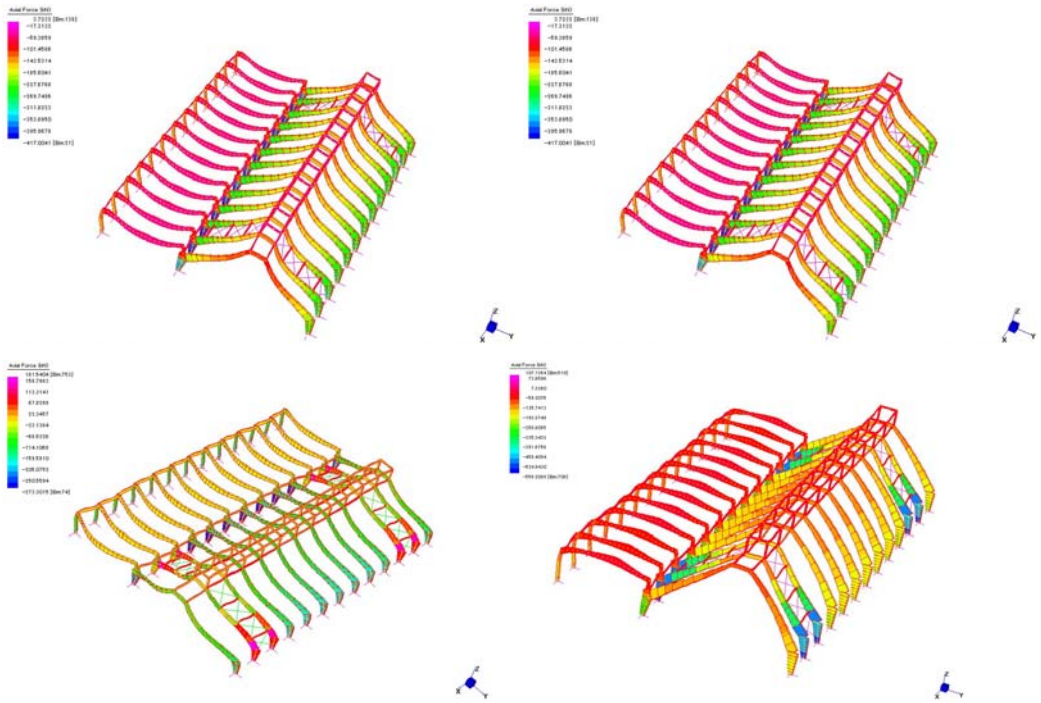

Figure 38: force distribution examples, snow+wind5, wind4+snow , SLV- and SLV+(from the left top, clockwise), Secondary body

4.3.5. Qualitative overview of the Spectral Response Analysis (ULS) (out-of-plane earthquake)

In case of seismic action, the combination of load becomes as below. According to EN1990-2002 (p54), wind load and snow load can be ignored as it is not extremely windy or snowy in Marghera. According to EN 1998-1 (p64), the combination of the horizontal components of the seismic action should be computed as below (4-17 and 4-18).

The combination of the load case in seismic action

$$G+A_{ed} \qquad (4\text{-}17)$$

$$A_{ed}=\gamma_I * A_{ek} \qquad (4\text{-}18)$$

(EN1990-2002 (p54))

Where:

γ_1 is the importance factor

$A_{Ed\ is}$ the design value of seismic action

A_{Ek} is the characteristic value of seismic action

γ_I=1.2 (importance factor for building class III)

The combination of the horizontal components

$$E_{Edx}+0.3E_{Edy} \quad (4\text{-}19)$$

$$0.3E_{Edx}+E_{Edy} \quad (4\text{-}20)$$

Where:

"+" implies "to be combined with"

E_{Edx} represents the action effects due to the application of the seismic action along the chosen horizontal axis *x* of the structure;

E_{Edy} represents the action effects due to the application of the seismic action along the chosen horizontal axis *y* of the structure.

(EN1998-1 p64)

In this section, earthquake is input in Y-direction on Principle body and in X-direction on Secondary body (Figure 39). Thus, the out-of-plane earthquake is discussed in the first place, as out-of-plane earthquake is thought to be more critical to the structure. Incidentally, the case with in-plane direction earthquake is discussed individually in the later section.

As the first step of the seismic analysis, the mass participation factor has to be confirmed. According to EN1998-1 (p59), the sum of the mass participation factor should be over 90%, and this condition is fulfilled in each structure -91.1% for Principle body and 90.7% for Secondary body (both with 100 modes). In Principle body, with mode 1 -43.1%- and mode 4 -20.4%- the participation factor shows high value. And so do mode1 -48.4%- and mode2 -19.2%- for the secondary body. When the result of the modal analysis is referred to, this outcome seems quite reasonable, as those modes show the global behaviour as mentioned above.

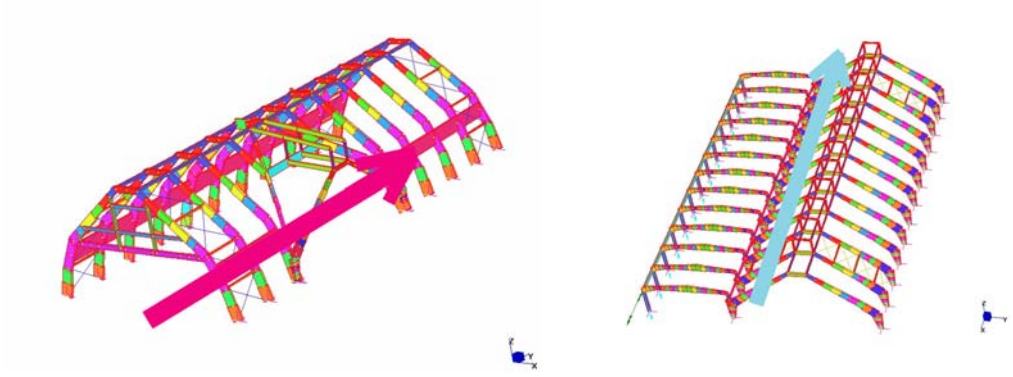

Figure 39: out-of-plane earthquake, Principle body and Secondary body (below)

Mode	Spectral Value	Excitation	Amplitude	Participation (%)
1	1.28E+00	5.73E+02	3.95E+00	43.083
2	1.35E+00	1.74E+01	9.91E-02	0.04
3	1.35E+00	7.80E+01	4.08E-01	0.799
4	1.35E+00	3.94E+02	1.51E+00	20.408
5	1.35E+00	1.03E+02	2.93E-01	1.382
6	1.35E+00	1.53E+01	4.26E-02	0.031
7	1.35E+00	3.64E+01	8.54E-02	0.174
8	1.35E+00	7.07E+00	1.60E-02	0.007
9	1.35E+00	6.94E+01	1.54E-01	0.633
10	1.35E+00	2.41E+02	4.20E-01	7.659

Mode	Spectral Value	Excitation	Amplitude	Participation (%)
1	2.94E+00	5.73E+02	9.08E+00	43.083
2	2.94E+00	1.74E+01	2.15E-01	0.04
3	2.94E+00	7.80E+01	8.85E-01	0.799
4	2.94E+00	3.94E+02	3.27E+00	20.408
5	2.94E+00	1.03E+02	6.35E-01	1.382
6	2.94E+00	1.53E+01	9.25E-02	0.031
7	2.94E+00	3.64E+01	1.85E-01	0.174
8	2.94E+00	7.07E+00	3.48E-02	0.007
9	2.94E+00	6.94E+01	3.34E-01	0.633
10	2.94E+00	2.41E+02	9.12E-01	7.659

Table 38: the mass participation, seismic analysis for Principle body (first 10 modes SLD) (first 10 modes SLV, below)

Mode	Spectral Value	Excitation	Amplitude	Participation (%)
1	1.20E+00	5.85E+02	4.29E+00	48.36
2	1.35E+00	3.68E+02	1.80E+00	19.197
3	1.35E+00	1.37E-01	4.98E-04	0
4	1.35E+00	3.14E-01	1.10E-03	0
5	1.35E+00	1.80E+01	6.29E-02	0.046
6	1.35E+00	1.55E+00	5.34E-03	0
7	1.35E+00	1.28E+00	4.38E-03	0
8	1.35E+00	8.18E-01	2.80E-03	0
9	1.35E+00	8.12E-01	2.75E-03	0
10	1.35E+00	8.72E-01	2.93E-03	0

Mode	Spectral Value	Excitation	Amplitude	Participation (%)
1	2.94E+00	5.85E+02	1.05E+01	48.36
2	2.94E+00	3.68E+02	3.91E+00	19.197
3	2.94E+00	1.37E-01	1.08E-03	0
4	2.94E+00	3.14E-01	2.39E-03	0
5	2.94E+00	1.80E+01	1.36E-01	0.046
6	2.94E+00	1.55E+00	1.16E-02	0
7	2.94E+00	1.28E+00	9.50E-03	0
8	2.94E+00	8.18E-01	6.07E-03	0
9	2.94E+00	8.12E-01	5.98E-03	0
10	2.94E+00	8.72E-01	6.36E-03	0

Table 39: the mass participation, Spectrum Response Analysis for Secondary body (first 10 modes SLD) (first 10 modes SLV, below)

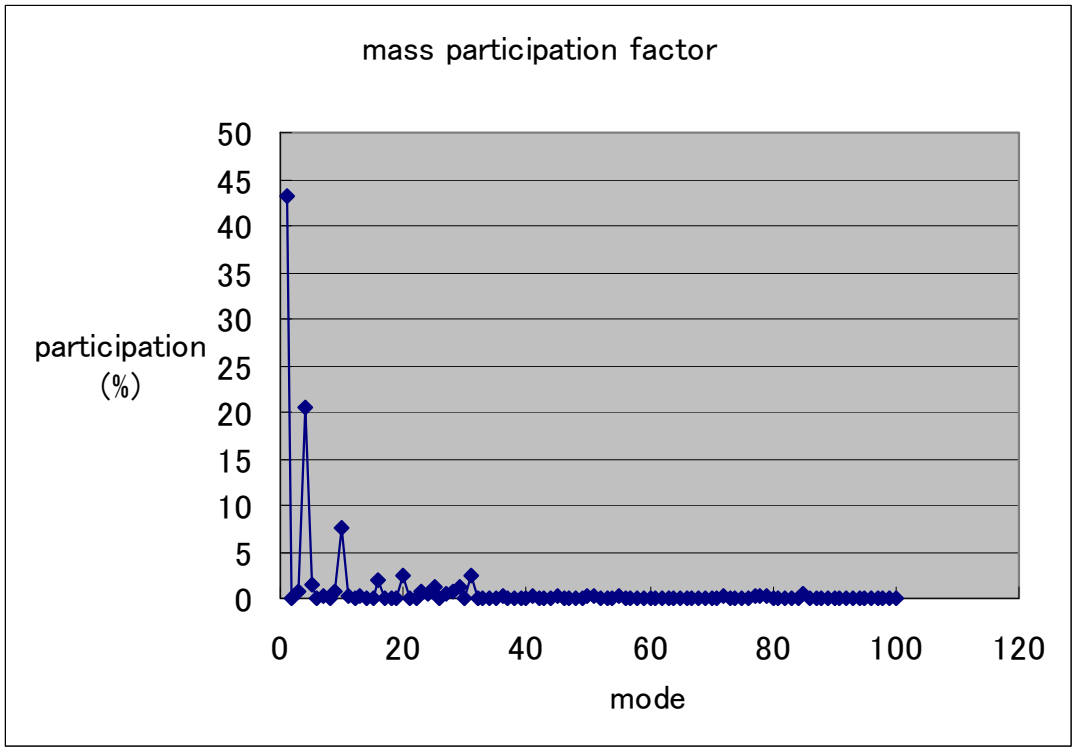

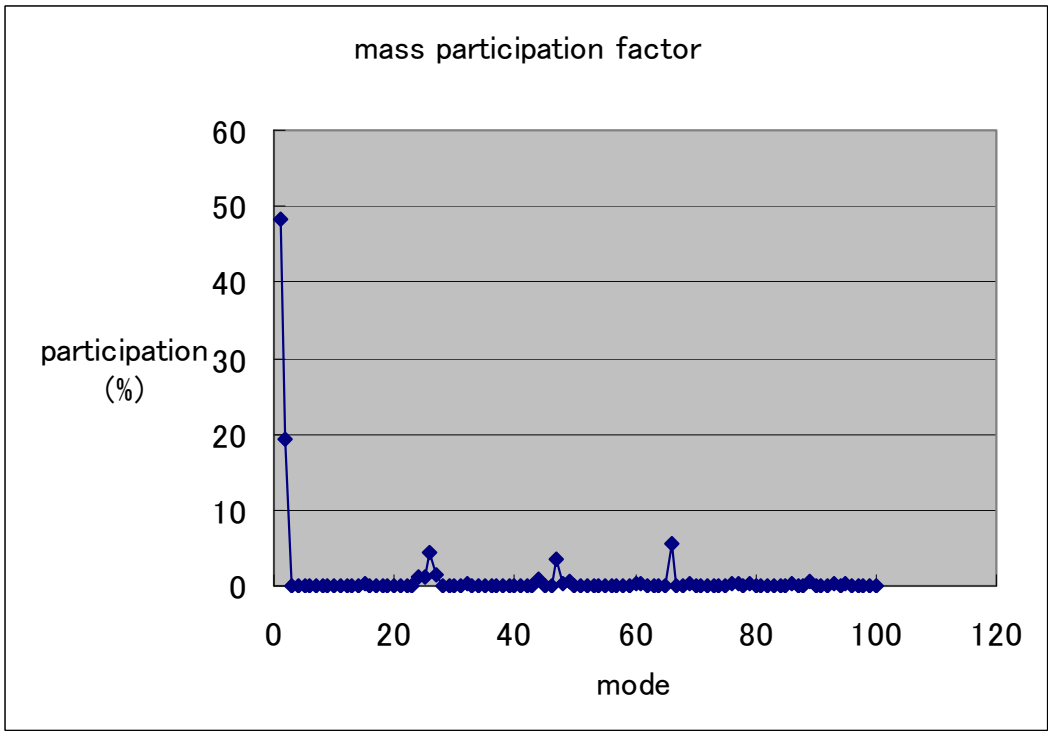

Figure 40: the participation factor in Principle body and Secondary body (below)

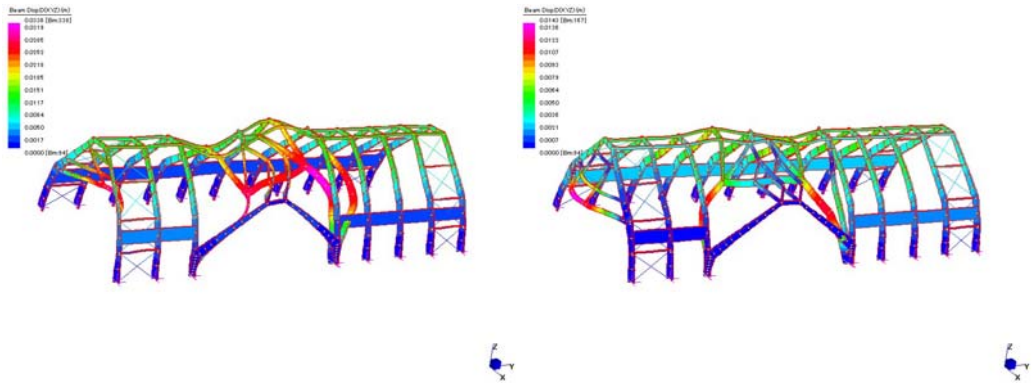

Figure 41: Mode1 Excitation, Mode4 Excitation (right), Displacement Principle body

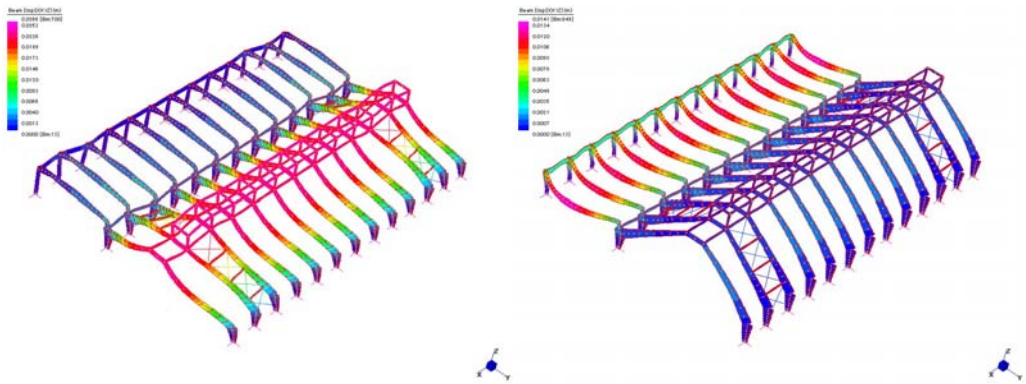

Figure 42: Mode1 Excitation, Mode2 Excitation (right), Displacement Secondary body

Displacement and Bending moment

As for the Principle body, the maximum displacement centres at the middle of 13th and 14th arch (beam 214 and 215). Given that the similar result of static analysis is also considered, it should be noted that these arches are quite fragile structurally. As mentioned above, it comes from the fact that this part does not have many vertical support members.

The maximum displacement value is 0.042 (m) over the span of 14.5 (m). That is, the value of deflection -displacement over the span- is 0.042/14.5=0.0029 in SLV+ and it is 0.044/14.5=0.003 in SLV-, and on the other hand in static analysis, as discussed above, the max deflection value is 0.0007 (=0.0085/12.1 in wind leading case). Hence, it can be said that the displacement in seismic analysis is four times as large as that of static analysis.

The max absolute bending-moment values are seen at the bottom of the 13th and 14th arch (beam 351 and 352) in Principle body. Its position (beam 351 and beam352) is the same as that of static analysis, but its value (-1643.2kNm at beam 352 in SLV-) is nearly twice as large as that of the max value in static analysis (-896.8kNm in at beam 352 in wind1+s). Moreover, in this analysis max value is found also in beam 366, and apparently this is due to the direction of the earthquake, and thus this part works as brace.

When it comes to Secondary body, max displacement is seen at the top of the arch part (beam 700), as this part is projected upwards without enough structural supporting members and hence is not so stiff. However, obviously this is not a structural member and when the distribution of the value (Figure 47 and 48) is referred, the maximum displacement is found at the middle of the arch. The value is 0.003(m) and hence, same here the max value of deflection is turned out to be 0.0023 (=0.03/13.1). This value is as about four times as large as that of static analysis-0.00053 at the beam 680 in wind5+s.

As for the bending moment max and min value is mostly found in the arches next to the steel braces. However, in the cases (SLD- and SLV-), the maximum value is found in the 6th arch -beam 92 (almost in the middle of the structure)- and in the cases (SLD+ and SLV+) the min value is found at the beam 718. These apparently come from the direction of applied force-that is out-of-plane the earthquake. Unlike Principle body, the max absolute value is not as different as that in static analysis. It is 490.2 (kNm) at the beam 832 in SLV+ and in static analysis it is 302.1 (kNm) in wind5+snow, and hence in seismic analysis it results in it is 1.5 times as big as max value in static analysis. Hence, when the values of bending moment are compared between static and seismic analysis, the difference is not as large as that of displacement in both Principle body and Secondary body.

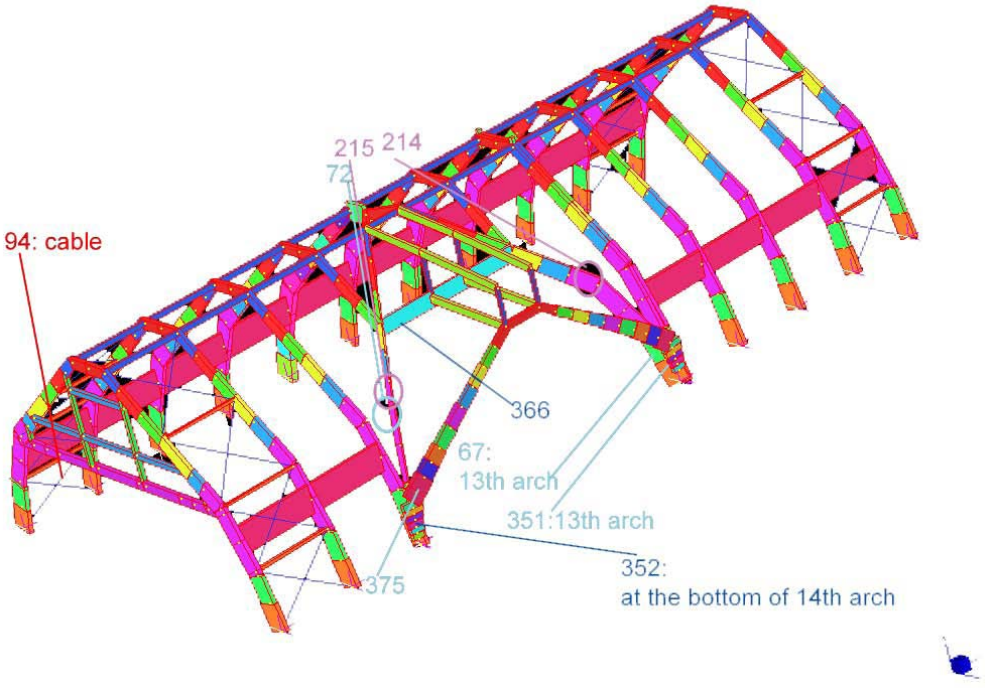

Figure 43: mapping of maximum and minimum displacement and bending moment in Spectral Response Analysis, Principle body

NB) purple-max. displacement, red-min displacement,

sky blue-max. bending moment, blue-min. bending moment

Principle	max. Dis.	Beam	min. Dis.	Beam	max BM	Beam	min BM	Beam
SLD+	0.0183	214	0	94	545.5	67	−186.6	366
SLV+	0.0420	214	0	94	1295.9	351	−164.2	366
SLD−	0.0202	215	0	94	261.2	72	−920	352
SLV−	0.044	215	0	94	206.3	375	−1643.2	352

Table 40: the list of max and min displacement and bending moment in Spectral Response Analysis, Principle body

NB). The spectral response is carried out with SRSS method. Hence, in case of superposition the positive and negative values should be considered, so four cases exist in the list. They are distinguished by + and -. e.g.) SLD+, SLD-

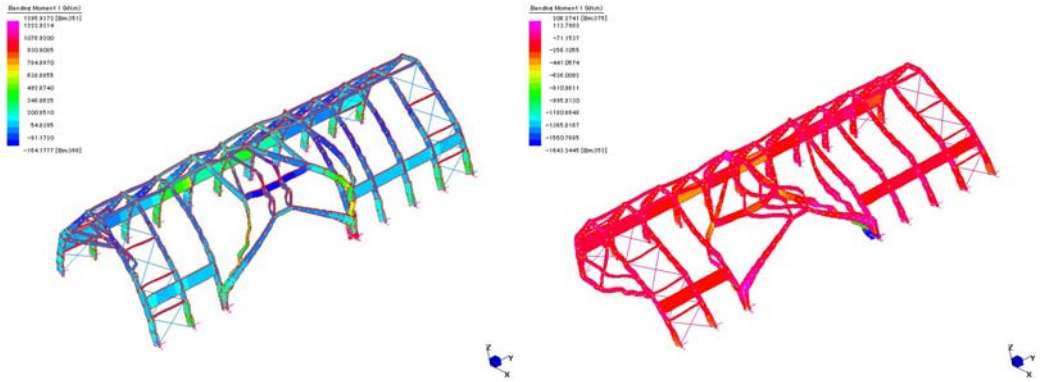

Figure 44: Superposition result SLV+ SLV- (right), Bending moment, Principle body

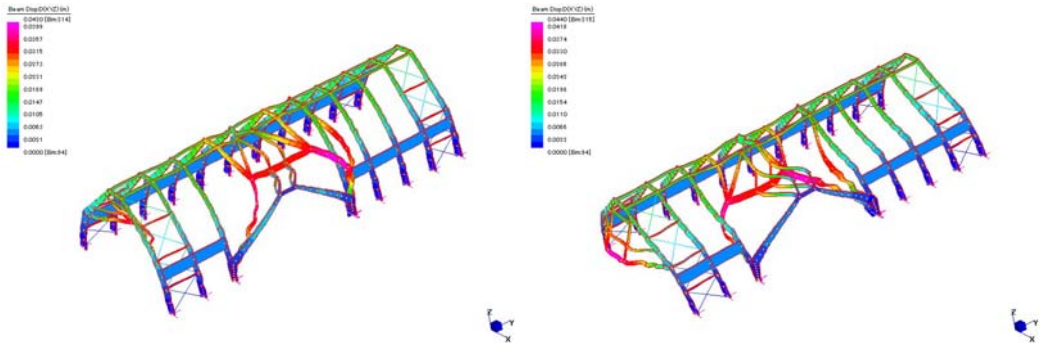

Figure 45: Superposition result SLV+, SLV- (right), Displacement Principle body

Secondary	max. Dis.	Beam	min. Dis.	Beam	max Mo..	Beam	min Mo.	Beam
SLD+	0.013	700	0	13	293.7	159	−139	718
SLV+	0.032	700	0	13	490.2	832	−137.7	718
SLD−	0.013	700	0	13	173.7	92	−189.1	452
SLV−	0.0321	700	0	13	169.6	92	−403.1	819

Table 41: the maximum and minimum displacement and bending moment in Spectral Response Analysis, Secondary body

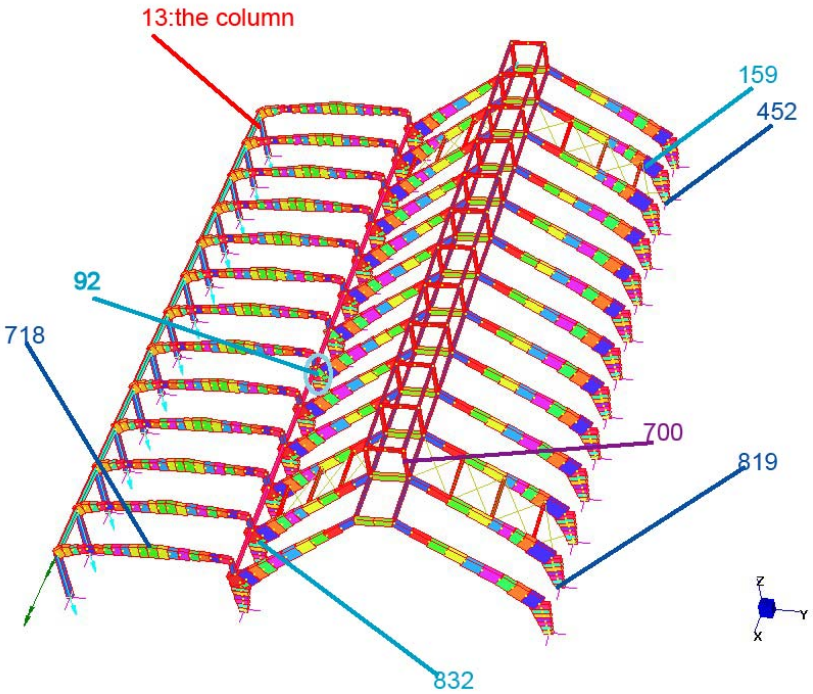

Figure 46: mapping of maximum and minimum displacement and bending moment in Spectral Response Analysis, Secondary body

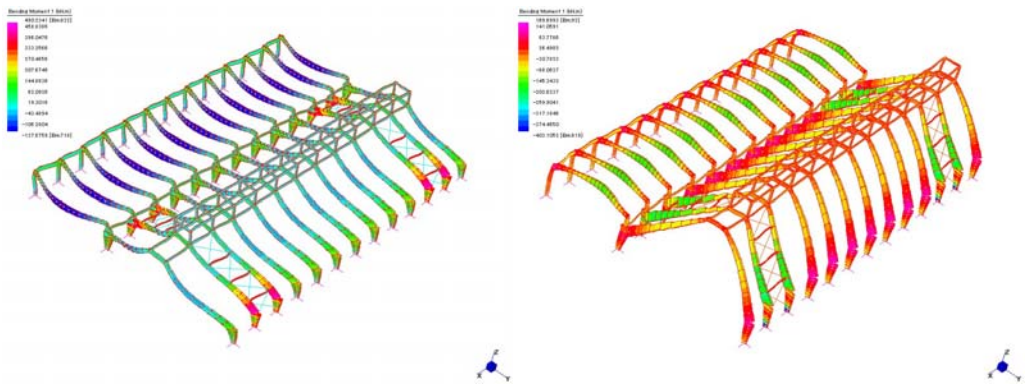

Figure 47: Superposition result SLV+ Bending Moment, SLV- (right), Bending Moment Secondary body

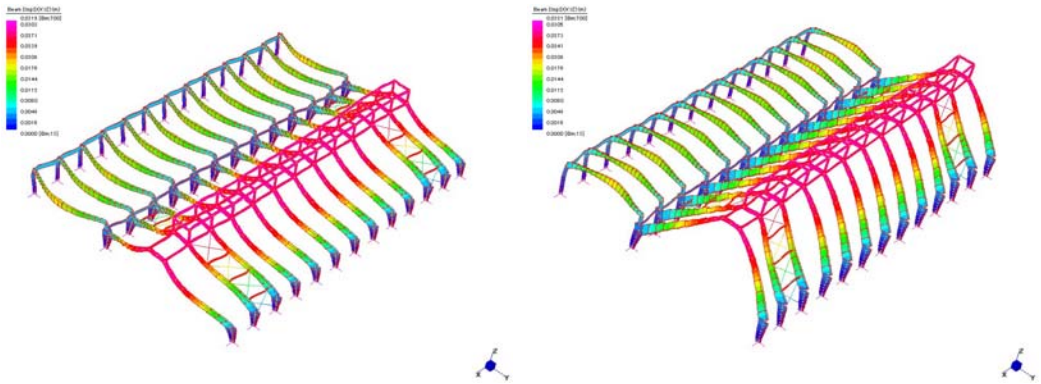

Figure 48: Superposition result SLV+, SLV- (right), Displacement Secondary body

4.3.6. Qualitative overview of the Spectral Response Analysis (ULS) (in-plane earthquake)

In this part, the in-plane earthquake is dealt with, and however so as to avoid the similar kind of discussion to that of out-of-plane earthquake, only the distinctive points from out-of-plane earthquake is pointed out.

Elastic Spectrum

The earthquake is input in-plane direction to each structure here (Figure 49). 280 modes are found for Principle body and 295 modes for Secondary body as for the modal analysis, since the requirement of the total mass participation factor. Unlike the out-of-plane earthquake, the relatively high participation factor can not be found-at most 15.1% in 5th mode in Principle body and 18.8% in 24th mode with Secondary body (Table 42 and 43). As a result 92.3% is acquired for Principle body and 93.4% for Secondary body.

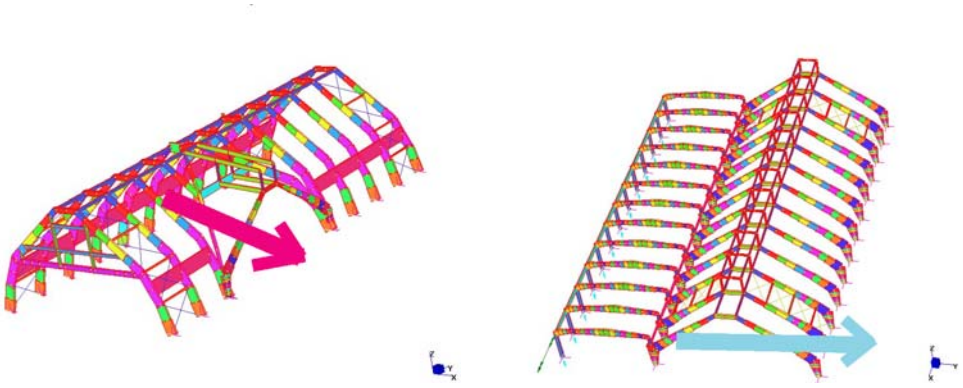

Figure 49: the direction of the applied earthquake Principle body and Secondary body (right)

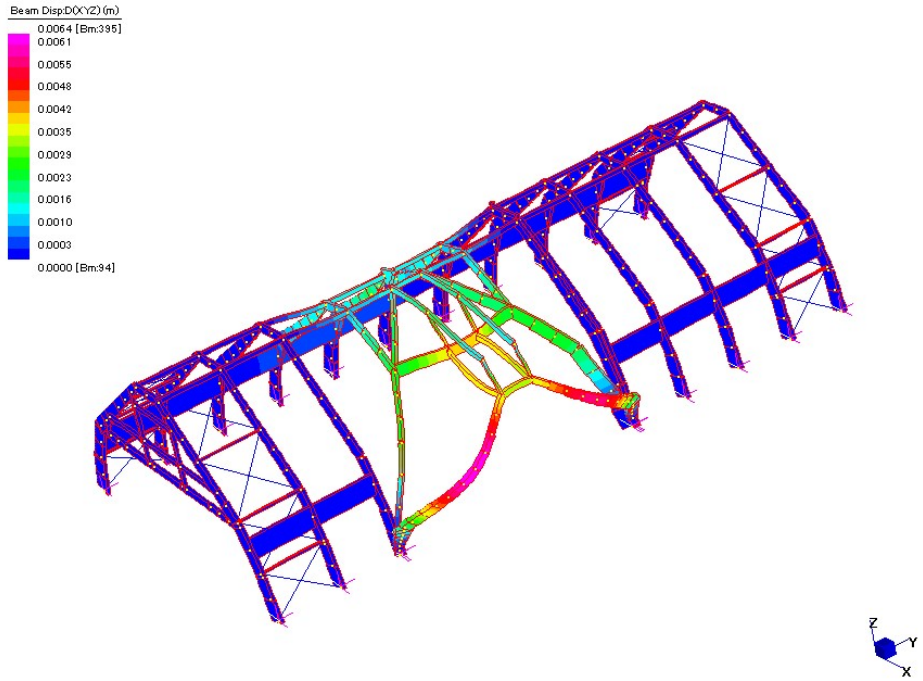

5th mode, Principle body

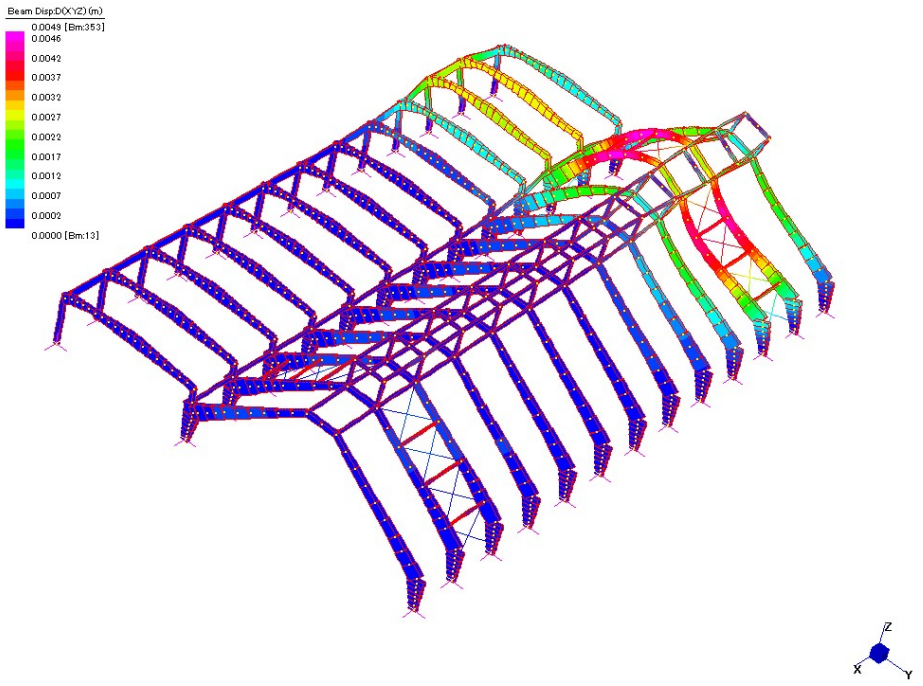

24th mode, Secondary body

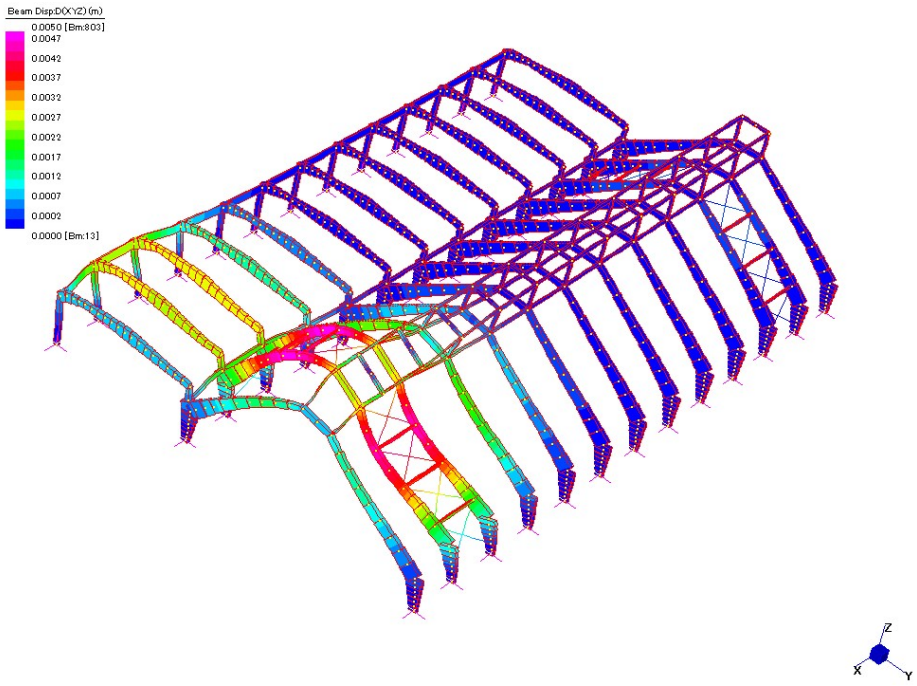

25th mode, Secondary body

Figure 50: mode Principle body and Secondary body

NF	Principle	
Mode	Eigenvalue	Frequency(Hz)
1	1.85E+02	2.17E+00
2	2.37E+02	2.45E+00
3	2.59E+02	2.56E+00
4	3.54E+02	3.00E+00
5	4.74E+02	3.47E+00
6	4.84E+02	3.50E+00
7	5.77E+02	3.82E+00
8	5.96E+02	3.88E+00
9	6.11E+02	3.93E+00
10	7.77E+02	4.44E+00
11	7.91E+02	4.48E+00
12	8.48E+02	4.63E+00
13	8.92E+02	4.75E+00
14	9.03E+02	4.78E+00
15	9.13E+02	4.81E+00

NF	Secondary	
Mode	Eigenvalue	Frequency/(Hz)
20	5.93E+02	3.88E+00
21	5.94E+02	3.88E+00
22	5.96E+02	3.89E+00
23	5.97E+02	3.89E+00
24	8.45E+02	4.63E+00
25	8.46E+02	4.63E+00
26	8.56E+02	4.66E+00
27	8.98E+02	4.77E+00
28	9.22E+02	4.83E+00
29	9.23E+02	4.84E+00
30	9.58E+02	4.93E+00
31	9.79E+02	4.98E+00
32	9.90E+02	5.01E+00
33	1.01E+03	5.06E+00
34	1.02E+03	5.10E+00
35	1.06E+03	5.18E+00

Table 42: natural frequency and eigenvalue Principle body and Secondary body (below)

Mode	Spectral Value	Excitation	Amplitude	Participation (%)
1	1.28E+00	1.70E+02	1.17E+00	3.816
2	1.35E+00	3.51E+00	2.00E-02	0.002
3	1.35E+00	2.50E+01	1.31E-01	0.082
4	1.35E+00	1.20E+02	4.59E-01	1.894
5	1.35E+00	3.39E+02	9.67E-01	15.118
6	1.35E+00	5.93E+00	1.66E-02	0.005
7	1.35E+00	1.17E+02	2.75E-01	1.801
8	1.35E+00	2.36E+01	5.35E-02	0.073
9	1.35E+00	6.80E+00	1.51E-02	0.006
10	1.35E+00	7.29E+01	1.27E-01	0.699

Mode	Spectral Value	Excitation	Amplitude	Participation (%)
20	1.35E+00	6.83E-02	1.56E-04	0
21	1.35E+00	7.11E-02	1.62E-04	0
22	1.35E+00	2.31E-01	5.25E-04	0
23	1.35E+00	1.99E-01	4.51E-04	0
24	1.35E+00	3.65E+02	5.84E-01	18.8
25	1.35E+00	3.20E+02	5.12E-01	14.47
26	1.35E+00	1.12E+02	1.77E-01	1.772
27	1.35E+00	3.37E+02	5.08E-01	16.063
28	1.35E+00	4.09E+00	6.01E-03	0.002
29	1.35E+00	8.01E+01	1.17E-01	0.908
30	1.35E+00	1.20E+01	1.70E-02	0.02

Table 43: list of mass participation factor, Principle body and Secondary body (below) in SLD

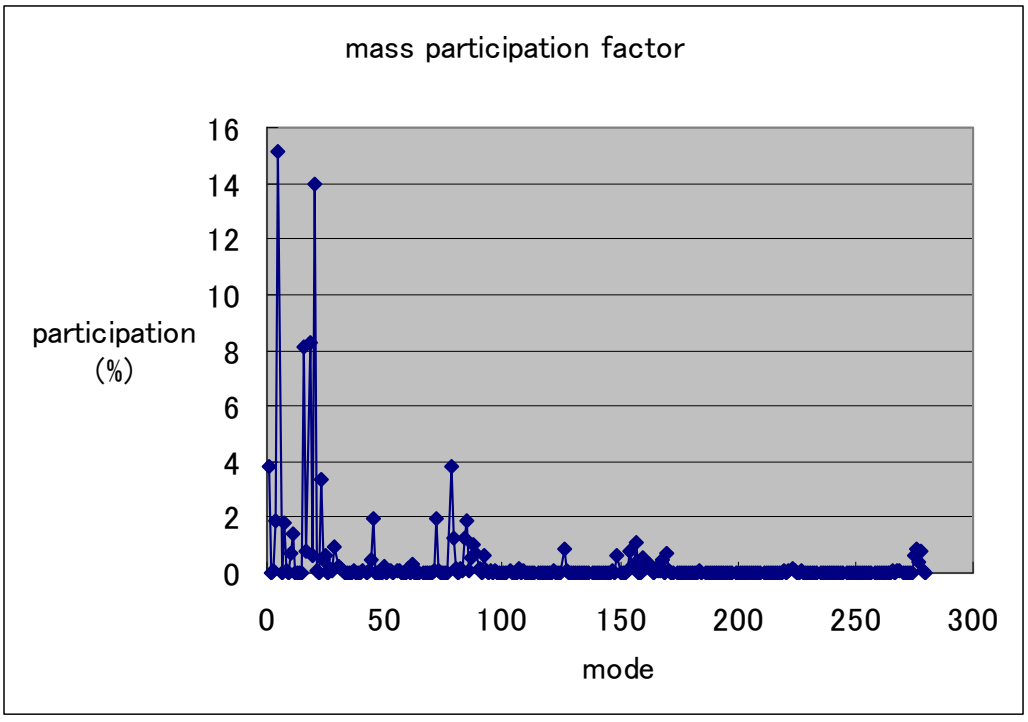

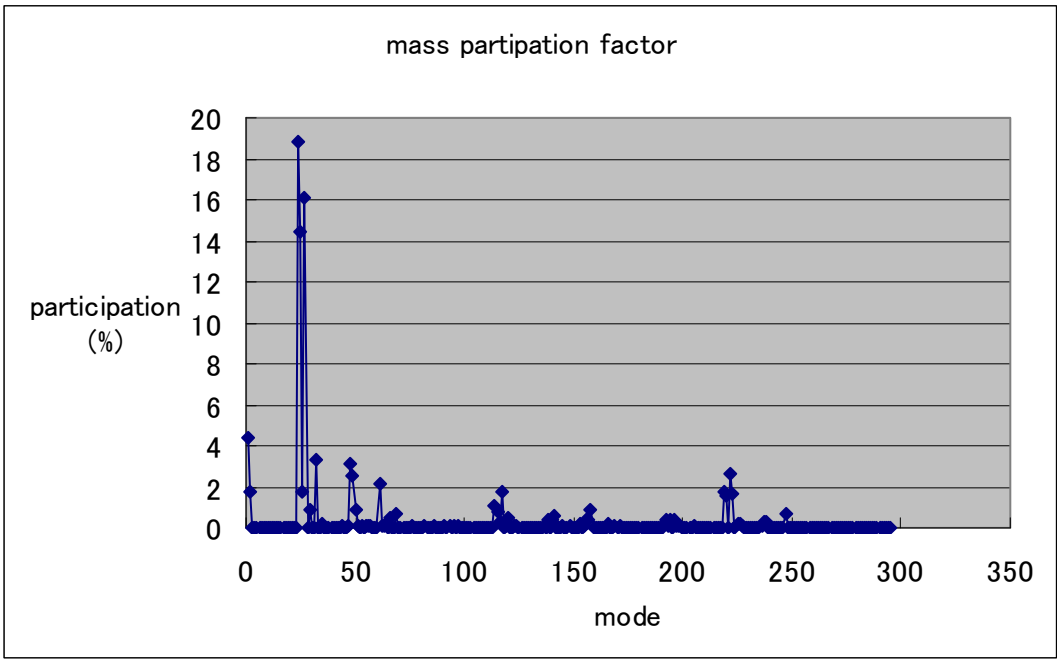

Figure 51: the mass participation factor, Principle body and Secondary body (below)

Displacement and Bending moment

In Principle body and Secondary body, the distribution of the force and the position of max and min values are similar to the static analysis in both cases bending moment and displacement and presumably it is due to the direction of the applied force. Rather, it should be noted that the absolute max value of bending moment is smaller than that in out-of-plane earthquake and is not so different from that of static analysis. The absolute max value is 976.1kNm at beam 352 in SLV- in Principle body, and on the other hand that in static analysis is 896.8kNm at beam 352 in wind1+s-incidentally in case of out-of-plane earthquake it is 1643.2kNm at beam 352. The same concept is also applied to Secondary body. The absolute max value is 302.1kNm at beam 452 in SLV-, and then that of static analysis is 302.1kNm at beam 684 in wind5+s-in case of out-of-plane earthquake it is 403.1kNm at beam 819. When it comes to displacement, in Principle body the max deflection value (displacement/span) is 0.0014 (=0.0182/13.1) at beam 395 in SLV+ and then in Secondary body it is 0.00057 (=0.0075/13.1) in SLV+. Here again like the seismic analysis of out-of-plane earthquake and static analysis, in general the values are larger in Principle body than in Secondary body in bending moment and deflection.

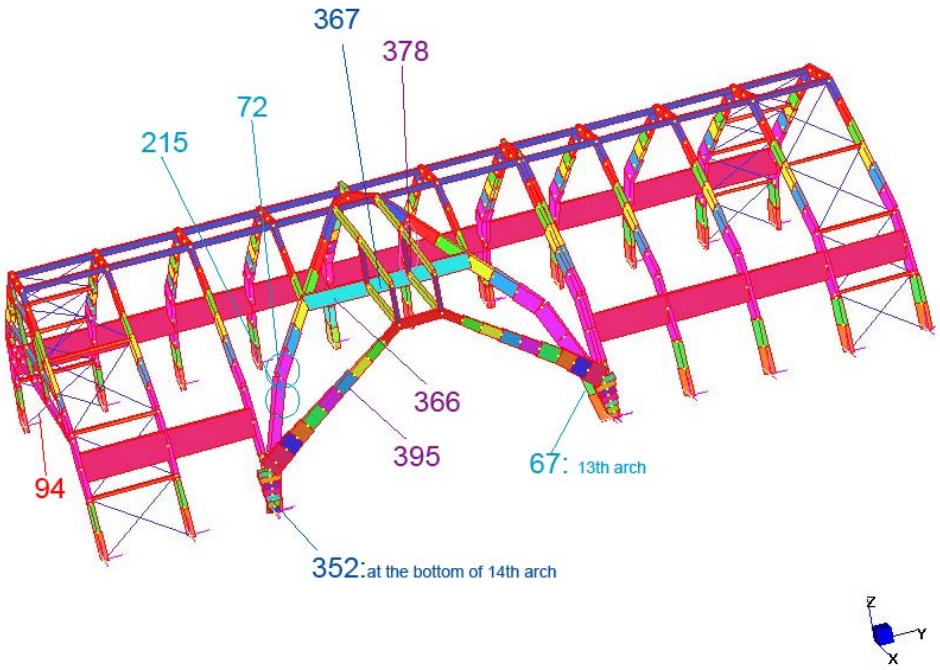

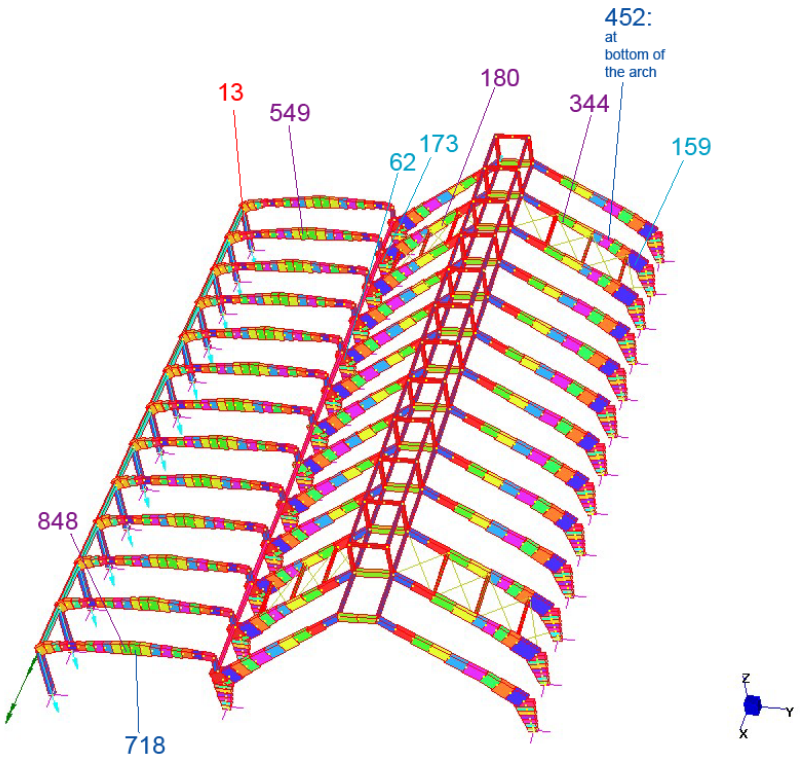

Figure 52: mapping of max and min BM and that of displacement Principle body and Secondary body (below)

Principle	max. Dis.	Beam	min. Dis.	Beam	max BM	Beam	min. BM	Beam
SLD+	0.009	395	0	94	388.3	215	−189	367
SLV+	0.0182	395	0	94	587.4	67	−169.7	367
SLD−	0.0101	366	0	94	286.6	72	−635.2	352
SLV−	0.0168	366	0	94	256.9	72	−976.1	352

Secondary	max. Dis.	Beam	min. Dis.	Beam	max BM	Beam	min. BM	Beam
SLD+	0.004	848	0	13	225	173	−137.1	718
SLV+	0.0075	180	0	13	288.8	159	−132.6	718
SLD−	0.0053	549	0	13	165.5	62	−154.2	452
SLV−	0.008	344	0	13	153.2	62	−298.5	452

Table 44: the list of max and min BM and that of displacement, in-plane earthquake, Principle body and Secondary body (below)

Principle	max. Dis.	Beam	min. Dis.	Beam	max BM	Beam	min BM	Beam
SLV+	0.0420	214	0	94	1295.9	351	−164.2	366
SLV−	0.044	215	0	94	206.3	375	−1643.2	352

Secondary	max. Dis.	Beam	min. Dis.	Beam	max Mo..	Beam	min Mo.	Beam
SLV+	0.032	700	0	13	490.2	832	−137.7	718
SLV−	0.0321	700	0	13	169.6	92	−403.1	819

Table 45 the maximum and minimum displacement and bending moment, out-of-plane earthquake, Principle body and Secondary body (below)

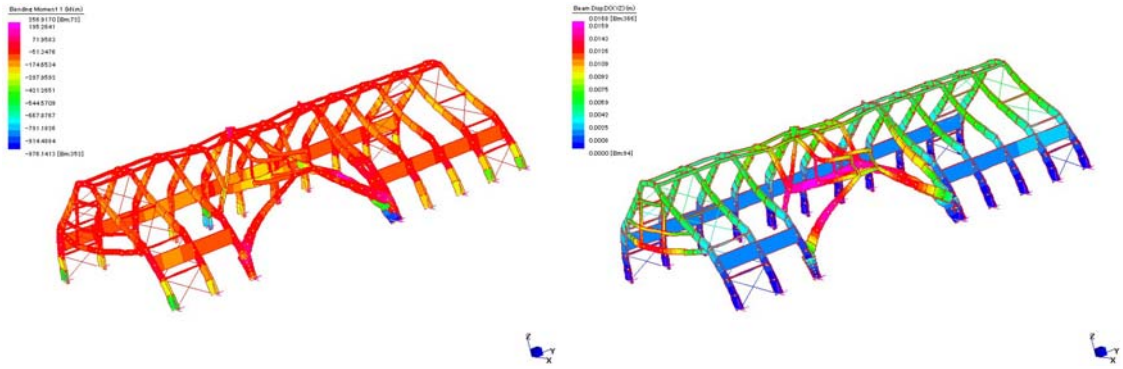

Figure 53: Superposition result SLV- Bending Moment, SLV- (right), Displacement, in-plane earthquake, Principle body

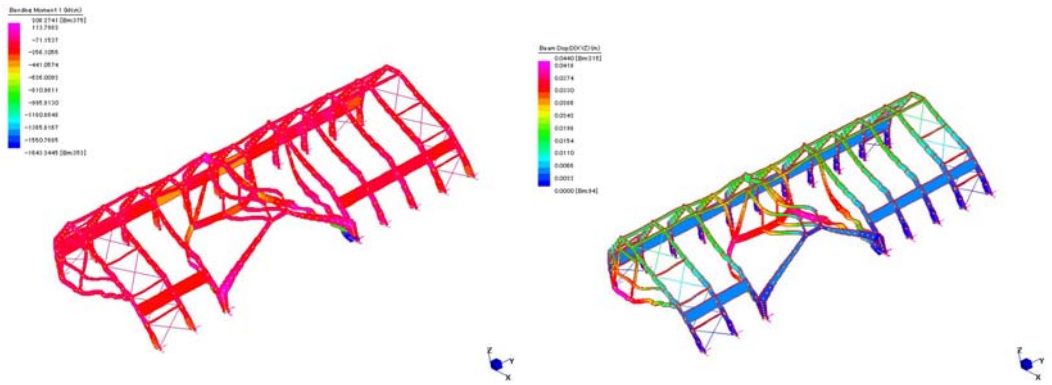

Figure 54: Superposition result SLV- Bending Moment, SLV- (right), Displacement, out-of-plane earthquake, Principle body

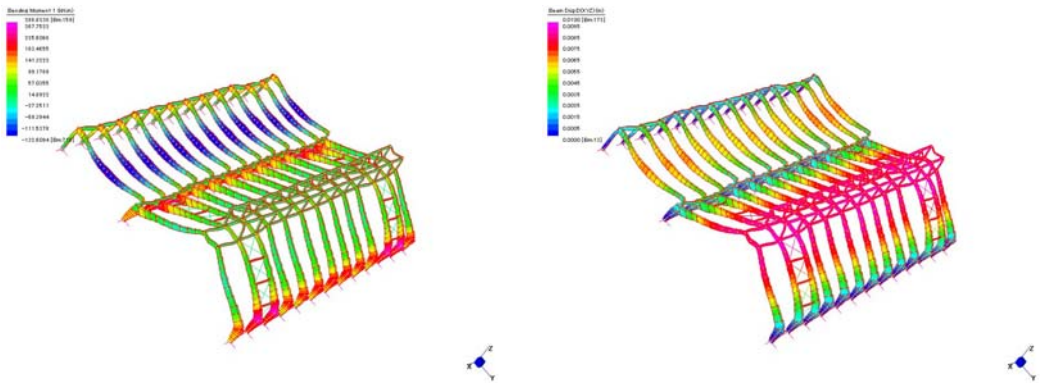

Figure 55: Superposition result SLV+ Bending Moment, SLV+ (right), Displacement in-plane earthquake, Secondary body

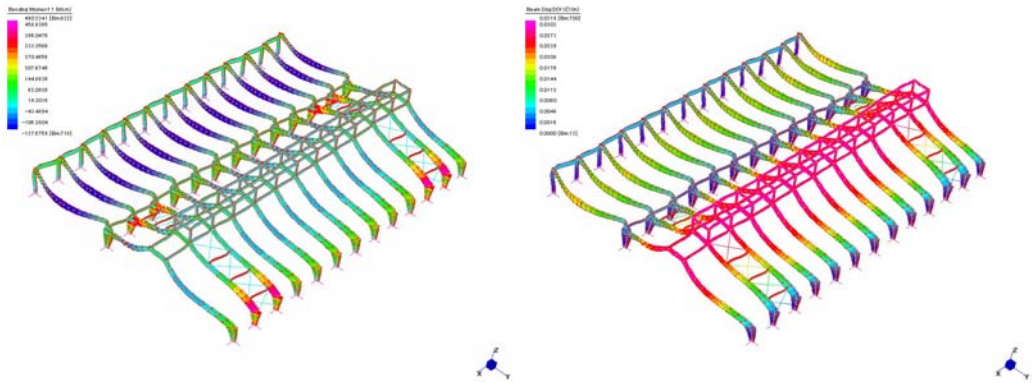

Figure 56: Superposition result SLV+ Bending Moment, SLV+ (right), Displacement, out-of-plane earthquake, Secondary body

Shear force

In Principle body, the distribution of the values is similar to that of out-of-plane earthquake. When max and min values are compared each other, almost the same values are found for max and min values. However, this similarity can not be seen in Secondary body, and hence the values and the distribution are quite different to each other and it is due to the steel brace, Thus, in case of out-of-plane earthquake, the values and distribution in these arches are different from that of other arches, but this tendency cannot be seen in case of in-plane earthquake. Thus the arches next to the steel brace are more likely to be effected by the out-of-plane earthquake than in-plane earthquake and it sounds reasonable given that the direction of the earthquake to the structure.

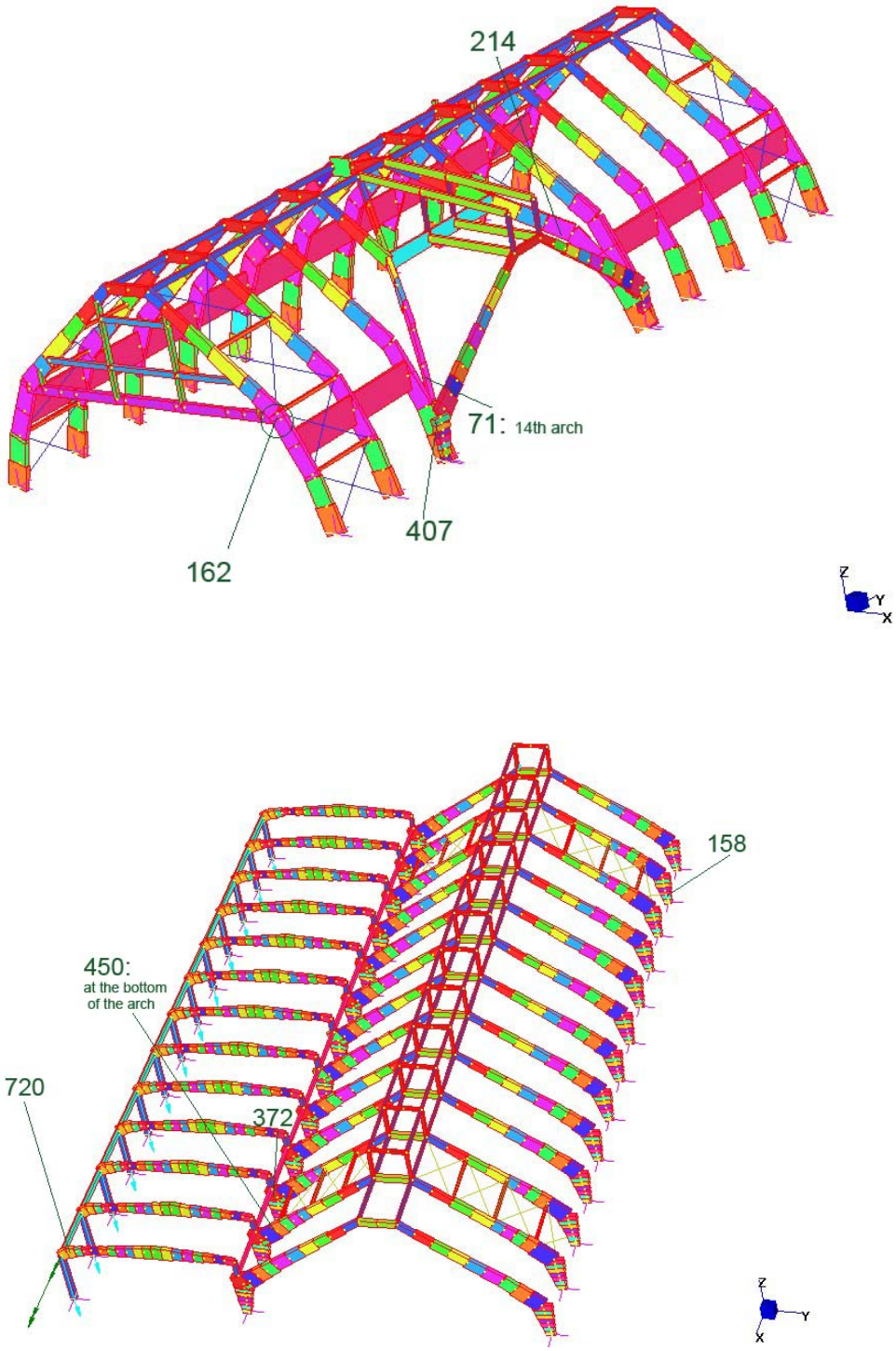

Figure 57: mapping of max and min shear force, Principle body and Secondary body (below)

Principle	max	Bm no	min	Bm no
SLV+	218.9	71	−72.3	162
SLV−	92.7	214	−144.5	407

Secondary	max	Bm no	min	Bm no
SLV+	149.5	158	−45.9	372
SLV−	51.9	720	−160.7	450

Table 46: the list of max and min shear force, in-plane earthquake, Principle body and Secondary body (below)

SH	max	Bm no	min	Bm no
SLV+	327.4	71	−68.9	155
SLV−	93.2	215	−146.2	407

SH	max	Bm no	min	Bm no
SLV+	284	752	−54.3	372
SLV−	64.5	108	−281.8	841

Table 47: max and min shear-force values, out-of-plane earthquake, Principle body and Secondary body (below)

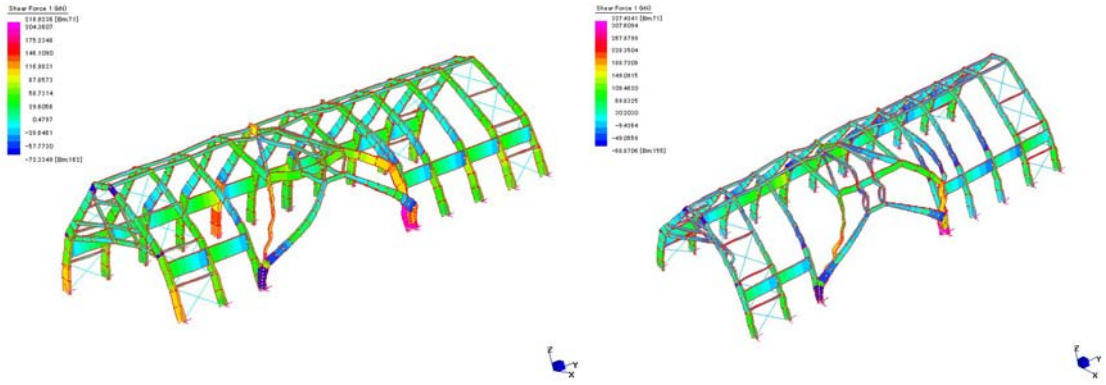

Figure 58: shear-force distribution In SLV+, in-plane earthquake, out-of-plane earthquake (right) Principle body

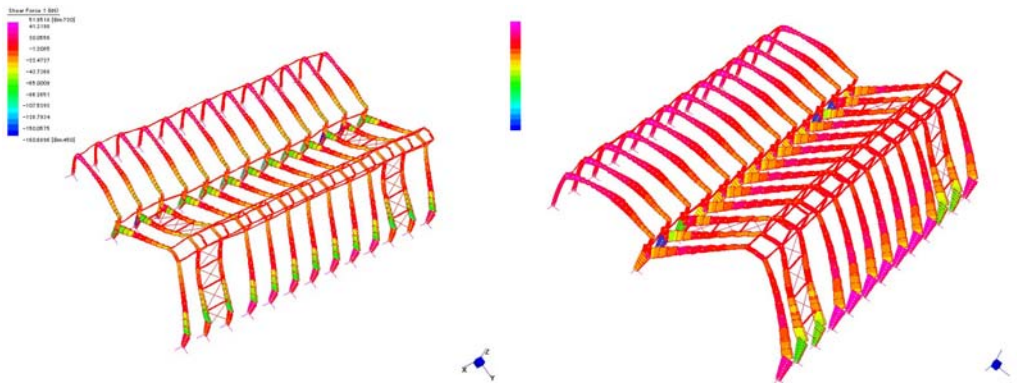

Figure 59: shear-force distribution In SLV-, in-plane earthquake, out-of-plane earthquake (right) Secondary body

Axial force

Principle body has the similar distribution of the force and the position of the max tensile and compressive value to that of static analysis and seismic analysis of out-of-plane earthquake and it can be guessed due to the effect of the gravity load. In axial force the values are also same as out-of-plane earthquake; for instance, in SLV+ 136.3kN-the max tensile value and 562kN the max compressive value in SLV+ in out-of-plane earthquake and on the other hand in case of in plane earthquake 105.2kN-tensile value and 513.8kN compressive value.

On the contrary, in Secondary body, the distribution of the values does not look similar to that of out-of-plane earthquake and the values are also not so close to each other. This phenomenon is also seen in shear-force case as discussed above.

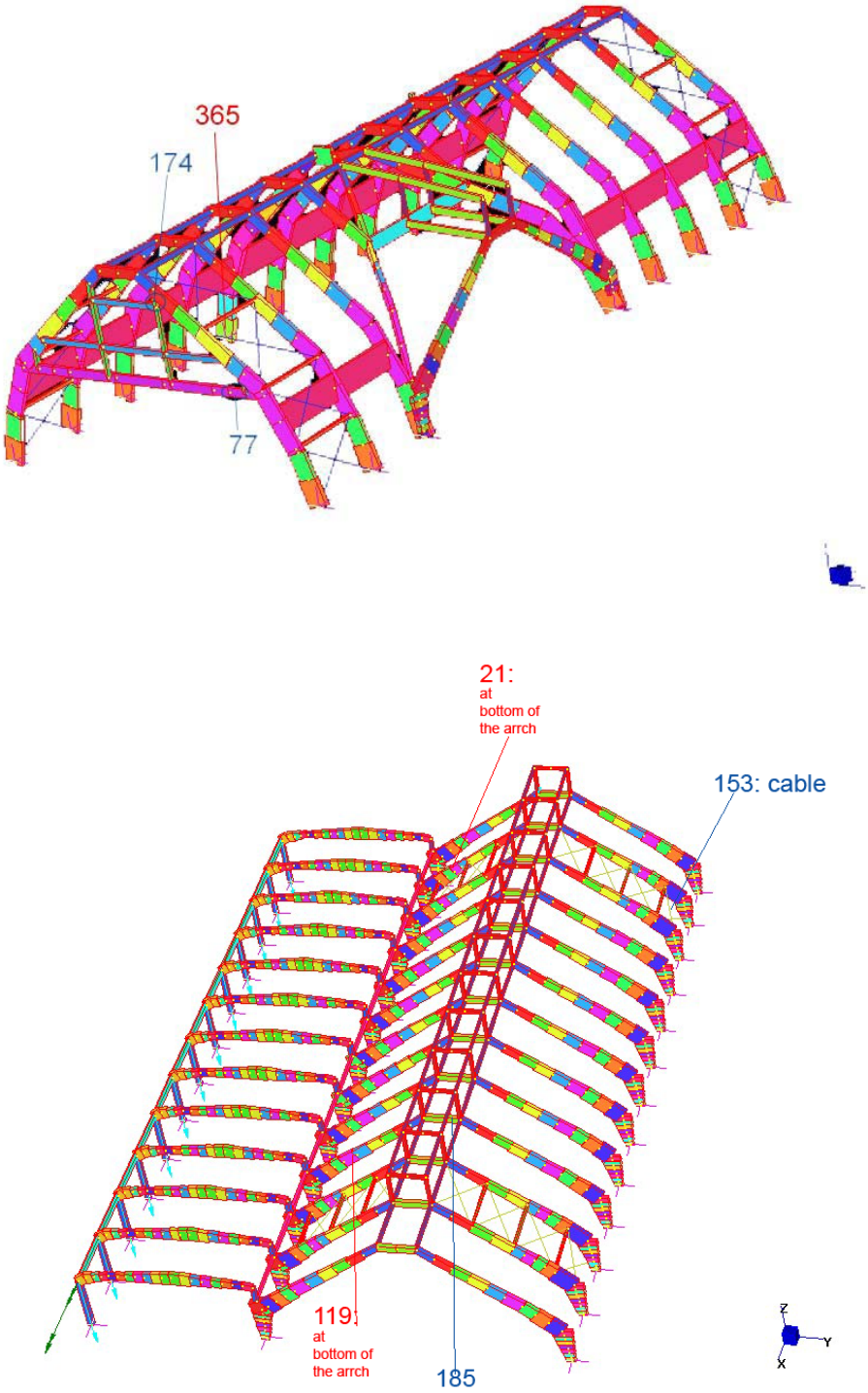

Figure 60: mapping of max and min axial force, in-plane earthquake, Principle body and Secondary body (below)

Principle	max	Bm no	min	Bm no
SLV+	105.2	77	−513.8	365
SLV−	68.4	174	−654.4	365

Secondary	max	Bm no	min	Bm no
SLV+	32.9	185	−265.2	119
SLV−	31.6	510	−364.4	21

Table 48: the list of max and min axial force, in-plane earthquake, Principle body and Secondary body (below)

AX	max	Bm no	min	Bm no
SLV+	136.3	331	−562	365
SLV−	74.8	81	−711	341

AX	max	Bm no	min	Bm no
SLV+	181.8	753	−272.6	74
SLV−	107.1	510	−558.2	708

Table 49: max and min axial-force values, out-of-plane earthquake, Principle body and Secondary body (below)

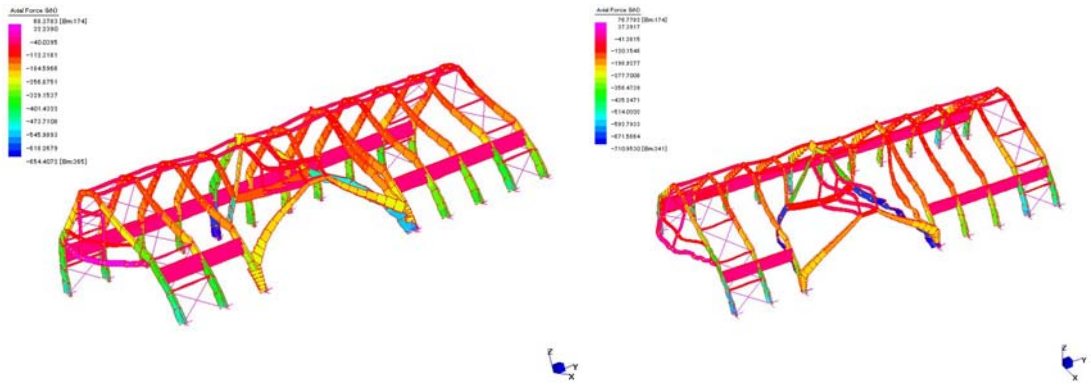

Figure 61: axial-force distribution In SLV-, in-plane earthquake, out-of-plane earthquake (right) Principle body

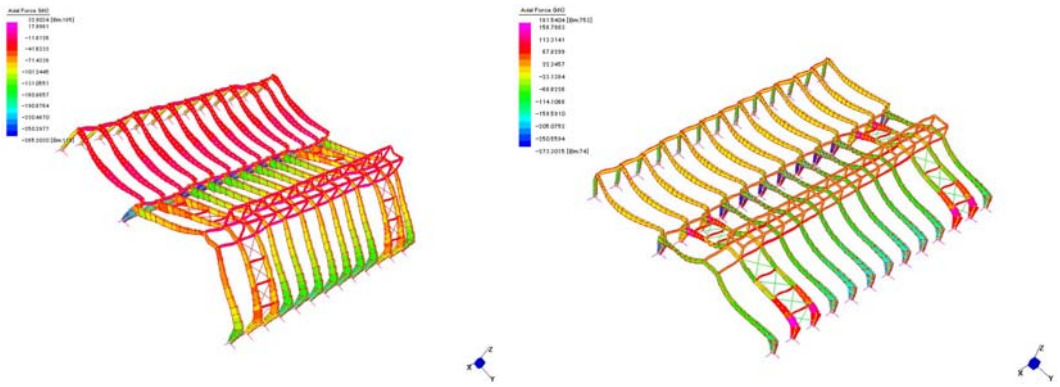

Figure 62: axial-force distribution In SLV+, in-plane earthquake, out-of-plane earthquake (right) Secondary body

4.3.7. Qualitative overview of the Linear Static Analysis (SLS)

In Serviceability Limit State, the combination of load case is different from that of ULS and it is shown as below:

1st case: snow is leading action

$$K_{FI} *G+ K_{FI} *S+K_{FI}*\psi_{0,1}*W \quad (4\text{-}21)$$

2nd case: wind is leading action

$$K_{FI}*G+ K_{FI}*\psi_{0,2}*S+ K_{FI}*W \quad (4\text{-}22)$$

where:

K_{FI}=1.1 (multiplication factor for RC3)

$\psi_{0,1}$=0.6 (reduction factor, wind load)

$\psi_{0,2}$=0.5 (reduction factor, snow load)

The result is more or less the same as that of ULS and hence this part is skipped to avoid the repetition of the similar discussion. However, as for the verification, apparently another criteria from the ULS is given, so in that chapter, the close analysis is carried out quantitatively.

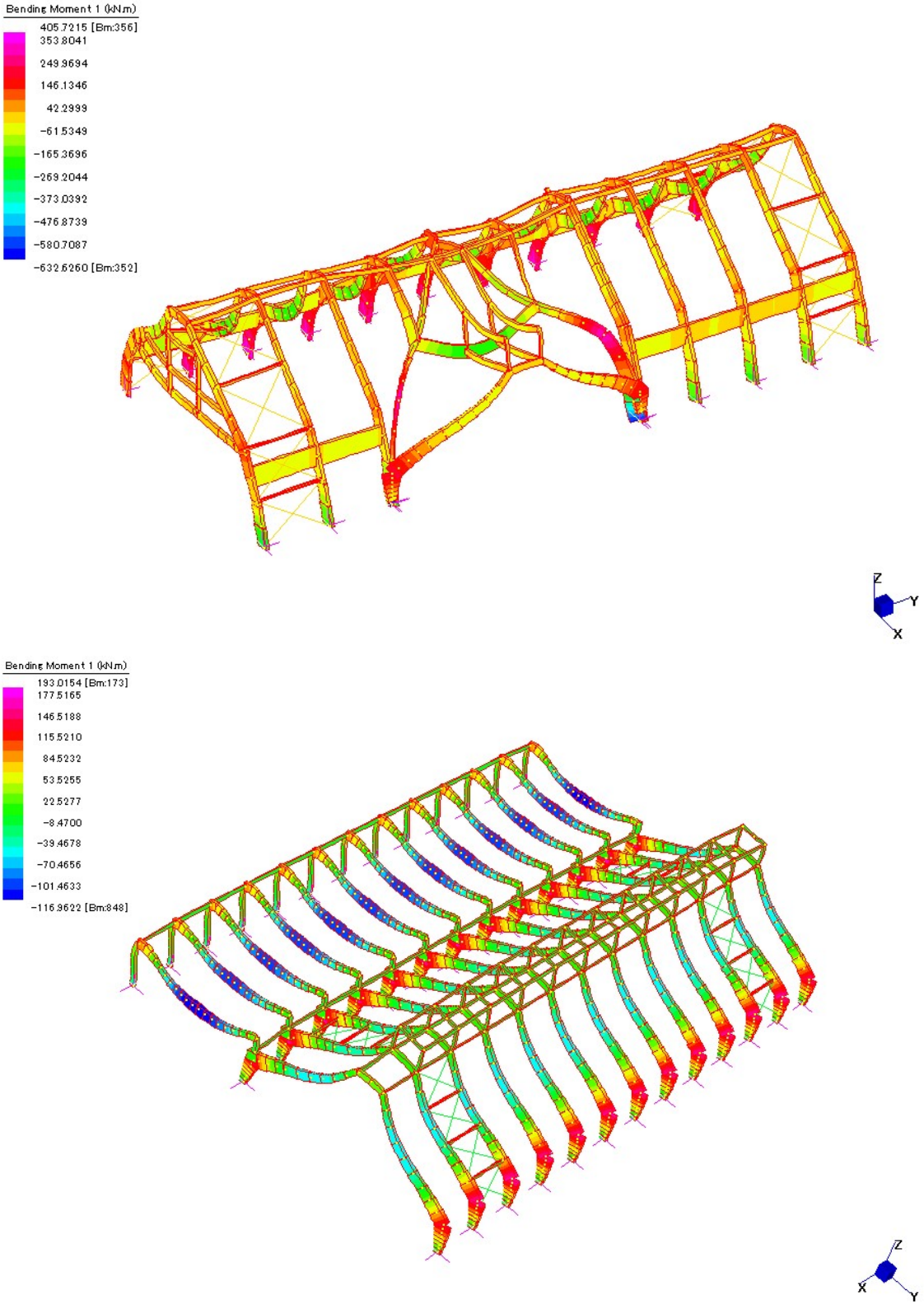

Figure 63: the combination of load, wind load leading case wind case 1 and 3-the top Principle body, the bottom Secondary body- Bending Moment

4.4. Conclusion

Modal analysis revealed the natural frequency of each structure.
As for Principle body, 1st mode (2.17Hz) and 4th mode (3.00Hz) are more relevant to the global behaviour of the structure and hence those modes are critical to the seismic analysis with out-of-plane earthquake. Just with these two modes, the sum of the participation factor results in nearly 65%. As for Secondary body, they are 1st mode (2.04Hz) and 2nd mode (2.65Hz) is dominant and again with those two modes, the sum of participation factor ends in nearly 70%. When it comes to in-plane earthquake, unlike out-of-plane earthquake, quite high mass participation factor is not found. In Principle body, in 5th mode (3.47Hz) it result in 15% and in Secondary body in 24th mode (18.8%), 25th mode (14.5%) and 27th mode (16.1%).

Linear static analysis is relevant to gravity, snow load and wind load.
In Principle body as for displacement, when the snow load (thus, vertical load) is dominant the maximum value (0.008m) is positioned in the middle of the long beam (12m span) in the entrance part. When it comes to the wind load, the maximum displacement (around0.0085m) is seen in the middle part of the continuous arch. The max and min value of the bending moment (about 500kNm and -750kNm) is found in the entrance part (beam: 72 and 215) in vertical-load (snow load) dominating case. It probably is due to the fact that this part does not have as many structural members as the other parts. In the wind-load dominant case, the max bending-moment value (around 600kNm) is seen at the bottom of the 3rd arch (beam 356) and the min value (about -900kNm) is found at the bottom of the 13th arch (beam 351). This result looks reasonable when the direction of the wind –lateral direction- is thought of. The max absolute value of shear force is found in the middle of the 14th or 15th arch and the reason should be the same as above- thus, due to the lack of sufficient vertical support member. The max compressive value is seen at the bottom of the 5th arch (beam 365) in any combination of the load case. Probably it is due to the size of the cross-section. When the force distribution is seen, the tensile values are not found as much as compressive value, and even when it is found, basically it is even smaller than compressive value. Presumably it can be said that in case of Principle body, larger value of each force (bending moment, shear force and axial force) is likely to concentrate in the entrance part- thus, the 13th,14th and 15th arches (Figure 64).

As for Secondary body in snow-load dominant case, the maximum displacements are always seen in the middle of the beam of beam part. The value is from 0.005 to 0.006m over the span of 15m. In wind-load leading case, the maximum displacement is found again at the middle of the arch of beam part or at the middle of the arch in the arch part. Apparently, the span of the beam in the beam part, is quite long-15m and hence this part is likely to get the max displacement. On the other hand, when the wind load is leading case, the max displacement is found at the middle of the arch of the arch part. In snow leading case, the max values of bending moment are found at the corner of the arch where the arch angle changes. They all are positioned in 12th arch, which are next to steel brace. On the other hand, min

value is found again at the middle of the beam of the beam part. In wind dominant case, the max value is positioned at the arch corner of the 2nd and 12th arch, and hence the steel brace effect is confirmed here again. In Secondary body, the max and min values of shear force are found around the steel brace. It is also true of axial force. As a result it would turn out that the max and min values in general are found in 2nd, 3rd, 11th and 12th arch in any load-case combination (Figure 64).

Seismic analysis is carried out in two cases: in-plane earthquake and out-of-plane earthquake. It turns out that the similar results are similar to that of the linear static analysis somehow. Thus, in any earthquake case, as for Principle boy the higher values of each force focus mostly on the 13th, 14th and 15th arch-entrance part (Figure 64). With regard to Secondary body, they are often found on 2nd, 3rd 11th and 12th arch-around the steel brace (Figure 64). However, due to the earthquake direction, in Secondary body sometimes the max or min value is found in some other part of the structure. Thus, when in-plane and out-of-plane earthquake are compared, the steel brace effects –that is, around the steel brace the higher value is found- become more obvious in Secondary body. On the other hand, the steel brace effect is so clear in Principle body, but it does not mean the steel does not work in Principle body. In fact, same phenomenon can be seen even in Principle body but in that body the entrance part show more remarkable outcome than arches with steel brace. The same tendency is seen in static analysis as well. In addition, in any analysis-especially in static analysis, the gravity load is dominant factor for the force location and distribution and presumably this derives from the fact that this structure is built of concrete whose density is relatively high compared to other structural material such as steel and timber.

So far, mostly the location and distribution of the value is discussed, so here the comparison of the max values is put down between three analyses-static analysis in-plane and out-of-plane seismic analysis (Table 50). In general larger value is shown, in turn: out-of-plane seismic analysis, in-plane earthquake analysis and static analysis. Moreover in any case, Principle body shows bigger values than Secondary body. Presumably this is due to the height of the building, total mass of the building and the shape of the structure: 15.5m high in Principle body and 10m high in Secondary body, $7.2*10^5$ (kg) in Principle body and $6.6*10^5$ (kg) in Secondary body, and rectangular-shaped plan in Principle body and square shaped plan in Secondary body. As a result, probably Secondary body undergo smaller value than Principle body in general. At any rate through the qualitative overview, the structural characteristic behaviour is revealed somehow. In accordance with this appreciation, they are analysed quantitatively in the verification chapter.

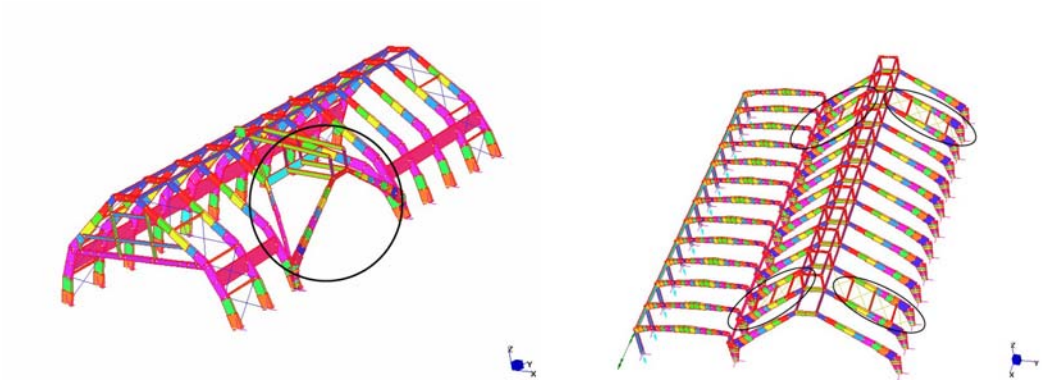

Figure 64: the entrance part in Principle body and the arches next to brace in Secondary body

Principle	max DF	LC	max abs .BM (kNm)	LC
Static	0.0007	wind2+s	896.8	wind1+s
Seismic/out	0.003	SLV−	1643.2	SLV−
Seismic/in	0.0014	SLV+	976.1	SLV−

Principle	max abs. SH (kN)	LC	max AX (kN)	LC	min AX (kN)	LC
Static	225.5	wind1+s	121.6	wind1+s	−852.7	wind1+s
Seismic/out	327.4	SLV+	136.8	SLV+	−711	SLV−
Seismic/in	218.9	SLV+	105.2	SLV+	−654.4	SLV−

Secondary	max DF	LC	max abs .BM (kNm)	LC
Static	0.00053	wind5+s	302.1	wind5+s
Seismic/out	0.0023	SLV−	490.2	SLV+
Seismic/in	0.00057	SLV+	298.5	SLV−

Secondary	max abs. SH (kN)	LC	max AX (kN)	LC	min AX (kN)	LC
Static	128.6	wind5+s	3.9	snow+w3	−425.4	snow+w6
Seismic/out	284	SLV+	181.8	SLV+	−558.2	SLV−
Seismic/in	160.7	SLV−	32.9	SLV+	−364.4	SLV−

Table 50: the list of max and min value in static analysis and seismic analysis for Principle body and Secondary body

DF-deflection, here it signifies displacement /span

Seismic/out means out-of-plane earthquake

Seismic/in means in-plane earthquake

5. THE VERIFICATION OF THE MEMBER

The verification is discussed in Eurocode2-EN1992-1-1:2004. In this chapter first, the procedure of the verification is discussed and then verification of the member is carried out: Serviceability Limit State and Ultimate Limit State, in turn. In this report, the double reinforcement is considered in any case, as unfortunately there is not sufficient information of upper reinforcement in ENCO (2008). The unit of equation and the value in table is "m, kN, kNm", unless it is not defined particularly.

5.1. The procedure

5.1.1. Serviceability Limit State

Deflection control

The deflection of the beam should not be over span/250 (p126 and p127, EN1992-1-1:2004).

Crack control

As for the crack control, In the crack control, the steel stress needs to be calculated, and hence the steel strain is obtained in the first place. It is acquired from the equilibrium of the force and of the bending moment of the cross-section. Incidentally, the axial force is neglected for the simplification.

Then, the relation between steel stress and bar spacing is used for the criterion for the verification in this report (Table 52). Incidentally, the correlation between steel stress and bar diameter can substitute this condition and thus not necessarily both conditions are satisfied. In Marghera it is especially close to the coast and hence the exposure class XS1 should be considered. Therefore the maximum w_{max} is set out to be 0.3 mm (Table 51).

equilibrium of the force

$$0.8*E_{cd}*\varepsilon_c*b*x+A_s'*E_s*((x-d_2')/x)*\varepsilon_c - A_s*E_s*((d-x)/x)*\varepsilon_c =0 \quad (5\text{-}1)$$

equilibrium of the bending moment (centre of the moment is taken at the position of the reinforcement in tension)

$$0.8*E_{cd}*\varepsilon_c*b*x*(d-0.4x-d_1')+ A_s*E_s*((x-d_2')/x)*\varepsilon_c*(d-d')- M_{Ed}=0 \quad (5\text{-}2)$$

$$\varepsilon_s=((d-x)/x)*\varepsilon_c \quad (5\text{-}3)$$

$$\sigma_{s=} E_s*\varepsilon_s \quad (5\text{-}4)$$

where:

$E_{cd:}$: Design value of modulus of elasticity of concrete

ε_c : Compressive strain in the concrete

b : Overall width of a cross-section,

A_s': Cross sectional area of reinforcement in compressive zone

A_s : Cross sectional area of reinforcement in tensile zone

E_s : Design value of modulus of elasticity of reinforcing steel

d : effective depth of the cross-section

d_1' : the distance between the surface of the reinforcement closest to the nearest concrete surface in tensile zone

d_2': the distance between the surface of the reinforcement closest to the nearest concrete surface in compressive zone

σ_s: tensile stress in the steel

M_{Ed} : design value of the applied internal bending moment

x : neutral axis depth

Exposure Class	Reinforced members and prestressed members with unbonded tendons	Prestressed members with bonded tendons
	Quasi-permanent load combination	Frequent load combination
X0, XC1	0,4[1]	0,2
XC2, XC3, XC4	0,3	0,2[2]
XD1, XD2, XS1, XS2, XS3		Decompression

Note 1: For X0, XC1 exposure classes, crack width has no influence on durability and this limit is set to guarantee acceptable appearance. In the absence of appearance conditions this limit may be relaxed.

Note 2: For these exposure classes, in addition, decompression should be checked under the quasi-permanent combination of loads.

Table 51: recommended value of w_{max}

(p119, EN1994-1-1 2004)

Steel stress[2] [MPa]	Maximum bar size [mm] w_k= 0,4 mm	w_k= 0,3 mm	w_k= 0,2 mm
160	40	32	25
200	32	25	16
240	20	16	12
280	16	12	8
320	12	10	6
360	10	8	5
400	8	6	4
450	6	5	-

Steel stress[2] [MPa]	Maximum bar spacing [mm] w_k=0,4 mm	w_k=0,3 mm	w_k=0,2 mm
160	300	300	200
200	300	250	150
240	250	200	100
280	200	150	50
320	150	100	-
360	100	50	-

Table 52: Maximum bar diameters and Maximum bar spacing for crack control

(p123, EN 1992-1-1 2004)

5.1.2. Ultimate Limit State

In the verification of the Ultimate Limit State, resistance value for each (axial force, bending moment, and shear force) should be calculated and the values -e.g. M_{Rd}- should be larger than the design value -e.g. M_{Ed}. The equation to acquire each value is shown below:

Axial Force

$$N_{Rd}=A_c*f_{cd}+A_s*f_{yd} \text{ (in compression)} \quad (5\text{-}5)$$

$$N_{Rd}=A_s*f_{yd} \text{ (in tension)} \quad (5\text{-}6)$$

where:

N_{Rd}: the design axial force resistance

b : overall width of a cross-section

h : overall depth of a cross-section

f_{cd}: Design value of concrete compressive strength

f_{yd}: Design yield strength of reinforcement

A_s : Cross sectional area of reinforcement in tension

A_c : Cross sectional area of concrete

Bending Moment

First, the position of the neutral axis is calculated (5-7), and the bending moment resistance is acquired (5-8). Moreover, the cross-section goes through the biaxial moment, and hence the biaxial bending condition should be satisfied (5-9).

x (neutral axis is given from the below equation)

$$N_{Ed}+0.8*x*b*f_{cu}-f_{yd}*A_s+A_s'*E_s*10^3*\varepsilon_{cu2}*(h/2-d')/x=0 \quad (5\text{-}7)$$

$$M_{Rd}=(A_s*f_{yd})*(h/2-d')+(A_s'*E_s*10^3*\varepsilon_{cu2}*(h/2-d')/x)*(h/2-d')+0.8*x*f_{cd}*b*(h/2-0.4*x) \quad (5\text{-}8)$$

$$(M_{Edz}/M_{Rdz})^a+(M_{Edz}/M_{Rdz})^a<1 \quad (5\text{-}9)$$

(P74, EN 1992-1-1 2004)

where:

M_{Rd}: the design bending moment resistance

N_{Ed}: design value of the applied axial force

A_s' : Cross sectional area of reinforcement in compresssion

E_s: design value of modulus of elasticity of reinforcement

d' : the distance between the surface of the reinforcement closest to the nearest concrete surface

x : neutral axis depth

ε_s: tensile strain of reinforcement

ε_{cu2}: Ultimate compressive strain in the concrete given by the Table 3.1 (p29, in EN1992-1-1:2004)

$\varepsilon_{ud:}$ design value of Ultimate tensile strain in the reinforcement

a*: the exponent (below)

N_{Ed}/N_{Rd}	0,1	0,7	1,0
a =	1,0	1,5	2,0

(P75, EN 1992-1-1 2004)

*in this analysis, a=1.5 is chosen for the conservative purpose.

Shear Force

First, shear stress (v_{Ed}) is obtained from the shear force of the cross section. Then, v_{Ed} should not be over "$v_{Rd,}$ max, cotθ=2.5" (Table 53). If this condition is fulfilled, the procedure can move to the equation (5-11 and 5-12) as a last step. However, if v_{Ed} is bigger than "$v_{Rd,}$ max, cotθ=2.5", at least "$v_{Rd,}$ max, cotθ=1" should be be bigger than $v_{Ed,}$ if it is satisfied, the exact theta should be calculated (5-13). With the theta, the equation (5-11) should be examined. Thus, in both cases, $A_{sw}/s>v_{Ed}*b_w/(b_w*f_{ywd}*\cot\theta)$ should be satisfied, and consequently the verification is obtained.

$$v_{Ed} = V_{Ed}/(b_w * z) \quad (5\text{-}10)$$

$v_{Ed} < v_{Rd,}$ max, $\cot\theta = 2.5$ is checked. In case this condition is satisfied,

$$A_{sw}/s > v_{Ed} * b_w/(b_w * f_{ywd} * \cot\theta) \quad (5\text{-}11)$$

Also,

$$s_{l,max} = 0.75d \quad (5\text{-}12)$$

If it is not satisfied, below case is examined

$v_{Ed} < v_{Rd,}$ max, $\cot\theta = 1$

If it is cleared, actual theta is calculated as below:

$$\theta = 0.5 * \sin^{-1}[v_{Ed} * b_w/(0.18 * f_{ck} * (1 - fck/250)] \quad (5\text{-}13)$$

eurocde2 http://www.eurocode2.info/main.asp?page=0

f_{ck}	$v_{Rd,max}$ cot▪=2.5	$v_{Rd,max}$ cot▪=1
20	2.54	3.68
25	3.1	4.5
28	3.43	4.97
30	3.64	5.28
32	3.84	5.58
35	4.15	6.02

Table 53: List of maximum design shear-stress resistance

(unit: MPa)

where:

v_{Ed} :design value of the applied shear stress of the cross-section

V_{Ed} :design value of the applied shear force of the cross-section

b_w : the minimum width between tension and compression chord

z: is the inner lever arm, the approximate value z=0.9d is employed-for the reinforced concrete without axial force

v_{Rd}: the design shear-stress resistance of the member

A_{sw} : the cross-sectional area of the shear reinforcement

s : the spacing of the stirrups

f_{ywd} : the design yield strength of the shear reinforcement

f_{ck} : the characteristic compressive strength of concrete

$s_{l,max}$: maximum spacing for vertical shear reinforcement

5.1.3. Selection of members for verification

Arches to be verified are chosen as seen in Figure 66. The choices depend on the result of the structural analysis in addition to the coring performed by ENCO (2008). Thus, basically, arches where the maximum values are found are chosen. From each arch, the bottom, middle and top part are chosen, and again those selections derive from the coring, as shown below.

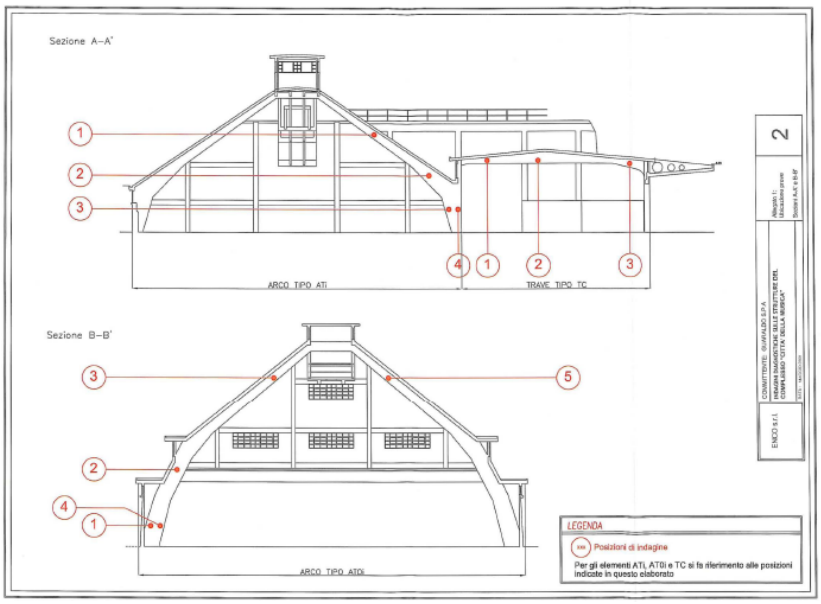

Figure 65: the point of the arch where testing was carried out

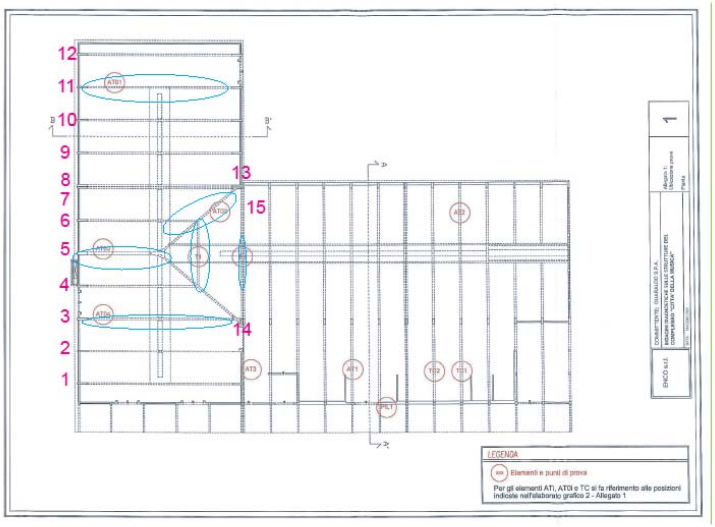

Figure 66: the numbering of the arch and the chosen arch for the verification, Principle body (ENCO, 2008 modified by author)

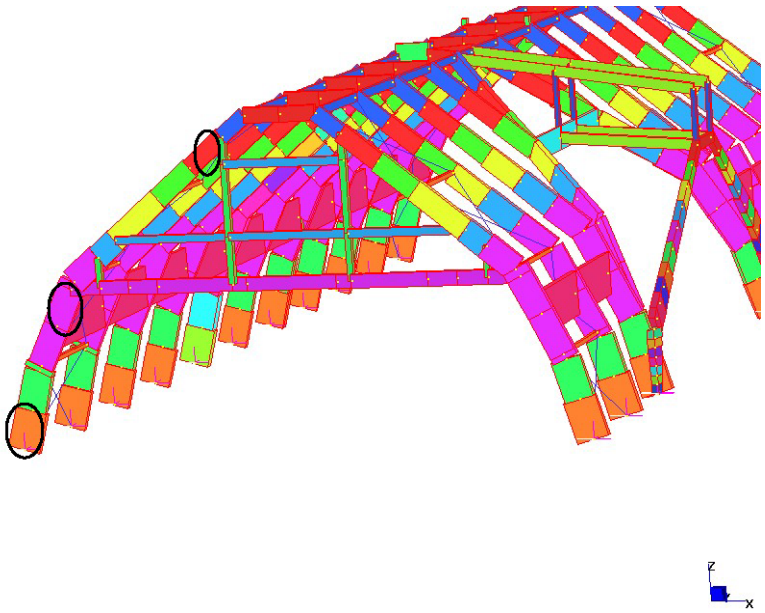

Figure 67: selection of the point of arch due to the testing, Principle body

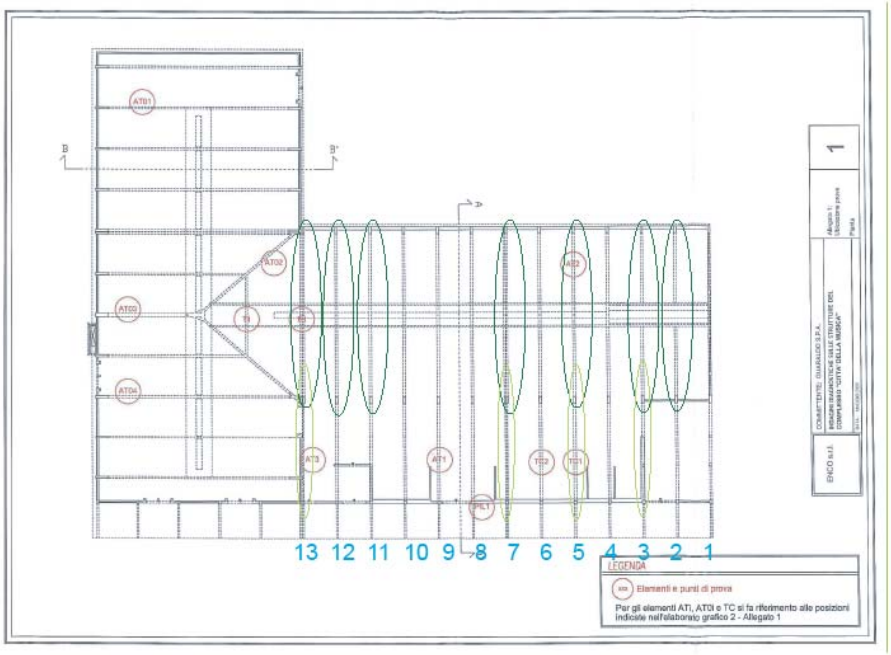

Figure 68: the numbering of the arch and the chosen arch for the verification, Principle body
(ENCO, 2008 modified by author)

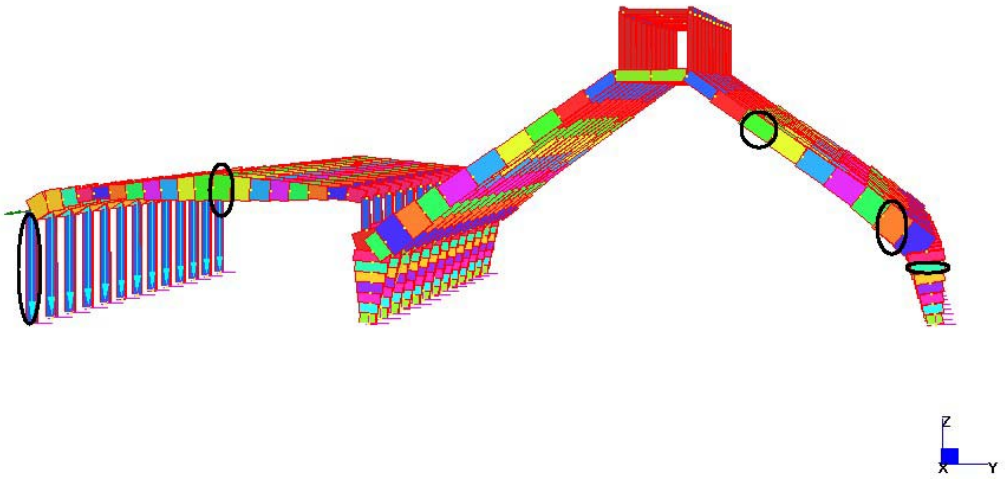

Figure 69: selection of the point of arch due to the testing, Principle body

5.2. Verification

In this part, there are various lists of values concerning the verification. However, the whole result is not given in the text for the saving of the space, basically, unverified members are put in the text for the discussion purpose and the whole result are put in the CD-R where the regarding excel file can be found. The CD-R has been handed in to UNIPD.

The material properties employed in the verification, including design value of concrete and steel strength, are defined as below (Table 54). The confidence factor is discussed in EN1998-3.
The value is determined in accordance with the knowledge about the building. In this case, there are the incomplete structural drawing and quite detailed result of in-situ and laboratory testing, and hence knowledge level 2 is applied (Table 55). Thus, the confidence factor turns out to be 1.2. Partial safety factor for steel and concrete are given in EN 1992-1-1 2004 and the values are shown in the equation.

First, Serviceability Limit State is examined and then the Ultimate Limit State is dealt with.

design value of concrete compressive strength

$$f_{cd}=\alpha_{cc}*f_{ck}/(\gamma_c* CF_{KL2}) \quad (5\text{-}14)$$

(p34, EN 1992-1-1 2004)

design value of steel tensile strength

$$f_{yd}=f_{yk}/(\gamma_s* CF_{KL2}) \quad (5\text{-}15)$$

(p44, EN 1992-1-1 2004 -modified by the author)

where:

γ_c : the partial safety factor for concrete: 1.5 is taken for static analysis and 1.2 is for seismic analysis*.

γ_s: the partial safety factor for reinforcing steel: 1.15 is for static analysis and 1.0 is for seismic analysis*.

α_{cc}: the coefficient taking account of long term effects on the compressive strength and of unfavorable effects resulting from the way the load is applied: The recommended value is 1.

*(p24, EN 1992-1-1 2004)

CF_{KL2}: the confidence factor coming from the knowledge on the existing building. KL2 signifies normal knowledge. The value is 1.2.

conc. prop.	snow, wind	Earthquake
f_{cdp}(MPa)	16.1	20.2
f_{cdsa}	13.3	16.7
f_{cdsb}	12.25	14.1
E_{cmp}(GPa)	35.1	35.1
E_{cmsa}	29.1	29.1
E_{cmsb}	27.3	27.3
ε_{c2}	0.002	0.002
ε_{cu2}	0.0035	0.0035

steel prop.	snow, wind	Earthquake
$_{fyd}$(MPa)	289.8	333.3
$(f_{tk}/f_{yd})k$	1.35	
ε_{ukp}	0.289	
ε_{udp}	0.26	
ε_{uks}	0.23	
ε_{uds}	0.21	
E_s(Gpa)	200	

Table 54: the property of concrete and steel -below- employed in the verification

NB) Some values are different from each body and they are distinguished as follows:

$f_{cd,p}$ -the design value of compressive strength in Principle body, $f_{cd,sa}$- that in arch part of Secondary body, $f_{cd,sb}$ -that in beam part in Secondary body

Table 3.1: Knowledge levels and corresponding methods of analysis (LF: Lateral Force procedure, MRS: Modal Response Spectrum analysis) and confidence factors (CF).

Knowledge Level	Geometry	Details	Materials	Analysis	CF
KL1	From original outline construction drawings with sample **visual** survey ***or*** from **full** survey	Simulated design in accordance with relevant practice ***and*** from **limited** *in-situ* inspection	Default values in accordance with standards of the time of construction ***and*** from **limited** *in-situ* testing	LF-MRS	CF_{KL1}
KL2		From incomplete original detailed construction drawings with **limited** *in-situ* inspection ***or*** from **extended** *in-situ* inspection	From original design specifications with **limited** *in-situ* testing ***or*** from **extended** *in-situ* testing	All	CF_{KL2}
KL3		From original detailed construction drawings with **limited** *in-situ* inspection ***or*** from **comprehensive** *in-situ* inspection	From original test reports with **limited** *in-situ* testing ***or*** from **comprehensive** *in-situ* testing	All	CF_{KL3}

NOTE The values ascribed to the confidence factors to be used in a country may be found in its National Annex. The recommended values are $CF_{KL1} = 1,35$, $CF_{KL2} = 1,20$ and $CF_{KL3} = 1,00$.

Table 55: **Confidence factor corresponding to knowledge level**

(EN1998-3, p18)

5.2.1. Serviceability Limit State-static analysis and seismic analysis -out-of-plane earthquake-

Deflection Control

For the deflection control, the below beams are verified. The result is shown below. Here, the verification is conducted in mathematical approach. The maximum design value of the displacement is compared with the minimum value -span/250- at the whole-structure level. That is, in case it is confirmed that its minimum upper-limit value (span/250) in the entire structure is larger than the maximum design value in the whole structure, it means that the whole structure is already verified.

The result is shown below. As for the Secondary Body, the maximum design value is 0.0136(m) -found in b- and on the other hand, minimum value is 0.0132(m) found in the combination of the load case SLD-. Hence, this structure is verified as for the deflection control.

However, with regard to Principle Body, in the load case of SLD+, SLD- this condition is not satisfied. Therefore, here another minimum upper-limit value should be taken and in addition, those beams which do not fulfill the condition should be verified individually: a, c, and C beams. Now those four beams are verified for each (fig) and hence as the minimum value can be taken as 0.0312(m). It is larger than 0.0239 (m) -the maximum design value found in the load case of SLD-, and hence this structure is also verified at this stage.

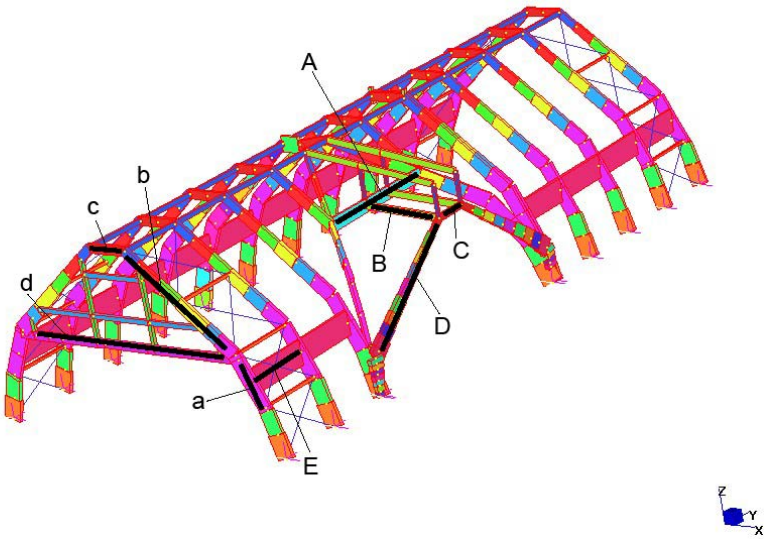

Figure 70: the verified beams for the deflection control, Principle Body

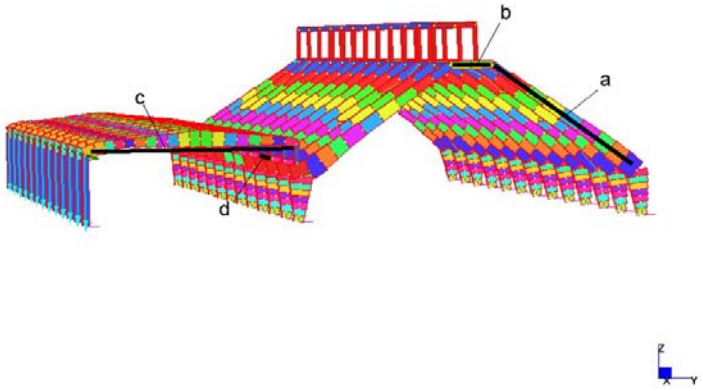

Figure 71: the verified beams for the deflection control, Secondary Body

Principle	span (m)	span/250
A	4.8	0.0192
B	12.1	0.0484
C	3.6	0.0144
D	22.5	0.09
A	12	0.048
B	7.8	0.0312
C	3.4	0.0136
D	13.1	0.0524
E	5.6	0.0224

Secondary	span (m)	span/250
A	13.1	0.0524
B	3.4	0.0136
C	15	0.06
D	5	0.02

Table 56: the upper limit value for the deflection control, Principle body and Secondary body (below)

Principle	
LC	displacement-xyz (m)
w1	0.0057
w2	0.0058
s1	0.006
s2	0.006
SLD+	0.0183
SLD-	0.0202

Secondary	
LC	displacement-xyz (m)
w3	0.0034
w4	0.0033
w5	0.0047
w6	0.004
s3	0.004
s4	0.0039
s5	0.0046
s6	0.0045
SLD+	0.013
SLD-	0.0132

Table 57: maximum value of xyz-displacement foe each load case, Principle body and Secondary body (below)

NB), From this chapter, the combination of the load case is abbreviated as below: for instance wind case 1 leading+ snow=w1, wind case 3+ snow leading=s3 As for SLD+,- they were already defined above.

a-right				a-left			
arch no	node	SLD+	SLD-	arch no	node	SLD+	SLD-
1	11	0.0025	0.0023	1	5	0.0021	0.0021
2	23	0.0025	0.0024	2	18	0.0021	0.0021
3	34	0.0025	0.0024	3	30	0.0022	0.0021
4				4	142	0.0022	0.0021
5				5	143	0.0021	0.002
6				6	144	0.0022	0.0021
7	256	0.009	0.009	7	145	0.0021	0.0021
8	105	0.0021	0.0022	8	146	0.0021	0.0021
9	65	0.0021	0.0022	9	147	0.0021	0.0021
10	74	0.0021	0.0022	10	148	0.0021	0.0021
11	84	0.0021	0.0022	11	149	0.0021	0.0021
12	95	0.0021	0.0022	12	150	0.0021	0.0021

c			
arch no	node	SLD+	SLD−
1	322	0.0063	0.0068
2	323	0.0063	0.0066
3	324	0.0062	0.0066
4	325	0.0093	0.0099
5	106	0.0058	0.0061
6	326	0.0094	0.0099
7	327	0.0063	0.0066
8	328	0.0063	0.0066
9	329	0.0063	0.0067
10	330	0.0063	0.0066
11	331	0.0064	0.0067
12	332	0.0065	0.0067
C	node	SLD+	SLD−
1	287	0.0014	0.0016

Table 58: the deflection in beam a, c and C, Principle body

Crack Control

The site is especially close to the coast and hence the exposure class XS1 should be considered . Therefore the maximum w_{max} is set out to be 0.3 mm (Table 59). The chosen arches are No3, 13 and P1 for the Principle body, and No 3 for the Secondary body arch part and No7 for the Secondary Body beam part, which includes the maximum value of steel stress. Then the above-mentioned calculation is performed on each arch. However as for the T1 section due to its complicated shape (Figure 72) another method is employed (5-16 and 5-17). In the verification step, the same mathematical approach as the deflection control is employed. That is, first maximum design value of the steel stress is picked up from the whole structure, and the maximum bar spacing is obtained. The actual spacing of each cross-section is compared with that maximum bar spacing. If it is satisfied, it means that the whole structure is verified.

As for the Principle body, the maximum design value is found to be 183.2 (MPa: beam 351, which is located at the bottom of 13th arch.) in SLD- load case. Therefore, according to the list (Table 60), 250 (mm) of the spacing is allowed. When the maximum bar spacing is referred, Principle body is verified (Table 61).

As for Secondary Body, the maximum design value is found to be 71.3 (MPa: beam 796, which is positioned at the top of the 3rd arch.) in w5 load case and hence 300 (mm) of the spacing is allowed.

Therefore, Secondary body is also verified. However, the cross-section P1L1 is not examined due to the lack of the information.

$$M_{Ed} = F*d \quad (5\text{-}16)$$

$$F/A_s = \sigma_s \quad (5\text{-}17)$$

where:

F: the tensile axial force of the cross-section

A_s: area of the steel under the tension

Figure 72:shape of T1

(ENCO 2008)

Exposure Class	Reinforced members and prestressed members with unbonded tendons	Prestressed members with bonded tendons
	Quasi-permanent load combination	Frequent load combination
X0, XC1	0,4[1]	0,2
XC2, XC3, XC4	0,3	0,2[2]
XD1, XD2, XS1, XS2, XS3		Decompression

Note 1: For X0, XC1 exposure classes, crack width has no influence on durability and this limit is set to guarantee acceptable appearance. In the absence of appearance conditions this limit may be relaxed.

Note 2: For these exposure classes, in addition, decompression should be checked under the quasi-permanent combination of loads.

Table 59: recommended value of w_{max} depending on the exposure class

(p119, EN1994-1-1 2004)

Steel stress[2] [MPa]	Maximum bar spacing [mm]		
	w_k=0,4 mm	w_k=0,3 mm	w_k=0,2 mm
160	300	300	200
200	300	250	150
240	250	200	100
280	200	150	50
320	150	100	-
360	100	50	-

Table 60: Maximum bar spacing for crack control

(p123, EN 1992-1-1 2004)

Principle	b (mm)	cover(mm)	no of bars	spacing (mm)
AT01-C2	300	30	4	80
AT01-C3	300	30	6	48
AT01-C5	300	38	6	44.8
AT02-C1	350	30	4	96.6
AT02-C2	300	30	4	80
AT02-C3	300	30	4	80
AT03-C1	500	36	4	142.6
AT03-C2	500	50	4	133.3
AT03-C3	400	30	7	56.6
AT04-3	300	30	6	48
T1	250	30	2	190
P1	250	40	3	85

Secondary	b (mm)	cover(mm)	no of bars	spacing (mm)
AT1-C1	350	28	4	98.0
AT1-C2	350	10	4	110.0
AT1-C3	350	30	8	41.4
AT2-C1	350	50	4	83.3
AT2-C2	350	60	4	76.7
AT2-C3	350	65	4	73.3
TC1-C2	240	30	3	90.0
TC2-C2	340	30	3	140.0

Table 61: The cross-section property for crack control, Principle body and Secondary body (below)

*the distance between the surface of the reinforcement closest to the nearest concrete lateral surface
As for AT01-C3, AT02-C3, AT03-C3, AT04-C3, T1 and TC1-C2 the value of the cover is not given in ENCO, and hence 30(mm) is assumed.

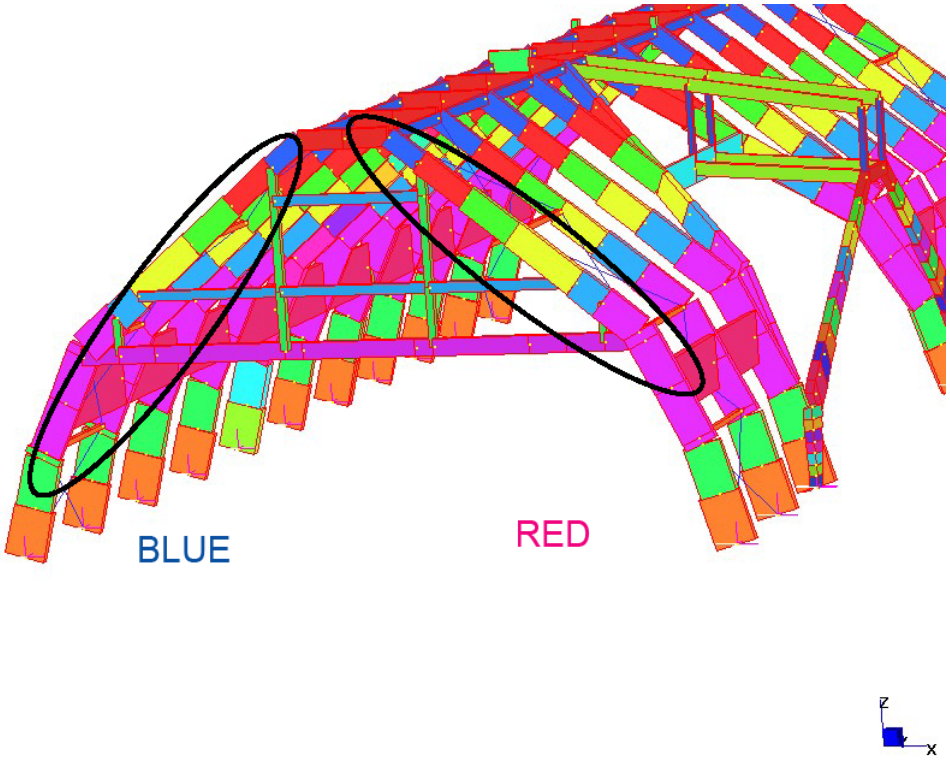

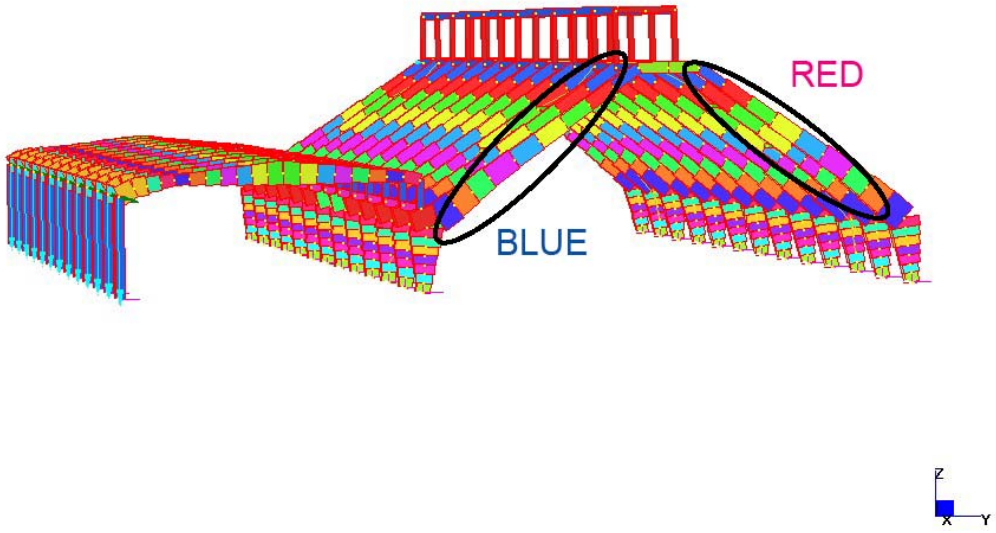

Figure 73: the colour indication, Principle body and Secondary body(below)

SLD-		x (m)	ε_c (−)	ε_s (−)	σ_s (MPa)
3top	259	0.213	0.0000417	0.000150	30.1
	AT01-C3	0.213	0.0000192	0.000069	13.8
middle	17	0.237	0.0000064	0.000028	5.5
	AT01-C2	0.208	0.0000094	0.000047	9.5
bottom	356	0.268	0.0000082	0.000034	6.8
	AT01-C1	0.268	0.0000074	0.000031	6.1
3top	241	0.213	0.0000396	0.000143	28.6
	AT01-C3	0.213	0.0000190	0.000068	13.7
middle	20	0.237	0.0000036	0.000016	3.1
	AT01-C2	0.208	0.0000208	0.000106	21.1
bottom	344	0.268	0.0000405	0.000167	33.4
	AT01-C1	0.268	0.0000336	0.000138	27.7
13 top	332	0.259	0.0000619	0.000173	34.5
	AT02-C3	0.259	0.0000845	0.000236	47.1
middle	68	0.237	0.0000603	0.000263	52.5

	AT02-C2	0.237	0.0001021	0.000444	88.8
bottom	351	0.290	0.0003858	0.000916	183.2
	AT02-C1	0.290	0.0003158	0.000750	150.0
P1	386	0.062	0.0000635	0.000151	30.2
		0.062	0.0001363	0.000324	64.9

w5		x (m)	ε_c (−)	ε_s (−)	σ_s (MPa)
3top	803	0.148	0.0000130	0.0000514	10.3
	AT2-C1	0.148	0.0000210	0.0000832	16.6
middle	798	0.190	0.0000358	0.0002104	42.1
	AT2-C2	0.190	0.0000215	0.0001266	25.3
bottom	839	0.190	0.0000220	0.0001295	25.9
	AT2-C3	0.190	0.0000335	0.0001971	39.4
3top	788	0.148	0.0000827	0.0003270	65.4
	AT2-C1	0.148	0.0000901	0.0003566	71.3
middle	796	0.190	0.0000381	0.0002245	44.9
	AT2-C2	0.190	0.0000168	0.0000991	19.8
bottom	813	0.190	0.0000514	0.0003024	60.5
	AT2-C3	0.190	0.0000579	0.0003406	68.1
TC/7	84	0.232	0.0000567	0.0002173	43.5
	TC2-C2	0.232	0.0000558	0.0002139	42.8

Table 62: the steel stress of each structure in the case where the maximum value is included (SLD-: Principle body, w5: Secondary body, below)

SLD-		shear1(kN)	BM1(kNm)	shear2	BM2	Axial (kN)	Torque (kN)
3top	259	13.0056	−76.3993	−4.9058	−10.8611	−116.137	−2.0542
	AT01-C3	24.3317	−35.1845	−4.9058	−12.9837	−106.788	−2.0542
middle	17	2.9299	−15.6673	−9.2344	−32.6536	−190.274	−4.4633
	AT01-C2	14.2534	20.4796	−9.2344	−37.9079	−167.615	−4.4633
bottom	356	−10.896	−25.0975	−10.5093	−34.0747	−370.861	−5.0935
	AT01-C1	−3.9307	−22.6583	−10.5093	−39.5017	−345.99	−5.0935
3top	241	10.5534	−72.572	−7.9984	−12.3874	−130.879	−3.1013
	AT01-C3	21.8795	−34.7879	−7.9984	−16.4201	−121.53	−3.1013

middle	20	−1.9726	8.81	−12.481	−37.0815	−204.787	−3.0717
	AT01−C2	9.3508	45.5422	−12.481	−44.7381	−182.128	−3.0717
bottom	344	−6.8357	−123.7594	−10.7056	−40.5663	−321.179	−9.3082
	AT01−C1	0.1296	−102.4937	−10.7056	−44.7561	−296.308	−9.3082
13 top	332	−32.5578	−138.066	−0.1017	−11.2712	−237.709	−3.9782
	AT02−C3	−15.5959	−188.5643	−0.1017	−6.4622	−248.322	−3.9782
middle	68	−25.8982	149.6584	−9.4424	−21.3648	−520.363	−14.7127
	AT02−C2	−10.9602	253.1842	−9.4424	−11.953	−497.704	−14.7127
bottom	351	5.2658	−894.1012	−20.3944	−116.414	−557.133	−16.4997
	AT02−C1	14.4545	−731.9375	−20.3944	−124.641	−532.262	−16.4997
P1	386	−24.3669	−10.1693	−23.2109	−33.9569	−118.925	−1.7974
		−8.3997	−21.8223	−23.2109	−51.2596	−118.925	−1.7974

w5		shear1(kN)	BM1(kNm)	shear2	BM2	Axial (kN)	Torque (kN)
3top	803	−8.7	−12.7	−0.270	0.562	−131.0	0.039
		0.2	−20.6	−0.270	0.066	−139.1	0.039
middle	798	−36.4	79.4	−0.238	0.587	−175.6	1.174
		−27.3	47.8	−0.238	0.351	−167.6	1.174
bottom	839	88.6	74.4	−0.429	−0.975	−266.5	0.516
		89.0	113.3	−0.429	−1.163	−260.6	0.516
3top	788	−12.2	−81.0	0.311	−0.735	−103.4	0.020
		4.2	−88.4	0.311	−0.162	−111.4	0.020
middle	796	−56.5	84.7	0.152	−0.037	−151.0	−0.921
		−44.4	37.4	0.152	0.106	−143.0	−0.921
bottom	813	48.8	173.8	0.411	1.008	−194.1	−1.268
		50.9	195.8	0.411	1.189	−188.3	−1.268
7	84	−2.5	−135.6	0.001	−0.010	−18.1	−0.002
		7.4	−133.5	0.001	−0.009	−17.6	−0.002

Table 63: corresponding design values corresponding to the figure above (SLD+: Principle body, w5: Secondary body, below)

T1	F (kN)	σ_s (MPa)
w1	171.4	94.7
w2	170.6	94.3
s1	173.6	95.9
s2	173.2	95.7
SLD+	148	81.8
SLD−	187.0	103.4

Table 64: the steel stress in cross-section T1

Bm367	shear1(kN)	BM1(kNm)	shear2	BM2	Axial (kN)	Torque (kN)
w1	−9.2	−205.6	0.2	2.6	−97.0	0.02
w2	−9.2	−204.7	0.2	2.7	−95.2	0.02
s1	−10.0	−208.4	0.2	3.9	−95.5	0.04
s2	−10.0	−207.8	0.2	3.9	−94.3	0.04
SLD+	7.7	−177.6	3.0	10.4	−73.1	2.01
SLD−	−24.9	−224.4	−2.6	0.7	−84.0	−1.87

Table 65: design value in cross-section T1 in each load case

5.2.2. Ultimate Limit State-static analysis and seismic analysis -out-of-plane earthquake-

As for the Ultimate Limit State, axial force, bending moment and shear force are discussed in turn.

Axial Force

Axial force verification is performed at the whole-structure level like Serviceability Limit State. The required cross-section properties are in Table 65. In Principle body, the minimum tensile axial-force resistance is 394.7kN (P1) and that of compression is 1529.7kN (T1) in **static analysis**. On the other hand, the maximum design tensile value is 121.6 kN (Bm:174 in w2,) and maximum design compressive value is -852.7kN (Bm:365 in w1) –Table 66. Then, when it comes to **seismic analysis**, the maximum design tensile value is 136.3 kN (Bm: 331 in SLV+) and the maximum design compressive value is -711kN (Bm: 341 in SLV-) –Table 66. The minimum tensile and compressive axial-force resistance are 454.0kN (tension, P1) and 1863.6kN (compression, T1) for each and they are larger than max and min design value. Hence, Principle body is verified. The same procedure is applied to Secondary body. As a result both Principle body and Secondary body are verified in terms of axial force.

	static		seismic	
	N_{Rd}+ (kN)	N_{Rd}− (kN)	N_{Rd}+ (kN)	N_{Rd}− (kN)
AT01-C1	711.4	7466.4	818.1	9288.1
AT01-C2	728.4	7000.9	837.8	8702.8
AT01-C3	1092.6	5917.6	1256.6	7306.6
AT01-C5	910.5	5735.5	1047.2	7097.2
AT02-C1	1138.2	9019.0	1309.0	11190.7
AT02-C2	728.4	7000.9	837.8	8702.8
AT02-C3	1427.7	6252.7	1642.0	7692.0
AT03-C1	728.4	11986.8	837.8	14954.4
AT03-C2	963.3	11417.5	1107.9	14216.3
AT03-C3	1542.5	7975.8	1774.0	9840.6
AT04-3	1092.6	5917.6	1256.6	7306.6
T1	524.5	1529.7	603.2	1863.6
P1	394.7	2405.1	454.0	2974.8

	static		seismic	
	N_{Rd}+ (kN)	N_{Rd}− (kN)	N_{Rd}+ (kN)	N_{Rd}− (kN)
AT1-C1	409.7	3909.7	471.2	4846.2
AT1-C2	728.4	7028.4	837.8	8712.8
AT1-C3	874.1	6474.1	1005.3	8005.3
AT2-C1	526.3	4026.3	605.3	4980.3
AT2-C2	460.5	6760.5	529.6	8404.6
AT2-C3	466.2	6066.2	536.2	7536.2
TC1-C2	722.5	3827.5	831.0	4718.0
TC2-C2	786.7	5185.5	904.8	6411.4
P1L1	178.5	1978.5	205.3	2458.6

Table 66: the design axial-force resistance Principle body, Secondary Body (below)

	max. N_{Ed}	Bm no.	min.N_{Ed}	Bm no.
w1	121.3	174	−852.7	365
w2	121.6	174	−847.3	365
s1	116.2	174	−852.1	365
s2	116.5	174	−848.9	365
SLV+	136.3	331	−579.4	365
SLV−	76.8	174	−711	341

	max. N_{Ed}	Bm no.	min.N_{Ed}	Bm no.
w3	3.5	138	−343.2	392
w4	3.4	138	−340.9	392
w5	3.3	138	−395.5	21
w6	3.7	138	−409.5	21
s3	3.9	138	−384.7	21
s4	3.8	138	−382	21
s5	3.7	138	−417	21
s6	4	138	−425	21
SLV+	181.8	753	−272.6	74
SLV−	107.1	510	−558	708

Table 67: the maximum and minimum design value of the applied axial force of the cross-section Principle body, Secondary Body (below)

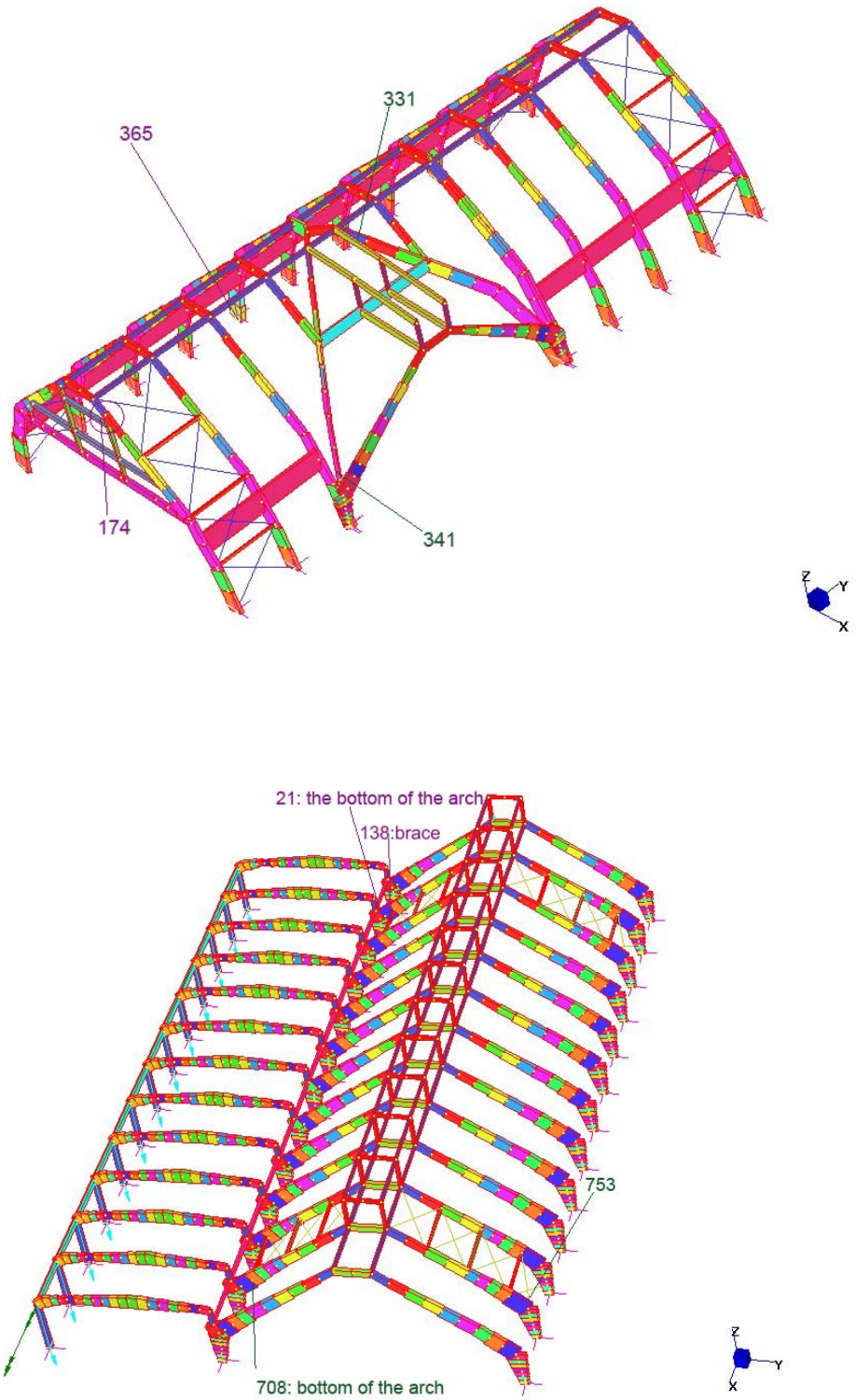

Figure 74: the mapping of the maximum and minimum design values of axial force Principle body, Secondary Body (below)

Bending Moment

The bending moment is verified in both plane 1 and plane 2. The required cross-section property for plane 1 and plane 2 is given in Table 68 and 69. Plane 1 means in-plane bending moment and plane 2 does that of out-of-plane.

As for the Principle body, for the first four cases-w1, w2, s1 and s2- the structure is verified. However, in the other cases (SLV+ and SLV-) several members can not be verified (Figure 75). Obviously, the result corresponds to the discussion in the structural analysis, and thus, the unverified members can be found in the entrance part and at the bottom of 5th arch (Table 70) in Plane 2. This cross-section goes through quite large value of the bending moment, and it will be the cause of the unverification. The unverification of P1 in plane2 comes from the insufficient height of the cross section in addition to less reinforcement, because the design values are not so large there, as it is seen (around -112kNm in both SLV+ and in SLV-).

As for the Secondary body, in **static analysis** the structure is verified in the case of w3 and w4, but in other cases-w5, w6, s3, s4, s5, s6, most of the columns P1L1 are not verified. This probably comes from relatively small square shaped area of the cross-section 0.16m^2- and the less reinforcement than other cross-sections. In Straus, the P1L1 is designed as one element, and as a result, end 1 means the bottom of the column and end 2 does the top of the column. In case of s3 and s4, the bottom of the column is verified but the top of the column is not verified (Table 72). In fact, the absolute value is not so different from each other-around 50kNm at the bottom and around 80kNm at the top-, but at any rate, in those cases, only the bottom part is verified. On the other hand in ENCO (2008) it is not clearly mentioned which part of the column P1L1 is examined for the position of the reinforcement steel, and in this verification it is assumed they have the same reinforcement steel irrespective of its position. Possibly, it is relevant to this outcome, but it is impossible to go further only with the current information.

In **seismic analysis**, again P1L1 is not verified. Like static analysis, only end2 (the top of the arch) are not verified in the verification of bending-moment resistance, but when it comes to biaxial-effect verification, both ends are not verified in both SLV+ and SLV-. In addition to P1L1, the bottom of the 2nd arch is not verified and the whole unverified result of them is shown below. In SLV+, various members in 2nd arch and 3rd arch are not verified: middle and bottom of 2nd arch and middle of 3rd arch. Presumably this is due to the steel braces which position between 2nd and 3rd arches and 11th and 12th arches. Because of these braces, those beam members experience higher value of bending moment compared to those of the other arches. Both in SLV+ and SLV-, middle of 5th arch is not verified in plane2 and this presumably comes from less steel reinforcement in this cross-section (AT2-C2) (Table 69). The same fact is applied to the middle of the 13th arch in SLV-.

In both static and seismic analysis, P1 member (at the top of the arch) is examined as this part turns out to be vulnerable through Principle-body verification, and they are all verified in Secondary body in both

analyses. This would be also due to the applied direction of the earthquake, and hence this part will be verified even in in-plane earthquake.

property of the cross section

Plane1	b (m)	h (m)	d_1' (m)	A (m^2)	Diameter(mm)	A_s	A_s whole	no of bars
AT01-C2	0.3	1.3	0.04	0.39	20	0.00031	0.00126	4
AT01-C3	0.3	1	0.021	0.3	20	0.00040	0.00240	6
AT01-C5	0.3	1	0.025	0.3	20	0.00031	0.00126	4
AT02-C1	0.35	1.4	0.025	0.49	25	0.00049	0.00196	4
AT02-C2	0.3	1.3	0.03	0.39	20	0.00031	0.00126	4
AT02-C3	0.3	1	0.02	0.3	28	0.00062	0.00246	4
AT03-C1	0.5	1.4	0.02	0.7	20	0.00031	0.00126	4
AT03-C2	0.5	1.3	0.035	0.65	23	0.00042	0.00166	4
AT03-C3	0.4	1	0.02	0.4	22	0.00048	0.00339	7
AT04-3	0.3	1	0.025	0.3	20	0.00040	0.00240	6
T1	0.25	0.25	0.03	0.0625	24	0.00045	0.00090	2
P1	0.25	0.5	0.03	0.125	17	0.00023	0.00068	3

Plane2	b (m)	h (m)	d_1' (m)	A (m^2)	Diameter(mm)	A_s	A_s whole	no of bars
AT01-C2	1.3	0.3	0.03	0.39	20	0.00031	0.00063	2
AT01-C3	1	0.3	0.03	0.3	20	0.00040	0.00080	2
AT01-C5	1	0.3	0.025	0.3	20	0.00031	0.00094	3
AT02-C1	1.4	0.35	0.04	0.49	25	0.00049	0.00098	2
AT02-C2	1.3	0.3	0.03	0.39	20	0.00031	0.00063	2
AT02-C3	1	0.3	0.02	0.3	28	0.00062	0.00123	2
AT03-C1	1.4	0.5	0.035	0.7	20	0.00031	0.00063	2
AT03-C2	1.3	0.5	0.05	0.65	23	0.00042	0.00083	2
AT03-C3	1	0.4	0.02	0.4	22	0.00048	0.00097	2
AT04-3	1	0.3	0.025	0.3	20	0.00040	0.00080	2
T1	0.25	0.25	0.03	0.0625	24	0.00045	0.00090	2
P1	0.5	0.25	0.04	0.125	17	0.00023	0.00045	2

Table 68: the properties of the cross-section for axial-force-resistance and bending-moment-resistance verification, Principle body, Plane1 and Plane2 (below)

Plane1	b (m)	h (m)	d_1' (m)	A (m^2)	Diameter(mm)	A_s	A_s whole	no of bars
AT1-C1	0.35	0.75	0.02	0.2625	15	0.00018	0.00071	4
AT1-C2	0.35	1.35	0.015	0.4725	20	0.00031	0.00126	4
AT1-C3	0.35	1.2	0.032	0.42	16	0.00020	0.00161	8
AT2-C1	0.35	0.75	0.017	0.2625	17	0.00023	0.00091	4
AT2-C2	0.35	1.35	0.04	0.4725	17	0.00023	0.00091	4
AT2-C3	0.35	1.2	0.03	0.42	16	0.00020	0.00080	4
TC1-C2	0.24	1.15	0.028	0.276	23	0.00042	0.00125	3
TC2-C2	0.34	1.15	0.03	0.391	24	0.00045	0.00136	3
P1L1	0.4	0.4	0.006	0.16	14	0.00015	0.00031	2
P1	0.25	0.5	0.03	0.125	17	0.00023	0.00068	3

Plane2	b (m)	h (m)	d_1' (m)	A (m^2)	Diameter(mm)	A_s	A_s whole	no of bars
AT1-C1	0.75	0.35	0.03	0.2625	15	0.00018	0.00035	2
AT1-C2	1.35	0.35	0.01	0.4725	20	0.00031	0.00063	2
AT1-C3	1.2	0.35	0.032	0.42	16	0.00020	0.00121	6
AT2-C1	0.75	0.35	0.05	0.2625	17	0.00023	0.00045	2
AT2-C2	1.35	0.35	0.06	0.4725	17	0.00023	0.00045	2
AT2-C3	1.2	0.35	0.065	0.42	16	0.00020	0.00040	2
TC1-C2	1.15	0.24	0.028	0.276	23	0.00042	0.00083	2
TC2-C2	1.15	0.34	0.03	0.391	24	0.00045	0.00090	2
P1L1	0.4	0.4	0.006	0.16	14	0.00015	0.00031	2
P1	0.5	0.25	0.04	0.125	17	0.00023	0.00045	2

Table 69: the properties of the cross-section for axial-force-resistance and bending-moment-resistance verification, Secondary body, Plane1 and Plane2 (below)

Principle body

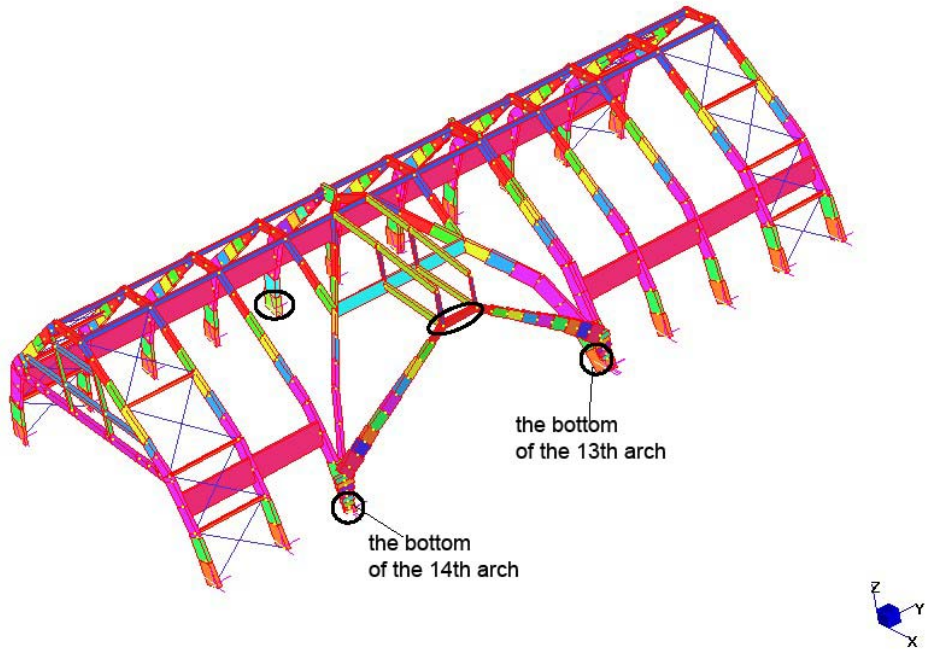

Figure 75: unverified part, Bending moment Principle body

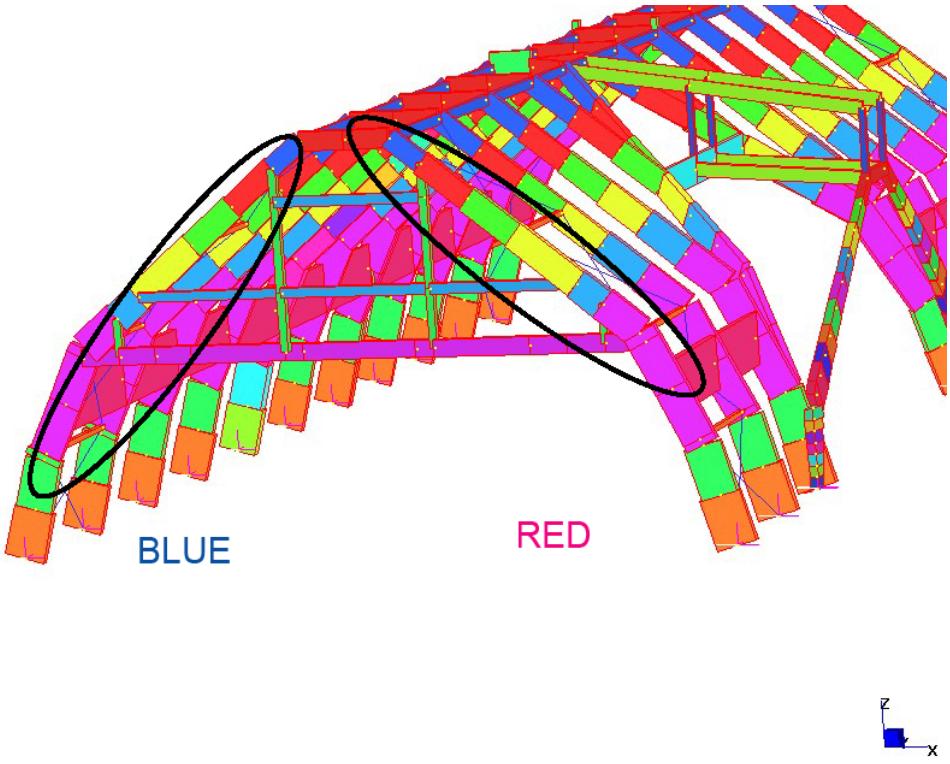

Figure 76: the colour indication, Principle body

verification, Principle body

w2		x(m)	M_{Rd1}(kNm)	safety factor	x	M_{Rd2}	safety factor	biaxial
3 top	259	0.0359	734.42	3.2045245	0.0296	145.8	187.75948	0.1747
	AT01-C3							
middle	17	0.0682	607.81	8.4386631	0.0282	139	154.59789	0.0413
	AT01-C2							
bottom	356	0.0614	1120.8	1.8235917	0.0413	247	243.51807	0.4063
	AT02-C1							
3 top	241	0.0379	762.83	312.68724	0.0315	149	245.99709	0.0004
	AT01-C3							
middle	20	0.0698	618.69	20.592778	0.0288	140.1	156.05311	0.0112
	AT01-C2							
bottom	344	0.0633	1137.7	2.9182951	0.0394	242	413.82156	0.2007
	AT02-C1							
5top	269	0.0368	1083.8	5.2965739	0.0286	237.8	111.77189	0.0829
	AT03-C3							
middle	220	0.0653	890.44	17.809644	0.046	340.7	84.31956	0.0146
	AT03-C2							
bottom	365	0.0841	1064.1	2.0426641	0.0499	339.2	80.098569	0.3439
	AT03-C1							

Verified members in case of w2

SLV+		x(m)	M_{Rd1}(kNm)	safety factor	x	M_{Rd2}	safety factor	biaxial
5top	269	0.037	1184.5	26.9	0.025	251.2	1.97	0.37
	AT03-C3							
middle	220	0.056	889.4	76.3	0.038	355.5	2.23	0.30
	AT03-C2							
bottom	365	0.053	951.2	50.1	0.034	321.7	0.98	1.04
	AT03-C1							
13 top	332	0.035	828.1	13.1	0.019	126.9	8.17	0.06
	AT02-C3							
middle	68	0.045	583.6	2.1	0.022	142.0	2.63	0.57

	AT02-C2							
bottom	351	0.044	1016.0	1.0	0.031	249.2	1.02	1.92
	AT02-C1							
14middle	72	0.046	588.6	2.1	0.022	142.5	2.72	0.55
	AT02-C2							
14 bottom	352	0.045	1020.7	1.1	0.032	249.7	0.96	1.95
	AT02-C1							
T1	367	0.043	805.0	5.4				
P1	386	0.044	124.7	1.7	0.036	71.6	0.84	1.76

unverified members in SLV+

SLV-		x(m)	M_{Rd1}(kNm)	safety factor	x	M_{Rd2}	safety factor	biaxial
5top	269	0.038	1207.1	21.3	0.0260	255.1	2.04	0.35
	AT03-C3							
middle	220	0.058	915.1	15.0	0.0389	360.3	2.19	0.32
	AT03-C2							
bottom	365	0.057	980.7	2.8	0.0357	328.1	1.00	1.20
	AT03-C1							
13 top	332	0.066	1120.9	5.2	0.0305	151.0	7.09	0.14
	AT02-C3							
middle	68	0.100	938.2	9.6	0.0381	184.7	3.71	0.17
	AT02-C2							
bottom	351	0.076	1352.2	0.8	0.0432	288.6	1.12	2.15
	AT02-C1							
14middle	72	0.053	657.6	6.7	0.0383	185.2	3.30	0.22
	AT02-C2							
14 bottom	352	0.077	1355.6	0.8	0.0433	289.0	1.17	2.13
	AT02-C1							
T1	367	0.045	821.7	3.2				

P1	386	0.046	129.5	3.0	0.0372	72.6	0.90	1.36

unverified members in SLV-

Table 70: neutral axis, bending-moment resistance, and BM and biaxial-bending verification*, Principle body

NB) biaxial verification means $(M_{Ed1}/M_{Rd1})^{1.5}+(M_{Ed2}/M_{Rd2})^{1.5}<1$

design value, Principle body

w2		shear1(kN)	BM1(kNm)	shear2	BM2	Axial (kN)	Torque (kN)
3 top	259	36.2	−229.2	0.2	0.8	−140.1	−0.5
	AT01−C3	66.3	−125.7	0.2	1.2	−126.4	−0.5
middle	17	−40.1	72.0	0.2	−0.9	−262.5	−0.8
	AT01−C2	−7.5	14.6	0.2	−0.5	−231.9	−0.8
bottom	356	−94.4	614.6	−0.3	1.0	−482.6	−0.5
	AT02−C1	−70.7	449.8	−0.3	0.4	−449.0	−0.5
3 top	241	7.4	−2.4	−0.2	−0.6	−199.6	1.3
	AT01−C3	21.5	26.7	−0.2	−1.1	−184.5	1.3
middle	20	51.0	−30.0	−0.2	0.9	−280.5	1.5
	AT01−C2	61.3	105.3	−0.2	0.3	−249.9	1.5
bottom	344	73.0	−389.8	0.4	−0.6	−416.2	−1.5
	AT02−C1	78.8	−238.3	0.4	0.2	−381.0	−1.5
5top	269	55.3	−204.6	0.6	2.1	−292.0	−0.7
	AT03−C3	96.1	−51.8	0.6	3.4	−269.5	−0.7
middle	220	−3.5	50.0	0.6	−4.0	−478.5	−1.9
	AT03−C2	39.8	93.7	0.6	−2.5	−426.5	−1.9
bottom	365	−68.4	520.9	−1.4	4.2	−847.3	0.4
	AT03−C1	−38.0	414.7	−1.4	1.4	−790.2	0.4

SLV+		shear1(kN)	BM1(kNm)	shear2	BM2	Axial (kN)	Torque (kN)
5top	269	35.2	44.1	11.6	127.5	−206.5	46.1

	AT03-C3	54.5	128.4	11.6	125.8	-190.6	46.1
middle	220	65.5	11.7	42.6	159.6	-329.0	67.2
	AT03-C2	84.8	157.4	42.6	185.6	-290.5	67.2
bottom	365	64.8	19.0	92.8	329.2	-562.0	118.3
	AT03-C1	76.6	122.2	92.8	374.8	-519.7	118.3
13 top	332	-12.6	63.4	7.1	15.5	128.8	16.3
	AT02-C3	4.4	18.1	7.1	23.7	118.2	16.3
middle	68	178.6	282.3	26.1	53.9	-99.3	7.8
	AT02-C2	193.6	423.2	26.1	44.2	-76.6	7.8
bottom	351	306.9	979.5	50.5	245.4	-193.5	11.8
	AT02-C1	316.1	1295.9	50.5	273.3	-168.7	11.8
14middle	72	180.8	277.7	23.3	52.3	-107.4	24.3
	AT02-C2	195.7	426.4	23.3	35.2	-84.7	24.3
14 bottom	352	310.3	938.5	48.5	260.8	-200.4	28.8
	AT02-C1	319.5	1264.1	48.5	283.1	-175.5	28.8
T1	367	27.8	-149.0	6.2	16.0	-66.7	4.4
		47.3	-118.9	6.2	20.7	-66.7	4.4
P1	386	30.1	74.6	53.4	85.1	-103.0	3.9
		46.1	104.7	53.4	125.6	-103.0	3.9

SLV-		shear1(kN)	BM1(kNm)	shear2	BM2	Axial (kN)	Torque (kN)
5top	269	29.0	-56.7	-10.8	-124.8	-253.8	-46.7
	AT03-C3	48.2	27.3	-10.8	-121.6	-237.9	-46.7
middle	220	27.1	-60.9	-41.9	-164.2	-371.0	-69.2
	AT03-C2	46.4	63.0	-41.9	-188.4	-332.5	-69.2
bottom	365	14.1	-344.5	-93.7	-326.5	-606.2	-119.2
	AT03-C1	26.0	-266.5	-93.7	-373.9	-563.9	-119.2
13 top	332	-40.0	-217.3	-2.8	-21.3	-378.1	-11.8
	AT02-C3	-23.0	-269.8	-2.8	-17.8	-388.7	-11.8
middle	68	-105.4	97.9	-23.3	-49.8	-683.3	-23.0
	AT02-C2	-90.5	184.7	-23.3	-32.8	-660.7	-23.0

bottom	351	−111.8	−1623.2	−47.7	−256.5	−697.8	−27.4
	AT02−C1	−102.6	−1520.9	−47.7	−278.7	−672.9	−27.4
14middle	72	−100.9	98.4	−26.4	−56.2	−689.2	−8.2
	AT02−C2	−85.9	194.6	−26.4	−47.1	−666.5	−8.2
14 bottom	352	−105.5	−1643.2	−51.6	−247.5	−702.9	−12.1
	AT02−C1	−96.3	−1530.3	−51.6	−276.2	−678.0	−12.1
T1	367	−45.0	−253.0	−5.8	−5.0	−90.4	−4.2
		−25.4	−275.9	−5.8	−8.5	−90.4	−4.2
P1	386	−45.3	−42.7	−53.3	−80.6	−124.8	−3.8
		−29.3	−70.4	−53.3	−120.7	−124.8	−3.8

Table 71: the design values of cross-sections, Principle Body

NB), Two values are shown for each beam and it comes from the fact that they have two ends: end1 and end2. The upper value is for end1 and the lower one is for end2.

Secondary Body

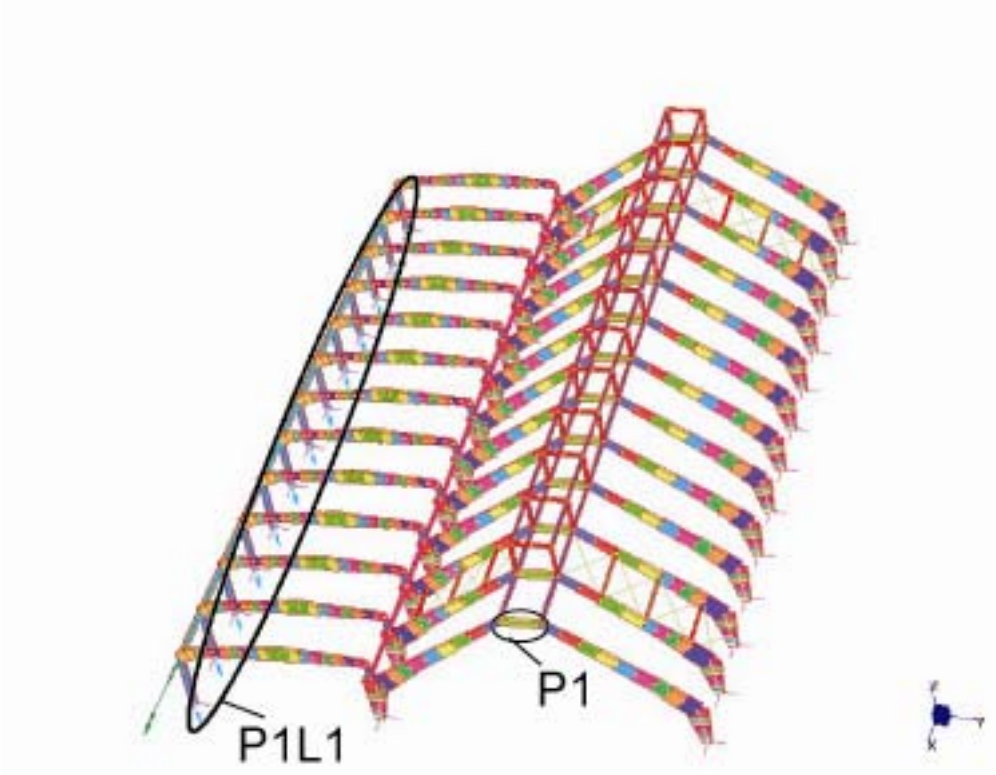

Figure 77: P1L1 and P1 in Secondary body

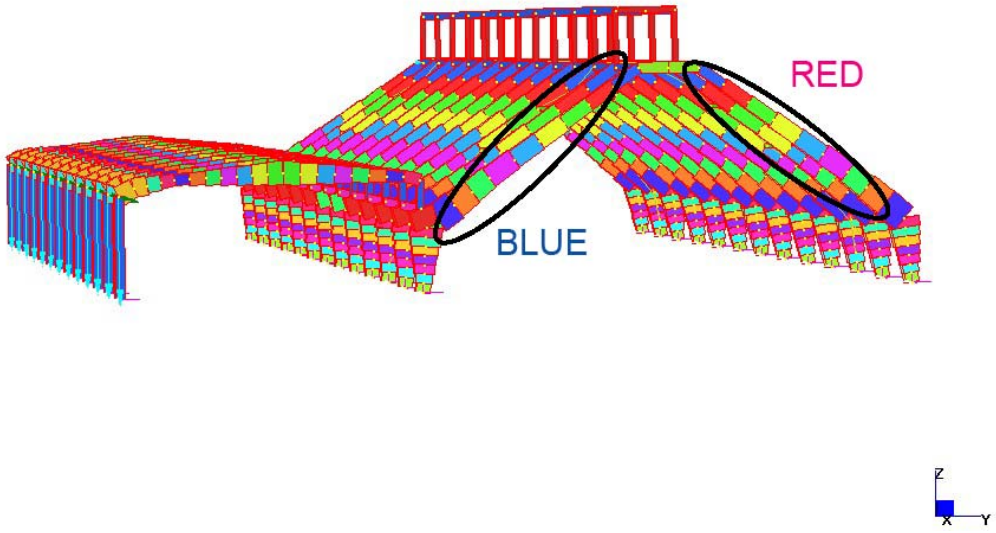

Figure 78: colour indication for Secondary body

verification, Secondary body

verified case

w6		x(m)	M_{Rd1}(kNm)	safety factor	x	M_{Rd2}	safety factor	biaxial
3top	803	0.034	254.3	6.5	0.044	67.2	90.5	0.061
	AT2-C1							
middle	798	0.067	492.3	4.0	0.030	30.7	37.9	0.127
	AT2-C2							
bottom	839	0.074	479.9	3.6	0.047	94.7	69.2	0.145
	AT2-C3							
3top	788	0.032	242.0	2.3	0.042	62.6	61.3	0.294
	AT2-C1							
middle	796	0.064	473.0	4.2	0.030	30.8	949.1	0.114
	AT2-C2							
bottom	813	0.060	421.0	1.8	0.042	81.3	60.0	0.404
	AT2-C3							
5top	301	0.034	252.6	8.6	0.044	66.6	1875.4	0.040

	AT2-C1							
middle	371	0.067	493.6	3.7	0.030	30.7	222.9	0.139
	AT2-C2							
bottom	431	0.072	474.8	2.7	0.046	93.5	2642.3	0.229
	AT2-C3							
5top	336	0.031	239.4	2.5	0.042	61.7	730.5	0.256
	AT2-C1							
middle	385	0.064	475.0	3.1	0.030	30.8	250.1	0.188
	AT2-C2							
bottom	503	0.059	417.6	2.0	0.042	80.5	647.9	0.367
	AT2-C3							

verified members in w6

SLV+	P1	x(m)	M_{Rd1}(kNm)	safety factor	x	M_{Rd2}	safety factor	biaxial
1	777	0.045	120.0	3.79	0.039	40.6	3.31	0.30
2	773	0.041	110.4	1.37	0.036	36.6	2.00	0.98
3	774	0.041	109.5	1.46	0.036	36.2	2.06	0.90
4	242	0.047	123.7	3.82	0.040	42.1	4.36	0.24
5	243	0.048	126.8	4.18	0.041	43.4	4.98	0.21
6	244	0.048	127.0	4.04	0.041	43.5	5.05	0.21
7	245	0.048	127.0	3.95	0.041	43.5	5.07	0.21
8	246	0.048	126.9	3.99	0.041	43.5	5.05	0.21
9	247	0.048	126.8	4.14	0.041	43.4	5.01	0.21
10	248	0.047	123.7	3.74	0.040	42.1	4.42	0.25
11	249	0.040	107.9	1.41	0.035	35.6	1.90	0.98
12	250	0.040	108.0	1.45	0.035	35.6	2.02	0.92
13	251	0.045	120.5	3.31	0.039	40.8	3.70	0.31

verified P1 in SLV-

unverified case

SLV+		x(m)	M_{Rd1}(kNm)	safety factor	x	M_{Rd2}	safety factor	biaxial
2middle	799	0.042	345.9	1.22	0.027	158.9	5.05	0.83
	AT2-C2							
bottom	833	0.037	315.6	0.84	0.030	56.3	3.00	1.50
	AT2-C3							
2middle	797	0.043	350.5	1.14	0.027	51.6	2.04	1.16
	AT2-C2							
bottom	819	0.030	233.6	0.74	0.026	38.0	0.28	8.22
	AT2-C3							
3top	803	0.026	228.8	84.32	0.034	54.1	10.67	0.03
	AT2-C1							
middle	798	0.044	358.4	1.30	0.027	29.9	0.93	1.78
	AT2-C2							
bottom	839	0.038	326.1	1.26	0.030	58.6	10.73	0.74
	AT2-C3							
3top	788	0.026	231.3	23.39	0.034	55.0	23.22	0.02
	AT2-C1							
middle	796	0.044	363.1	1.21	0.027	30.7	1.18	1.53
	AT2-C2							
bottom	813	0.032	263.3	1.10	0.027	44.6	1.82	1.28
	AT2-C3							
5top	301	0.029	252.6	9.97	0.037	63.0	2.25	0.33
	AT2-C1							
middle	371	0.056	480.6	5.18	0.032	48.3	1.01	1.07
	AT2-C2							
bottom	431	0.055	447.2	3.12	0.037	86.1	12.54	0.20
	AT2-C3							
5top	336	0.029	252.8	15.86	0.037	63.1	1.92	0.39
	AT2-C1							
middle	385	0.057	483.9	4.38	0.032	48.7	1.37	0.73
	AT2-C2							
bottom	503	0.048	405.4	3.41	0.035	76.6	1.30	0.83

	AT2-C3							

unverified members in SLV+

SLV-		x(m)	M_{Rd1}(kNm)	safety factor	x	M_{Rd2}	safety factor	biaxial
2middle	799	0.076	612.8	4.19	0.029	37.7	1.17	0.91
	AT2-C2							
bottom	833	0.083	578.1	5.16	0.046	116.5	5.63	0.16
	AT2-C3							
2middle	797	0.076	611.4	3.92	0.029	63.0	2.44	0.39
	AT2-C2							
bottom	819	0.089	600.7	1.49	0.047	121.9	0.92	1.68
	AT2-C3							
5top	336	0.030	256.6	6.21	0.037	64.6	1.96	0.43
	AT2-C1							
middle	385	0.058	491.7	5.00	0.029	38.0	1.06	1.00
	AT2-C2							
bottom	503	0.049	409.1	4.80	0.035	77.4	1.31	0.76
	AT2-C3							
13top	271	0.030	260.2	4.72	0.038	65.9	2.29	0.39
	AT2-C1							
middle	359	0.058	495.0	15.44	0.029	38.8	0.88	1.23
	AT2-C2							
bottom	400	0.048	403.3	4.13	0.038	89.5	5.37	0.20
	AT2-C3							
13top	266	0.030	260.0	5.87	0.038	65.8	1.91	0.45
	AT2-C1							
middle	357	0.058	497.4	7.59	0.029	38.0	1.06	0.97
	AT2-C2							
bottom	467	0.050	413.6	5.37	0.035	78.4	1.35	0.72
	AT2-C3							

unverified members in SLV-

P1L1 members

s3	P1L1	x	M_{Rd1}	safety factor	x	M_{Rd2}	safety factor	biaxial
1	725	0.024	67.8	1.4	0.024	67.8	87.3	0.6
		0.019	61.9	0.9	0.019	61.9	38.9	1.3
2	710	0.025	69.7	1.3	0.025	69.7	366.4	0.7
		0.021	63.8	0.9	0.021	63.8	182.0	1.2
3	696	0.025	69.4	1.2	0.025	69.4	6543.1	0.7
		0.02	63.5	0.9	0.02	63.5	1469.0	1.2
4	136	0.025	69.7	1.2	0.025	69.7	4525.3	0.8
		0.021	63.8	0.8	0.021	63.8	3866.3	1.3
5	121	0.025	69.7	1.2	0.025	69.7	8300.4	0.8
		0.021	63.8	0.8	0.021	63.8	6447.3	1.3
6	106	0.025	69.5	1.2	0.025	69.5	36554.6	0.8
		0.02	63.6	0.9	0.02	63.6	15132.7	1.2
7	91	0.025	69.4	1.2	0.025	69.4	14775.2	0.8
		0.02	63.5	0.9	0.02	63.5	37380.7	1.2
8	76	0.025	69.2	1.2	0.025	69.2	4644.6	0.7
		0.02	63.3	0.9	0.02	63.3	4306.7	1.2
9	61	0.025	69.5	1.2	0.025	69.5	2968.9	0.8
		0.02	63.6	0.9	0.02	63.6	2605.5	1.3
10	46	0.025	69.5	1.2	0.025	69.5	2055.0	0.8
		0.02	63.6	0.9	0.02	63.6	1686.0	1.2
11	32	0.025	69.4	1.2	0.025	69.4	18746.1	0.7
		0.02	63.5	0.9	0.02	63.5	2094.5	1.2
12	23	0.025	69.4	1.2	0.025	69.4	347.6	0.7
		0.02	63.5	0.9	0.02	63.5	179.6	1.1
13	13	0.023	67.4	1.4	0.023	67.4	88.6	0.6
		0.019	61.5	0.9	0.019	61.5	39.0	1.2

unverified P1L1 in s3

SLV−	P1L1	x	M_{Rd1}	safety factor	x	M_{Rd2}	safety factor	biaxial
1	725	0.020	66.7	1.46	0.020	66.7	1.32	1.23
		0.018	62.7	1.49	0.018	62.7	0.87	1.77
2	710	0.020	66.2	0.85	0.020	66.2	1.21	2.02

		0.017	62.2	66.29	0.017	62.2	0.76	1.52
3	696	0.019	65.2	0.84	0.019	65.2	1.21	2.04
		0.017	61.2	23.40	0.017	61.2	0.77	1.50
4	136	0.019	64.7	1.32	0.019	64.7	1.20	1.43
		0.016	60.7	1.38	0.016	60.7	0.76	2.14
5	121	0.019	64.7	1.33	0.019	64.7	1.20	1.41
		0.016	60.7	1.34	0.016	60.7	0.76	2.16
6	106	0.019	64.7	1.28	0.019	64.7	1.20	1.45
		0.016	60.7	1.42	0.016	60.7	0.76	2.11
7	91	0.019	64.6	1.25	0.019	64.6	1.20	1.48
		0.016	60.6	1.47	0.016	60.6	0.76	2.08
8	76	0.019	64.7	1.26	0.019	64.7	1.20	1.46
		0.016	60.7	1.46	0.016	60.7	0.76	2.09
9	61	0.019	64.7	1.32	0.019	64.7	1.20	1.43
		0.016	60.6	1.36	0.016	60.6	0.76	2.15
10	46	0.019	64.8	1.31	0.019	64.8	1.20	1.43
		0.016	60.8	1.40	0.016	60.8	0.76	2.12
11	32	0.019	65.1	0.84	0.019	65.1	1.21	2.04
		0.017	61.0	20.75	0.017	61.0	0.76	1.51
12	23	0.020	66.0	0.87	0.020	66.0	1.20	2.00
		0.017	62.0	50.61	0.017	62.0	0.76	1.52
13	13	0.020	66.8	1.34	0.020	66.8	1.35	1.28

unverified P1L1 in SLV-

Table 72: neutral axis, bending moment resistance, and verification, Secondary body

Design value, Secondary body

verified case

w6		shear1(kN)	BM1(kNm)	shear2	BM2	Axial (kN)	Torque (kN)
3top	803	−14.6	−38.9	−0.4	0.7	−182.8	0.1
	AT2−C1	1.1	−51.2	−0.4	0.1	−193.8	0.1
middle	798	−61.3	121.6	−0.3	0.8	−243.8	1.6
	AT2−C2	−47.0	67.9	−0.3	0.5	−232.9	1.6
bottom	839	119.5	131.5	−0.5	−1.4	−375.5	0.7
	AT2−C3	120.0	184.0	−0.5	−1.6	−367.4	0.7
3top	788	−18.8	−106.6	0.4	−1.0	−148.3	0.0
	AT2−C1	4.3	−119.9	0.4	−0.2	−159.3	0.0
middle	796	−76.7	111.5	0.2	0.0	−213.1	−1.2
	AT2−C2	−59.9	47.5	0.2	0.2	−202.3	−1.2
bottom	813	70.8	229.1	0.6	1.4	−270.0	−1.7
	AT2−C3	73.9	261.0	0.6	1.6	−262.2	−1.7
5top	301	−20.3	−29.4	0.0	0.0	−178.2	0.0
	AT2−C1	−7.1	−50.5	0.0	0.0	−187.4	0.0
middle	371	−63.9	132.5	0.0	0.1	−245.8	0.0
	AT2−C2	−48.1	71.1	0.0	0.1	−233.9	0.0
bottom	431	−119.9	177.6	0.0	0.0	−366.3	0.1
	AT2−C3	−119.3	123.1	0.0	0.0	−374.7	0.1
5top	336	−27.2	−96.4	0.0	−0.1	−141.0	0.0
	AT2−C1	−7.8	−123.4	0.0	0.0	−150.3	0.0
middle	385	−87.2	155.7	0.0	−0.1	−216.3	0.0
	AT2−C2	−64.8	60.7	0.0	−0.1	−201.9	0.0
bottom	503	69.6	213.8	0.0	−0.1	−264.0	−0.1
	AT2−C3	72.8	246.5	0.0	−0.1	−255.8	−0.1

SLV+	P1	shear1(kN)	BM1(kNm)	shear2	BM2	Axial (kN)	Torque (kN)
1	777	5.1	31.7	4.7	12.3	−59.9	3.5
2	773	0.0	80.7	7.1	18.3	−18.1	2.4

3	774	−0.6	75.0	7.2	17.6	−14.3	2.2
4	242	−2.5	32.4	3.3	9.7	−76.3	2.1
5	243	−2.5	30.4	3.1	8.7	−89.6	1.5
6	244	−1.4	31.4	2.8	8.6	−90.4	1.3
7	245	−0.7	32.1	2.8	8.6	−90.6	1.2
8	246	−1.0	31.8	2.9	8.6	−90.3	1.4
9	247	−2.0	30.6	3.1	8.7	−89.4	1.6
10	248	−2.0	33.1	3.4	9.5	−75.9	2.2
11	249	0.3	76.5	7.2	18.7	−7.2	2.4
12	250	−0.1	74.7	6.9	17.6	−7.9	2.2
13	251	−1.9	36.4	3.5	11.0	−62.1	2.5

Unverified case

SLV+		shear1(kN)	BM1(kNm)	shear2	BM2	Axial (kN)	Torque (kN)
2middle	799	−25.1	283.1	12.5	31.5	67.8	7.9
	AT2-C2	−15.0	249.0	12.5	34.7	75.4	7.9
bottom	833	155.4	376.8	31.1	18.8	−12.9	46.0
	AT2-C3	155.8	376.1	31.1	22.2	−18.9	46.0
2middle	797	−22.6	307.3	10.8	25.3	60.5	8.1
	AT2-C2	−13.4	279.2	10.8	27.7	68.2	8.1
bottom	819	283.1	315.1	93.9	134.4	130.8	33.1
	AT2-C3	283.5	375.1	93.9	145.5	134.1	33.1
3top	803	14.4	−2.7	1.3	5.1	−31.6	5.7
	AT2-C1	25.1	−19.7	1.3	4.7	−39.1	5.7
middle	798	−26.6	275.8	12.0	32.1	48.2	10.0
	AT2-C2	−16.5	241.1	12.0	34.8	55.8	10.0
bottom	839	255.9	259.3	29.7	5.5	−31.3	47.2
	AT2-C3	256.3	263.2	29.7	2.5	−25.3	47.2
3top	788	19.2	9.9	2.0	2.4	−38.7	1.5
	AT2-C1	29.9	−4.9	2.0	2.8	−46.2	1.5
middle	796	−22.5	299.8	11.0	26.1	40.8	6.1
	AT2-C2	−13.3	271.8	11.0	28.6	48.4	6.1
bottom	813	258.2	239.6	9.8	24.5	78.7	30.7

	AT2-C3	258.9	251.0	9.8	25.7	84.7	30.7
5top	301	-11.1	-25.3	4.2	28.0	-98.2	5.9
	AT2-C1	-2.2	-39.6	4.2	28.0	-104.5	5.9
middle	371	-42.4	92.7	17.2	47.7	-144.3	5.9
	AT2-C2	-31.3	48.5	17.2	52.1	-135.9	5.9
bottom	431	-43.6	143.3	34.8	6.9	-244.8	43.6
	AT2-C3	-43.2	116.7	34.8	7.9	-251.1	43.6
5top	336	-10.0	-15.9	4.5	32.8	-98.9	6.2
	AT2-C1	-1.0	-26.8	4.5	31.9	-105.2	6.2
middle	385	-39.1	110.6	17.8	35.6	-149.5	5.5
	AT2-C2	-26.9	64.4	17.8	40.7	-139.4	5.5
bottom	503	78.4	118.8	21.8	58.9	-170.8	44.4
	AT2-C3	79.2	152.2	21.8	61.3	-164.6	44.4

SLV-		shear1(kN)	BM1(kNm)	shear2	BM2	Axial (kN)	Torque (kN)
2middle	799	-62.3	-146.2	-12.1	-32.3	-354.5	-10.0
	AT2-C2	-52.2	-188.9	-12.1	-35.0	-346.8	-10.0
bottom	833	-261.5	-112.1	-30.7	-20.7	-480.2	-46.7
	AT2-C3	-261.1	-157.6	-30.7	-23.9	-486.2	-46.7
2middle	797	-53.2	-156.1	-10.9	-25.8	-352.2	-6.4
	AT2-C2	-44.0	-190.5	-10.9	-28.3	-344.6	-6.4
bottom	819	-154.4	-403.1	-97.5	-131.8	-521.9	-31.2
	AT2-C3	-154.0	-397.9	-97.5	-144.8	-518.6	-31.2
5top	336	-12.7	-41.3	-4.5	-32.9	-109.5	-6.3
	AT2-C1	-3.7	-51.7	-4.5	-31.9	-115.8	-6.3
middle	385	-48.1	98.4	-17.8	-35.8	-161.8	-5.5
	AT2-C2	-35.9	50.9	-17.8	-40.8	-151.6	-5.5
bottom	503	62.7	85.2	-21.8	-59.0	-177.5	-44.6
	AT2-C3	63.5	116.9	-21.8	-61.5	-171.2	-44.6
13top	271	-19.2	-55.1	-5.1	-28.8	-119.6	-6.6
	AT2-C1	-10.2	-69.8	-5.1	-28.8	-125.9	-6.6
middle	359	-49.4	32.1	-17.9	-44.2	-167.1	-6.6

	AT2-C2	-38.3	-11.6	-17.9	-48.7	-158.7	-6.6
bottom	400	-76.6	97.6	-23.8	-16.7	-270.7	-49.2
	AT2-C3	-76.2	74.1	-23.8	-14.9	-276.9	-49.2
13top	266	-16.5	-44.3	-4.0	-34.4	-119.0	-7.9
	AT2-C1	-7.6	-56.6	-4.0	-33.3	-125.3	-7.9
middle	357	-48.1	65.5	-17.7	-36.0	-170.9	-7.1
	AT2-C2	-35.8	18.7	-17.7	-40.9	-160.8	-7.1
bottom	467	41.3	77.0	-21.7	-58.1	-185.3	-45.9
	AT2-C3	42.1	106.0	-21.7	-60.5	-179.1	-45.9

P1L1 members

s3	P1L1	shear1(kN)	BM1(kNm)	shear2	BM2	axial(kN)	torque(kN)
1	725	25.9	-49.9	0.48	-0.78	-157.2	0.08
		23.0	71.7	0.48	1.59	-128.7	0.08
2	710	28.4	-55.2	-0.11	0.19	-166.3	0.09
		22.5	71.5	-0.11	-0.35	-137.8	0.09
3	696	28.8	-56.4	0.01	-0.01	-164.6	0.00
		22.9	72.4	0.01	0.04	-136.0	0.00
4	136	29.9	-59.0	-0.01	0.02	-166.2	0.02
		24.0	75.2	-0.01	-0.02	-137.7	0.02
5	121	30.3	-60.1	0.00	0.01	-166.4	0.00
		24.5	76.4	0.00	-0.01	-137.8	0.00
6	106	29.4	-58.0	0.00	0.00	-165.0	-0.01
		23.5	73.5	0.00	0.00	-136.5	-0.01
7	91	29.3	-58.0	0.00	0.00	-165.0	0.00
		23.5	73.4	0.00	0.00	-136.5	0.00
8	76	28.8	-57.0	0.01	-0.01	-163.8	0.00
		22.9	71.8	0.01	0.01	-135.3	0.00
9	61	29.6	-58.6	0.01	-0.02	-165.1	0.00
		23.7	74.0	0.01	0.02	-136.6	0.00
10	46	29.3	-57.9	0.01	-0.03	-165.1	-0.02
		23.4	73.3	0.01	0.04	-136.5	-0.02
11	32	29.0	-56.9	-0.01	0.00	-164.6	0.01
		23.1	72.7	-0.01	-0.03	-136.1	0.01

12	23	28.1	−55.6	0.11	−0.20	−164.9	−0.08
		22.2	69.5	0.11	0.35	−136.4	−0.08
13	13	25.2	−49.7	−0.47	0.76	−155.2	−0.08
		22.3	68.5	−0.47	−1.58	−126.7	−0.08

s3

SLV−	P1L1	shear1(kN)	BM1(kNm)	shear2	BM2	axial(kN)	torque(kN)
1	725	15.1	−45.8	−18.2	−50.5	−139.7	−19.6
		15.1	42.1	−18.2	−71.9	−118.5	−19.6
2	710	5.7	−77.5	−21.7	−54.9	−136.7	−16.2
		5.7	0.9	−21.7	−82.2	−115.5	−16.2
3	696	6.1	−77.3	−21.0	−53.9	−131.5	−16.5
		6.1	2.6	−21.0	−79.9	−110.3	−16.5
4	136	16.0	−49.2	−21.1	−54.1	−129.0	−15.3
		16.0	44.1	−21.1	−80.4	−107.9	−15.3
5	121	16.3	−48.6	−21.1	−54.0	−129.1	−15.5
		16.3	45.2	−21.1	−80.2	−107.9	−15.5
6	106	15.8	−50.4	−21.1	−54.0	−128.9	−15.7
		15.8	42.8	−21.1	−80.2	−107.8	−15.7
7	91	15.5	−51.6	−21.1	−54.0	−128.2	−15.7
		15.5	41.2	−21.1	−80.2	−107.1	−15.7
8	76	15.5	−51.2	−21.1	−54.0	−129.0	−15.5
		15.5	41.6	−21.1	−80.2	−107.8	−15.5
9	61	16.2	−49.1	−21.1	−54.0	−128.7	−15.5
		16.2	44.5	−21.1	−80.2	−107.6	−15.5
10	46	15.9	−49.6	−21.1	−54.1	−129.7	−15.4
		15.9	43.6	−21.1	−80.3	−108.6	−15.4
11	32	6.3	−77.0	−21.0	−53.8	−130.8	−16.5
		6.3	2.9	−21.0	−79.9	−109.7	−16.5
12	23	5.9	−75.8	−21.6	−55.2	−135.6	−16.0
		5.9	1.2	−21.6	−81.7	−114.4	−16.0
13	13	15.0	−49.7	−18.9	−49.3	−139.9	−19.7
		15.0	40.6	−18.9	−74.1	−118.8	−19.7

SLV-

Shear Force

Again, here plane 1 and plane 2 is examined. As mentioned, plane1 is in-plane direction and plane2 is out-of-plane direction.

In **static analysis**, Principle body is verified in any combination of the load case. As for Secondary body only in w6, the structure is verified, and in the other cases most of the P1L1 is not verified. There are 2 mentions about the spacing on P1L1 in ENCO:250, 160(mm) (fig). Presumably, it tells that the spacing of the stirrup is between 160 and 250 (mm)-probably the spacing becomes narrow at the both end. At any rate, when the spacing is 250 (mm), P1L1 are not verified in above-mentioned cases, but when the spacing becomes 160 (mm), in case of w5, s5 and s6 P1L1 still are not verified.

In **seismic analysis**, Principle body is verified again in SLV+ and SLV-. In Secondary body, In SLV+ in case of spacing of 250 (mm), P1L1 is not verified. On the other hand, in SLV- the whole structure is verified.

In both static and seismic analysis, most of P1L1 members are not verified throughout the arch and hence, obvious steel-brace effect is not confirmed unlike bending-moment verification except for SLV+, though beams in 2^{nd}, 3^{rd}, 11^{th} and 12^{th} arches undergo higher values of shear force compared to the other arches.

Property of the cross section

Principle	b_w (m)	d(m)	z(m)	diameter(mm)	$A_{sw}(m^2)$	spacing(m)	A_{sw}/s
AT01-C2	0.3	1.3	1.17	8	0.000101	0.2	0.000503
AT01-C3	0.3	1	0.9	8	0.000101	0.25	0.000402
AT01-C5	0.3	1	0.9	8	0.000101	0.2	0.000503
AT02-C1	0.35	1.4	1.26	8	0.000101	0.2	0.000503
AT02-C2	0.3	1.3	1.17	8	0.000101	0.2	0.000503
AT02-C3	0.3	1	0.9	10	0.000157	0.25	0.000628
AT03-C1	0.5	1.4	1.26	8	0.000101	0.25	0.000402
AT03-C2	0.5	1.3	1.17	8	0.000101	0.2	0.000503
AT03-C3	0.4	1	0.9	7	0.000077	0.3	0.000257
AT04-3	0.3	1	0.9	8	0.000101	0.3	0.000335
T1	0.25	0.5	0.45	9	0.000127	0.25	0.000509
P1	0.25	0.5	0.45	8	0.000101	0.25	0.000402

Secondary	b_w (m)	d(m)	z(m)	diameter(mm)	$A_{sw}(m^2)$	spacing(m)	A_{sw}/s
AT1-C1	0.35	0.75	0.675	8	0.000101	0.2	0.000503
AT1-C2	0.35	1.35	1.215	8	0.000101	0.25	0.000402
AT1-C3	0.35	1.2	1.08	6	0.000057	0.2	0.000283
AT2-C1	0.35	0.75	0.675	8	0.000101	0.2	0.000503
AT2-C2	0.35	1.35	1.215	8	0.000101	0.2	0.000503
AT2-C3	0.35	1.2	1.08	6	0.000057	0.2	0.000283
TC1-C2	0.24	1.15	1.035	8	0.000101	0.7	0.000144
TC2-C2	0.34	1.15	1.035	8	0.000101	0.7	0.000144
P1L1	0.4	0.4	0.36	6	0.000057	0.25	0.000226
P1	0.25	0.5	0.45	8	0.000101	0.25	0.000402

Table 73: the property of the cross-section for the shear-force resistance, Principle body and Secondary body (below)

verification, Principle body

SLV+	Bm no	v_{Ed1}(kN)	verification	v_{Ed2}	verification
3 top	259	0.073	0.00037	0.041	0.00039
	AT02-C3				
middle	17	0.079	0.00048	0.059	0.00048
	AT01-C2				
bottom	356	0.093	0.00047	0.085	0.00047
	AT01-C1				
3 top	241	0.199	0.00032	0.099	0.00036
	AT02-C3				
middle	20	0.104	0.00047	0.076	0.00048
	AT01-C2				
bottom	344	0.077	0.00048	0.063	0.00048
	AT01-C1				
P1	386	0.267	0.00022	0.475	0.00009
SLV-					
P1	386	-0.402	0.00013	-0.474	0.00009

Table 74: the design applied value of shear stress and verification*, Principle body

*verification signifies: $A_{sw}/s\text{-}v_{Ed}*b_w/(b_w*f_{ywd}*\cot\theta)>0$, $\cot\theta=2.5$

design value, Principle body

SLV+	Bm no	shear1(kN)	BM1(kNm)	shear2	BM2	Axial (kN)	Torque (kN)
3 top	259	19.7	-13.9	11.1	25.0	-73.7	3.8
	AT02-C3	31.0	29.5	11.1	30.4	-64.3	3.8
middle	17	27.7	42.4	20.6	70.0	-150.1	8.3
	AT01-C2	39.1	89.3	20.6	82.3	-127.4	8.3
bottom	356	25.2	225.5	23.1	77.3	-238.1	11.2
	AT01-C1	32.2	245.7	23.1	88.7	-213.3	11.2
3 top	241	20.8	-3.8	17.0	25.2	-43.7	9.4
	AT02-C3	32.1	38.4	17.0	33.0	-34.4	9.4
middle	20	36.7	48.5	26.8	83.7	-122.1	9.5
	AT01-C2	48.0	87.5	26.8	99.3	-99.5	9.5

bottom	344	53.6	226.4	26.8	85.4	−210.5	18.0
	AT01−C1	60.6	277.5	26.8	100.0	−185.6	18.0
P1	386	30.1	74.6	53.4	85.1	−103.0	3.9
SLV−							
P1	386	−45.3	−42.7	−53.3	−80.6	−124.8	−3.8

Table 75: the design value of applied force including shear force. Principle body verification, Secondary body

w6	Bm no	v_{Ed1}(kN)	verification	v_{Ed2}	verification
3top	803	−0.0616	0.000459	−0.0015	0.000502
	AT2−C1				
middle	798	−0.1442	0.000445	−0.0008	0.000502
	AT2−C2				
bottom	839	0.3162	0.000141	−0.0014	0.000282
	AT2−C3				
3top	788	−0.0794	0.000446	0.0018	0.000501
	AT2−C1				
middle	796	−0.1803	0.000431	0.0005	0.000502
	AT2−C2				
bottom	813	0.1874	0.000199	0.0015	0.000282
	AT2−C3				
7top	291	−0.0854	0.000442	−0.0001	0.000503
	AT1−C1				
middle	367	−0.1505	0.000342	−0.0001	0.000402
	AT1−C2				
bottom	419	−0.3209	0.000139	0.0001	0.000283
	AT1−C3				
7top	326	−0.1149	0.000420	0.0001	0.000503
	AT1−C1				
middle	381	−0.2050	0.000321	0.0001	0.000402
	AT1−C2				
bottom	491	0.1837	0.000201	0.0001	0.000283
	AT1−C3				

Verified in static analysis

P1L1 members

s6	P1L1	v_{Ed1}(kN)	verification	v_{Ed2}	verification
1	725	0.2032	−0.000085	0.0034	0.000221
		0.1828	−0.000054	0.0034	0.000221
2	710	0.2394	−0.000141	−0.0007	0.000225
		0.1985	−0.000078	−0.0007	0.000225
3	696	0.2431	−0.000147	0.0001	0.000226
		0.2022	−0.000084	0.0001	0.000226
4	136	0.2454	−0.000150	0.0000	0.000226
		0.2045	−0.000087	0.0000	0.000226
5	121	0.2494	−0.000156	0.0000	0.000226
		0.2085	−0.000093	0.0000	0.000226
6	106	0.2459	−0.000151	0.0000	0.000226
		0.2050	−0.000088	0.0000	0.000226
7	91	0.2459	−0.000151	0.0000	0.000226
		0.2050	−0.000088	0.0000	0.000226
8	76	0.2421	−0.000145	0.0000	0.000226
		0.2012	−0.000082	0.0000	0.000226
9	61	0.2456	−0.000150	0.0001	0.000226
		0.2047	−0.000088	0.0001	0.000226
10	46	0.2455	−0.000150	0.0001	0.000226
		0.2046	−0.000088	0.0001	0.000226
11	32	0.2432	−0.000147	0.0000	0.000226
		0.2023	−0.000084	0.0000	0.000226
12	23	0.2360	−0.000136	0.0007	0.000225
		0.1951	−0.000073	0.0007	0.000225
13	13	0.1967	−0.000075	−0.0033	0.000221
		0.1764	−0.000044	−0.0033	0.000221

s6, s=0.25

s6	P1L1	v_{Ed1}(kN)	verification	v_{Ed2}	verification
1	725	0.2032	0.000042	0.0034	0.000348
		0.1828	0.000073	0.0034	0.000348
2	710	0.2394	−0.000014	−0.0007	0.000352

		0.1985	0.000049	−0.0007	0.000352
3	696	0.2431	−0.000019	0.0001	0.000353
		0.2022	0.000043	0.0001	0.000353
4	136	0.2454	−0.000023	0.0000	0.000353
		0.2045	0.000040	0.0000	0.000353
5	121	0.2494	−0.000029	0.0000	0.000353
		0.2085	0.000034	0.0000	0.000353
6	106	0.2459	−0.000024	0.0000	0.000353
		0.2050	0.000039	0.0000	0.000353
7	91	0.2459	−0.000024	0.0000	0.000353
		0.2050	0.000039	0.0000	0.000353
8	76	0.2421	−0.000018	0.0000	0.000353
		0.2012	0.000045	0.0000	0.000353
9	61	0.2456	−0.000023	0.0001	0.000353
		0.2047	0.000039	0.0001	0.000353
10	46	0.2455	−0.000023	0.0001	0.000353
		0.2046	0.000040	0.0001	0.000353
11	32	0.2432	−0.000020	0.0000	0.000353
		0.2023	0.000043	0.0000	0.000353
12	23	0.2360	−0.000008	0.0007	0.000352
		0.1951	0.000054	0.0007	0.000352
13	13	0.1967	0.000052	−0.0033	0.000348
		0.1764	0.000083	−0.0033	0.000348

s6, s=0.16

SLV+	P1L1	v_{Ed1}(kN)	verification	v_{Ed2}	verification
1	725	0.1516	0.000024	0.1315	0.000051
		0.1517	0.000024	0.1315	0.000051
2	710	0.2255	−0.000075	0.1499	0.000026
		0.2257	−0.000075	0.1499	0.000026
3	696	0.2258	−0.000075	0.1457	0.000032
		0.2259	−0.000075	0.1457	0.000032
4	136	0.1614	0.000011	0.1466	0.000031
		0.1615	0.000011	0.1466	0.000031

5	121	0.1594	0.000014	0.1462	0.000031
		0.1595	0.000013	0.1462	0.000031
6	106	0.1633	0.000008	0.1463	0.000031
		0.1635	0.000008	0.1463	0.000031
7	91	0.1657	0.000005	0.1463	0.000031
		0.1658	0.000005	0.1463	0.000031
8	76	0.1650	0.000006	0.1462	0.000031
		0.1651	0.000006	0.1462	0.000031
9	61	0.1602	0.000013	0.1463	0.000031
		0.1603	0.000012	0.1463	0.000031
10	46	0.1623	0.000010	0.1466	0.000031
		0.1625	0.000010	0.1466	0.000031
11	32	0.2246	−0.000073	0.1455	0.000032
		0.2247	−0.000073	0.1455	0.000032
12	23	0.2182	−0.000065	0.1510	0.000025
		0.2183	−0.000065	0.1510	0.000025
13	13	0.1616	0.000011	0.1265	0.000058
		0.1618	0.000011	0.1265	0.000058

SLV+, s=0.25

SLV+	P1L1	v_{Ed1}(kN)	verification	v_{Ed2}	verification
1	725	0.1516	0.000151	0.1315	0.000178
		0.1517	0.000151	0.1315	0.000178
2	710	0.2255	0.000053	0.1499	0.000154
		0.2257	0.000053	0.1499	0.000154
3	696	0.2258	0.000052	0.1457	0.000159
		0.2259	0.000052	0.1457	0.000159
4	136	0.1614	0.000138	0.1466	0.000158
		0.1615	0.000138	0.1466	0.000158
5	121	0.1594	0.000141	0.1462	0.000158
		0.1595	0.000141	0.1462	0.000158
6	106	0.1633	0.000136	0.1463	0.000158
		0.1635	0.000135	0.1463	0.000158
7	91	0.1657	0.000133	0.1463	0.000158

		0.1658	0.000132	0.1463	0.000158
8	76	0.1650	0.000133	0.1462	0.000158
		0.1651	0.000133	0.1462	0.000158
9	61	0.1602	0.000140	0.1463	0.000158
		0.1603	0.000140	0.1463	0.000158
10	46	0.1623	0.000137	0.1466	0.000158
		0.1625	0.000137	0.1466	0.000158
11	32	0.2246	0.000054	0.1455	0.000159
		0.2247	0.000054	0.1455	0.000159
12	23	0.2182	0.000062	0.1510	0.000152
		0.2183	0.000062	0.1510	0.000152
13	13	0.1616	0.000138	0.1265	0.000185
		0.1618	0.000138	0.1265	0.000185

SLV-, s=0.16

Table 76: the design applied value of shear stress and verification, Secondary body

from the top, verified part in w6, P1L1 in s6 with 250mm spacing, in s6 with 160mm in SLV- with 250mm and in SLV- with 160mm

design value, Secondary body

w6	Bm no	shear1(kN)	BM1(kNm)	shear2	BM2	Axial (kN)	Torque (kN)
3top	803	−14.6	−38.9	−0.4	0.7	−182.8	0.070
	AT2-C1	1.1	−51.2	−0.4	0.1	−193.8	0.070
middle	798	−61.3	121.6	−0.3	0.8	−243.8	1.596
	AT2-C2	−47.0	67.9	−0.3	0.5	−232.9	1.596
bottom	839	119.5	131.5	−0.5	−1.4	−375.5	0.693
	AT2-C3	120.0	184.0	−0.5	−1.6	−367.4	0.693
3top	788	−18.8	−106.6	0.4	−1.0	−148.3	0.026
	AT2-C1	4.3	−119.9	0.4	−0.2	−159.3	0.026
middle	796	−76.7	111.5	0.2	0.0	−213.1	−1.223
	AT2-C2	−59.9	47.5	0.2	0.2	−202.3	−1.223
bottom	813	70.8	229.1	0.6	1.4	−270.0	−1.665
	AT2-C3	73.9	261.0	0.6	1.6	−262.2	−1.665

7top	291	−20.2	−29.1	0.0	0.0	−177.9	0.000
	AT1−C1	−7.0	−50.1	0.0	0.0	−187.2	0.000
middle	367	−64.0	133.7	0.0	0.2	−245.6	0.004
	AT1−C2	−48.2	72.2	0.0	0.1	−233.7	0.004
bottom	419	−121.3	179.1	0.0	−0.1	−355.1	0.112
	AT1−C3	−120.8	123.9	0.0	0.0	−363.5	0.112
7top	326	−27.1	−96.5	0.0	−0.1	−140.7	−0.008
	AT1−C1	−7.8	−123.6	0.0	0.0	−150.0	−0.008
middle	381	−87.2	155.6	0.0	−0.1	−216.1	−0.014
	AT1−C2	−64.9	60.6	0.0	−0.1	−201.6	−0.014
bottom	491	69.4	214.0	0.0	−0.1	−263.8	−0.114
	AT1−C3	72.6	246.6	0.0	−0.1	−255.6	−0.114

P1L1 members

s6	P1L1	shear1(kN)	BM1(kNm)	shear2	BM2	Axial (kN)	Torque (kN)
1	725	29.3	−57.5	0.5	−0.8	−160.877	0.1104
		26.3	80.9	0.5	1.6	−132.343	0.1104
2	710	34.5	−68.7	−0.1	0.2	−173.074	0.1211
		28.6	88.2	−0.1	−0.3	−144.536	0.1211
3	696	35.0	−70.3	0.0	0.0	−171.341	−0.0025
		29.1	89.3	0.0	0.0	−142.803	−0.0025
4	136	35.3	−71.3	0.0	0.0	−171.814	0.0123
		29.5	90.0	0.0	0.0	−143.277	0.0123
5	121	35.9	−72.4	0.0	0.0	−173.226	−0.0002
		30.0	91.8	0.0	0.0	−144.689	−0.0002
6	106	35.4	−71.5	0.0	0.0	−171.795	−0.0024
		29.5	90.1	0.0	0.0	−143.258	−0.0024
7	91	35.4	−71.5	0.0	0.0	−171.736	−0.0056
		29.5	90.1	0.0	0.0	−143.199	−0.0056
8	76	34.9	−70.5	0.0	0.0	−170.572	−0.0046
		29.0	88.4	0.0	0.0	−142.034	−0.0046
9	61	35.4	−71.4	0.0	0.0	−171.716	−0.0026
		29.5	90.0	0.0	0.0	−143.178	−0.0026

10	46	35.3	−71.3	0.0	0.0	−171.806	−0.0173
		29.5	90.0	0.0	0.0	−143.268	−0.0173
11	32	35.0	−70.4	0.0	0.0	−171.343	0.0139
		29.1	89.4	0.0	0.0	−142.806	0.0139
12	23	34.0	−68.9	0.1	−0.2	−171.588	−0.1189
		28.1	85.7	0.1	0.3	−143.051	−0.1189
13	13	28.3	−56.8	−0.5	0.8	−158.567	−0.1121
		25.4	76.9	−0.5	−1.6	−130.032	−0.1121

SLV+	P1L1	shear1(kN)	BM1(kNm)	shear2	BM2	Axial (kN)	Torque (kN)
1	725	21.8	−26.7	18.9	49.3	−97.3	19.729
		21.9	69.5	18.9	74.2	−76.1	19.729
2	710	32.5	1.3	21.6	55.2	−116.9	16.241
		32.5	113.0	21.6	81.7	−95.8	16.241
3	696	32.5	−0.3	21.0	53.9	−119.5	16.493
		32.5	112.3	21.0	80.0	−98.4	16.493
4	136	23.2	−30.2	21.1	54.1	−122.6	15.367
		23.3	72.0	21.1	80.3	−101.5	15.367
5	121	23.0	−30.9	21.1	54.0	−122.5	15.508
		23.0	71.0	21.1	80.2	−101.3	15.508
6	106	23.5	−29.2	21.1	54.0	−122.7	15.684
		23.5	73.5	21.1	80.2	−101.5	15.684
7	91	23.9	−28.0	21.1	54.0	−123.4	15.688
		23.9	75.1	21.1	80.2	−102.2	15.688
8	76	23.8	−28.3	21.1	53.9	−122.6	15.506
		23.8	74.5	21.1	80.2	−101.5	15.506
9	61	23.1	−30.4	21.1	54.0	−122.8	15.509
		23.1	71.7	21.1	80.2	−101.7	15.509
10	46	23.4	−29.7	21.1	54.0	−122.0	15.326
		23.4	72.5	21.1	80.4	−100.8	15.326
11	32	32.3	−0.4	20.9	53.8	−120.1	16.485
		32.4	111.9	20.9	79.9	−99.0	16.485

12	23	31.4	0.2	21.7	54.9	−115.8	15.976
		31.4	108.9	21.7	82.2	−94.7	15.976
13	13	23.3	−26.8	18.2	50.4	−97.3	19.602
		23.3	73.6	18.2	71.8	−76.2	19.602

Table 77: the design value of applied force including shear force corresponding to the verification result above. Secondary body

5.2.3. Serviceability Limit State-seismic analysis (in-plane earthquake)

Deflection control

As for the deflection control, the same procedure is taken as that of out-of-plane earthquake.

As a result, the minimum upper-limit value is found to be 0.0136 (m)-beam C for Principle body and beam b for Secondary body. On the other hand, the maximum displacement in each load case for each body is shown as below. Hence, with regard to the deflection control, both structures are verified.

Principle	Span(m)	span/250
a	4.8	0.0192
b	12.1	0.0484
c	3.6	0.0144
d	22.5	0.09
A	12	0.048
B	7.8	0.0312
C	3.4	0.0136
D	13.1	0.0524
E	5.6	0.0224

Secondary	span/m	span/250
a	13.1	0.0524
b	3.4	0.0136
c	15	0.06
d	5	0.02

Table 78: the upper limit value for the deflection control, Principle body and Secondary body (below)

Principle		
LC	displacement-xyz (m)	Bm no
SLD+	0.009	395
SLD-	0.0094	378

Seconadry		
LC	displacement-xyz (m)	Bm no
SLD+	0.004	848
SLD-	0.0053	549

Table 79: maximum value of xyz-displacement in seismic analysis, Principle body and Secondary body (below)

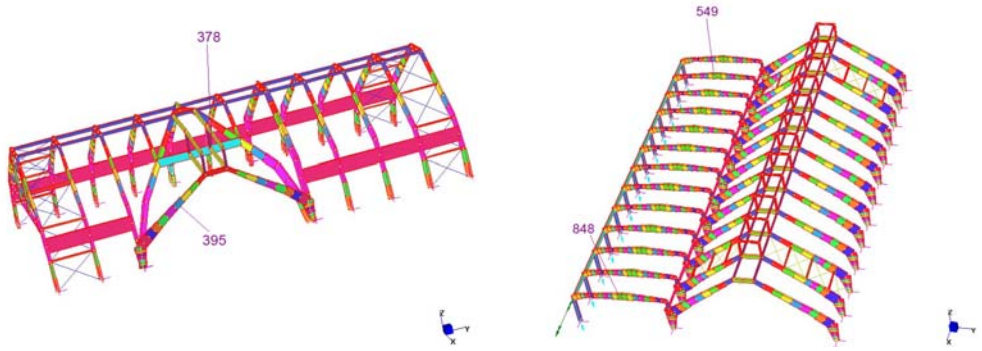

Figure 79: the position of the maximum displacement in SLD+ and SLD- in Principle body and Secondary body (right)

Crack control

As discussed, the maximum w_{max} is set out to be 0.3 mm. Then, the maximum design value of the steel stress is 121.8 (MPa)-at the bottom of 13th arch- in Principle body and 66.3 (MPa)-at the bottom of 3rd arch- in Secondary body. Hence, each allows over 300 (mm) for bar-spacing (Table 80). Hence, each structure is verified in crack control as well.

Steel stress[2] [MPa]	Maximum bar spacing [mm] w_k=0,4 mm	w_k=0,3 mm	w_k=0,2 mm
160	300	300	200
200	300	250	150
240	250	200	100
280	200	150	50
320	150	100	-
360	100	50	-

Table 80: Maximum bar spacing for crack control

(p123, EN 1992-1-1 2004)

Principle	b (mm)	cover(mm)	no of bars	spacing (mm)
AT01-C2	300	30	4	80
AT01-C3	300	30	6	48
AT01-C5	300	38	6	44.8
AT02-C1	350	30	4	96.6
AT02-C2	300	30	4	80
AT02-C3	300	30	4	80
AT03-C1	500	36	4	142.6
AT03-C2	500	50	4	133.3
AT03-C3	400	30	7	56.6
AT04-3	300	30	6	48
T1	250	30	2	190
P1	250	40	3	85

Secondary	b (mm)	cover(mm)	no of bars	spacing (mm)
AT1-C1	350	28	4	98.0
AT1-C2	350	10	4	110.0
AT1-C3	350	30	8	41.4
AT2-C1	350	50	4	83.3
AT2-C2	350	60	4	76.7
AT2-C3	350	65	4	73.3
TC1-C2	240	30	3	90.0
TC2-C2	340	30	3	140.0

Table 81: The cross-section property, Principle body and Secondary body (below)

*the distance between the surface of the reinforcement closest to the nearest concrete lateral surface
As for AT01-C3, AT02-C3, AT03-C3, AT04-C3, T1 and TC1-C2 the value of the cover is not given in ENCO, and hence 30(mm) is assumed.

SLD−		x (m)	ε_c (−)	ε_s (−)	σ_s (MPa)
3top	259	0.213	0.0000436	0.000157	31.4
	AT01−C3	0.213	0.0000213	0.000077	15.3
middle	17	0.237	0.0000052	0.000022	4.5
	AT01−C2	0.208	0.0000110	0.000056	11.2
bottom	356	0.268	0.0000127	0.000052	10.5
	AT01−C1	0.268	0.0000123	0.000051	10.2
3top	241	0.213	0.0000405	0.000146	29.2
	AT01−C3	0.213	0.0000197	0.000071	14.2
middle	20	0.237	0.0000037	0.000016	3.2
	AT01−C2	0.208	0.0000198	0.000100	20.0
bottom	344	0.268	0.0000343	0.000142	28.3
	AT01−C1	0.268	0.0000265	0.000109	21.9
13 top	332	0.259	0.0000426	0.000119	23.8
	AT02−C3	0.259	0.0000641	0.000179	35.8
middle	68	0.237	0.0000706	0.000307	61.4
	AT02−C2	0.237	0.0001147	0.000499	99.8
bottom	351	0.290	0.0002368	0.000562	112.5
	AT02−C1	0.290	0.0001544	0.000367	73.3
P1	386	0.062	0.0000282	0.000067	13.4
		0.062	0.0000112	0.000027	5.3

SLD+		x (m)	ε_c (−)	ε_s (−)	σ_s (MPa)
3top	803	0.148	0.0000065	0.000026	5.2
	AT2−C1	0.148	0.0000150	0.000059	11.9
middle	798	0.190	0.0000438	0.000258	51.5
	AT2−C2	0.190	0.0000259	0.000152	30.4
bottom	839	0.190	0.0000468	0.000275	55.1
	AT2−C3	0.190	0.0000552	0.000325	64.9
3top	788	0.148	0.0000003	0.000001	0.2
	AT2−C1	0.148	0.0000040	0.000016	3.2
middle	796	0.190	0.0000402	0.000237	47.3
	AT2−C2	0.190	0.0000268	0.000157	31.5

bottom	813	0.190	0.0000465	0.000274	54.7
	AT2-C3	0.190	0.0000564	0.000332	66.3
TC/7	84	0.232	0.0000537	0.000206	41.2
	TC2-C2	0.232	0.0000545	0.000209	41.8

Table 82: design value of steel stress including maximum value in Principle body and Secondary body (below)

SLD-		shear1(kN)	BM1(kNm)	shear2	BM2	Axial (kN)	Torque (kN)
3top	259	12.6	-79.8	-3.2	-5.8	-108.5	-0.7
	AT01-C3	24.0	-39.0	-3.2	-7.1	-99.1	-0.7
middle	17	2.9	-12.7	-4.3	-15.7	-183.5	-3.0
	AT01-C2	14.2	24.1	-4.3	-18.0	-160.9	-3.0
bottom	356	-13.7	-38.7	-3.2	-9.0	-344.4	-2.1
	AT01-C1	-6.7	-37.7	-3.2	-10.7	-319.5	-2.1
3top	241	11.1	-74.2	-4.0	-6.8	-111.3	0.2
	AT01-C3	22.4	-36.1	-4.0	-9.0	-102.0	0.2
middle	20	1.5	9.0	-5.2	-15.7	-186.5	-1.0
	AT01-C2	12.9	43.2	-5.2	-19.1	-163.8	-1.0
bottom	344	-1.5	-104.9	-1.7	-9.2	-294.3	-3.8
	AT01-C1	5.5	-81.0	-1.7	-8.9	-269.4	-3.8
13 top	332	-29.0	-95.1	0.7	-6.8	-154.7	-0.2
	AT02-C3	-12.0	-143.1	0.7	-0.4	-165.4	-0.2
middle	68	11.3	175.0	-0.3	-15.3	-432.7	-11.8
	AT02-C2	26.2	284.6	-0.3	-11.3	-410.1	-11.8
bottom	351	61.6	-548.8	-8.7	-44.1	-480.3	-12.5
	AT02-C1	70.8	-357.9	-8.7	-46.4	-455.5	-12.5
P1	386	-13.9	4.5	-3.9	-16.8	-130.2	-1.8
		2.0	1.8	-3.9	-17.4	-130.2	-1.8

SLD+		shear1(kN)	BM1(kNm)	shear2	BM2	Axial (kN)	Torque (kN)
3top	803	−5.8	−6.4	−0.1	0.7	−99.0	0.4
		4.8	−14.7	−0.1	0.2	−106.4	0.4
middle	798	−34.5	97.2	0.0	0.9	−137.9	1.5
		−24.4	57.4	0.0	0.7	−130.3	1.5
bottom	839	89.2	158.3	1.2	−0.2	−249.3	1.7
		89.6	186.6	1.2	−0.6	−243.4	1.7
3top	788	−5.8	−0.3	0.5	−0.4	−96.9	0.4
		4.9	−3.9	0.5	0.1	−104.4	0.4
middle	796	−26.7	89.3	0.6	0.2	−138.7	−0.7
		−17.5	59.4	0.6	0.3	−131.1	−0.7
bottom	813	90.7	157.2	0.8	1.5	−172.0	−1.0
		91.4	190.6	0.8	1.7	−166.0	−1.0
7	84	−4.4	−128.5	0.3	0.3	−15.2	0.2
		4.9	−130.4	0.3	0.4	−14.7	0.2

Table 83: design value of each force corresponding beam Principle body and Secondary body (below)

5.2.4. Ultimate Limit State-seismic analysis (in-plane earthquake)

Axial force

The maximum design value of axial force is found in Table 84. Each maximum design value is compared with the minimum axial-force resistance of each body, and as a result the verification of each body is confirmed.

	seismic	
	N_{Rd}+ (kN)	N_{Rd}− (kN)
AT01−C1	818.1	9288.1
AT01−C2	837.8	8702.8
AT01−C3	1256.6	7306.6
AT01−C5	1047.2	7097.2
AT02−C1	1309.0	11190.7
AT02−C2	837.8	8702.8
AT02−C3	1642.0	7692.0
AT03−C1	837.8	14954.4
AT03−C2	1107.9	14216.3
AT03−C3	1774.0	9840.6
AT04−3	1256.6	7306.6
T1	603.2	1863.6
P1	454.0	2974.8

	seismic	
	N_{Rd}+ (kN)	N_{Rd}− (kN)
AT1−C1	471.2	4846.2
AT1−C2	837.8	8712.8
AT1−C3	1005.3	8005.3
AT2−C1	605.3	4980.3
AT2−C2	529.6	8404.6
AT2−C3	536.2	7536.2
TC1−C2	831.0	4718.0
TC2−C2	904.8	6411.4
P1L1	205.3	2458.6

Table 84: the design axial-force resistance Principle body, Secondary Body (below)

	max. N_{Ed}	Bm no.	min.N_{Ed}	Bm no.
SLV+(p)	102.5	77	−413.9	365
SLV−(p)	68.7	174	−654.4	365
SLV+(s)	20.9	153	−265.5	44
SLV−(s)	3.2	668	−296.8	21

Table 85: the maximum and minimum design value of the applied axial force of the cross-section Principle body, Secondary Body (below)

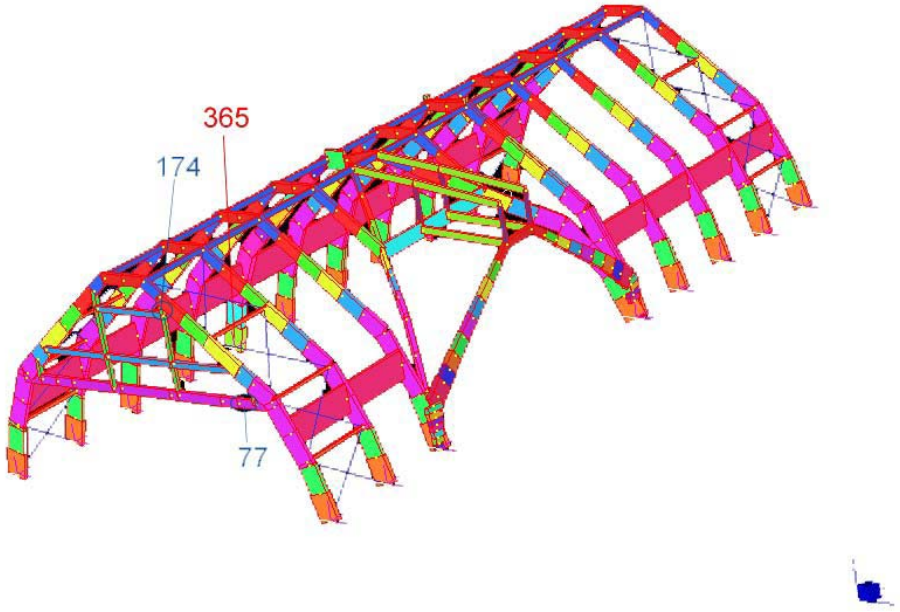

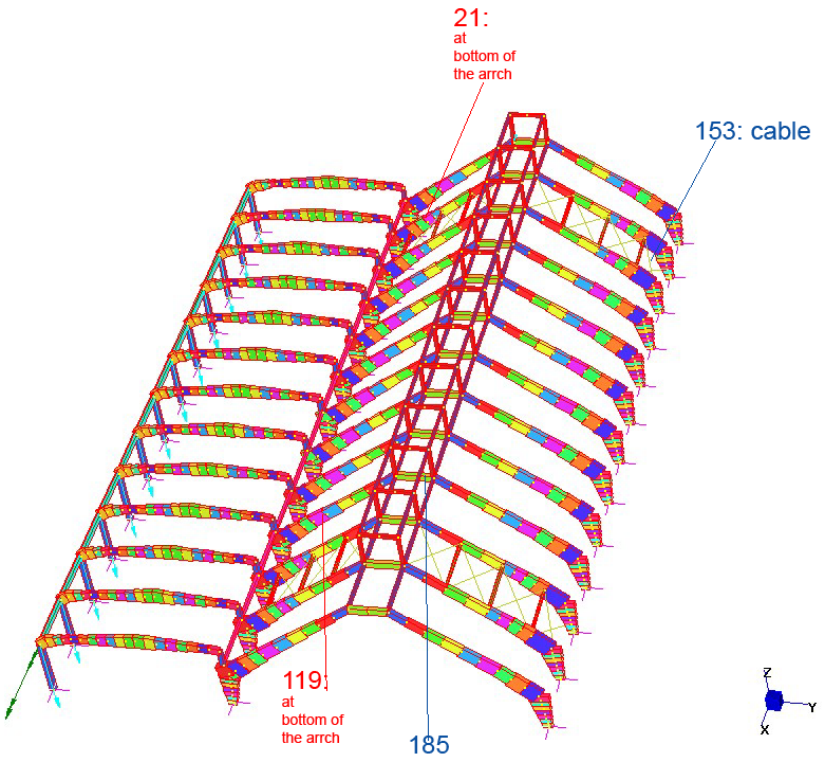

Figure 80: the mapping of the max and min axial force, Principle body and Secondary body (below)

Bending moment

Principle body is always verified. When the result of out-of-plane earthquake in Principle body as discussed, P1 members in Secondary body are likely not to verified, but turned out to be verified. As for Secondary body, P1L1 is not verified.

verification, Principle body

s2		x(m)	M_{Rd1}(kNm)	safety factor	x	M_{Rd2}	Safety f	biaxial
13 top	332	0.0360	777.3	9.4	0.0264	126.8	40.0	0.04
	AT02-C3							
middle	68	0.0978	834.3	3.3	0.0401	163.7	45.3	0.17
	AT02-C2							
bottom	351	0.0730	1214.9	1.7	0.0470	261.4	109.6	0.45
	AT02-C1							
T1	367	0.0480	725.3	2.6				

P1	386	0.0510	124.3	4.7	0.0427	67.5	14.8	0.12

verified members in s2

SLV+		x(m)	M_{Rd1}(kNm)	safety f	x	M_{Rd2}	Safety f	biaxial
13 top	332	0.0332	801.0	40.7	0.0220	133.0	19.0	0.02
	AT02-C3							
middle	68	0.0564	686.6	3.0	0.0260	152.6	3.6	0.34
	AT02-C2							
bottom	351	0.0513	1114.0	3.7	0.0344	259.7	2.4	0.41
	AT02-C1							
T1	367	0.0618	937.1	4.1				
P1	386	0.0726	176.2	0.6	0.0523	83.6	0.7	3.23

including unverified members in SLV+

Table 86: neutral axis, bending-moment resistance, and BM and biaxial-bending verification, Principle body

design value, Principle body

s2		shear1(kN)	BM1(kNm)	shear2	BM2	Axial (kN)	Torque (kN)
13 top	332	−34.3	−82.8	2.8	−3.2	−190.0	4.9
	AT02-C3	−12.3	−146.8	2.8	4.4	−206.1	4.9
middle	68	78.6	255.7	1.2	3.6	−599.4	−9.8
	AT02-C2	96.4	481.7	1.2	6.8	−568.8	−9.8
bottom	351	182.5	−714.3	1.2	−2.4	−663.7	−9.4
	AT02-C1	193.0	−329.5	1.2	0.1	−630.1	−9.4
T1	367	−13.7	−281.5	0.3	5.1	−129.7	0.1
		17.2	−276.0	0.3	5.9	−129.7	0.1
P1	386	−12.4	26.5	0.1	4.6	−162.9	0.0
		13.6	28.3	0.1	4.9	−162.9	0.0

s2

SLV+		shear1(kN)	BM1(kNm)	shear2	BM2	Axial (kN)	Torque (kN)
13 top	332	−19.3	−19.7	5.6	7.0	−24.5	9.0
	AT02-C3	−2.4	−69.2	5.6	12.3	−35.1	9.0

middle	68	105.8	232.4	9.6	42.6	−266.4	2.7
	AT02−C2	120.7	358.6	9.6	43.8	−243.7	2.7
bottom	351	197.1	303.6	27.6	106.6	−339.5	4.0
	AT02−C1	206.3	563.9	27.6	122.8	−314.6	4.0
T1	367	2.5	−165.2	6.8	24.4	−43.1	1.6
		22.1	−158.3	6.8	28.9	−43.1	1.6
P1	386	9.6	45.6	18.0	50.1	−78.4	4.1
		25.6	58.1	18.0	56.9	−78.4	4.1

SLV+

Table 87: the design values corresponding beam, Principle Body

verification, Secondary body

w6	P1L1	x(m)	M_{Rd1}(kNm)	safety f	x	M_{Rd2}	safety f	biaxial
1	725	0.0229	66.8	1.21	0.0229	66.8	88.0	0.75
		0.0186	60.9	0.84	0.0186	60.9	39.3	1.30
2	710	0.0235	67.6	1.03	0.0235	67.6	348.1	0.96
		0.0191	61.7	0.86	0.0191	61.7	168.9	1.26
3	696	0.0232	67.2	1.00	0.0232	67.2	4767.0	1.01
		0.0189	61.3	0.84	0.0189	61.3	1365.6	1.31
4	136	0.0233	67.3	0.99	0.0233	67.3	7827.6	1.02
		0.0189	61.4	0.83	0.0189	61.4	8650.5	1.31
5	121	0.0237	67.8	0.97	0.0237	67.8	29482.4	1.04
		0.0193	61.9	0.81	0.0193	61.9	77388.0	1.38
6	106	0.0233	67.3	0.99	0.0233	67.3	16026.5	1.02
		0.0189	61.4	0.83	0.0189	61.4	5532.6	1.32
7	91	0.0233	67.3	0.99	0.0233	67.3	8108.1	1.02
		0.0189	61.4	0.83	0.0189	61.4	7973.8	1.32
8	76	0.0232	67.2	0.99	0.0232	67.2	4665.1	1.01
		0.0188	61.3	0.84	0.0188	61.3	4472.9	1.30
9	61	0.0233	67.3	0.99	0.0233	67.3	3235.3	1.02
		0.0189	61.4	0.83	0.0189	61.4	3054.5	1.31
10	46	0.0233	67.3	0.99	0.0233	67.3	2033.6	1.02
		0.0189	61.4	0.83	0.0189	61.4	1611.9	1.31

11	32	0.0232	67.2	0.99	0.0232	67.2	35377.2	1.01
		0.0189	61.3	0.84	0.0189	61.3	1588.5	1.31
12	23	0.0233	67.3	1.02	0.0233	67.3	325.4	0.97
		0.0189	61.4	0.89	0.0189	61.4	164.9	1.20
13	13	0.0226	66.4	1.19	0.0226	66.4	89.7	0.77
		0.0183	60.5	0.87	0.0183	60.5	39.5	1.24

w6

SLV-	P1L1	x(m)	M_{Rd1}(kNm)	safety factor	x	M_{Rd2}	safety factor	biaxial
1	725	0.018	64.1	1.0	0.018	64.1	4.0	1.1
		0.016	60.1	3.7	0.016	60.1	2.8	0.4
2	710	0.020	65.8	0.7	0.020	65.8	3.9	1.7
		0.017	61.8	3.6	0.017	61.8	2.4	0.4
3	696	0.019	65.6	0.7	0.019	65.6	3.9	1.8
		0.017	61.6	3.3	0.017	61.6	2.5	0.4
4	136	0.019	65.3	1.0	0.019	65.3	3.9	1.2
		0.017	61.3	3.2	0.017	61.3	2.4	0.4
5	121	0.019	65.2	1.0	0.019	65.2	3.9	1.2
		0.017	61.2	3.5	0.017	61.2	2.5	0.4
6	106	0.019	65.4	0.9	0.019	65.4	3.9	1.4
		0.017	61.4	8.0	0.017	61.4	2.5	0.3
7	91	0.019	65.4	0.8	0.019	65.4	3.9	1.5
		0.017	61.4	67.8	0.017	61.4	2.5	0.3
8	76	0.019	65.4	0.8	0.019	65.4	3.9	1.4
		0.017	61.4	18.0	0.017	61.4	2.5	0.3
9	61	0.019	65.3	0.9	0.019	65.3	3.9	1.3
		0.017	61.2	4.4	0.017	61.2	2.5	0.4
10	46	0.019	65.4	1.0	0.019	65.4	3.9	1.2
		0.017	61.4	3.7	0.017	61.4	2.5	0.4
11	32	0.019	65.7	0.7	0.019	65.7	3.9	1.9
		0.017	61.7	2.5	0.017	61.7	2.5	0.5
12	23	0.020	65.9	0.7	0.020	65.9	3.8	1.9
		0.017	61.9	2.2	0.017	61.9	2.5	0.6

13	13	0.018	64.2	0.9	0.018	64.2	4.3	1.2
		0.016	60.2	4.9	0.016	60.2	2.5	0.3

SLV-

SLV+	P1	x	M_{Rd1}	safety factor	x	M_{Rd2}	safety factor	biaxial
1	777	0.0	121	3.7	0.0392	40.8	4.9	0.23
2	773	0.0	121	1.9	0.0394	41.1	6.3	0.43
3	774	0.0	122	2.0	0.0396	41.4	7.1	0.4
4	242	0.0	126	2.8	0.0409	43.1	6.5	0.27
5	243	0.0	126	2.9	0.041	43.2	8.5	0.24
6	244	0.0	126	2.6	0.0409	43.1	8.8	0.28
7	245	0.0	126	2.5	0.0409	43	9.6	0.29
8	246	0.0	126	2.5	0.0409	43.1	9.2	0.28
9	247	0.0	126	2.8	0.041	43.2	8.3	0.25
10	248	0.0	126	2.7	0.0409	43	6.3	0.29
11	249	0.0	121	1.9	0.0394	41.2	6.2	0.44
12	250	0.0	121	1.9	0.0394	41.2	7.0	0.43
13	251	0.0	123	2.5	0.0401	42	3.8	0.39

SLV+

design value, Secondary body

w6	P1L1	shear1(kN)	BM1(kNm)	shear2	BM2	Axial (kN)	Torque (kN)
1	725	28.1	−55.3	0.5	−0.8	−152.2	0.126
		23.2	72.3	0.5	1.6	−123.7	0.126
2	710	32.6	−65.9	−0.1	0.2	−156.0	0.143
		22.8	72.1	−0.1	−0.4	−127.5	0.143
3	696	33.2	−67.5	0.0	0.0	−154.2	−0.008
		23.4	73.2	0.0	0.0	−125.7	−0.008
4	136	33.4	−68.1	0.0	0.0	−154.7	0.009
		23.6	73.6	0.0	0.0	−126.2	0.009
5	121	34.3	−69.8	0.0	0.0	−157.1	−0.001
		24.5	76.6	0.0	0.0	−128.5	−0.001

6	106	33.4	−68.3	0.0	0.0	−154.7	−0.004
		23.6	73.8	0.0	0.0	−126.1	−0.004
7	91	33.4	−68.3	0.0	0.0	−154.6	−0.005
		23.6	73.7	0.0	0.0	−126.1	−0.005
8	76	33.1	−67.7	0.0	0.0	−154.0	−0.005
		23.3	72.9	0.0	0.0	−125.5	−0.005
9	61	33.4	−68.2	0.0	0.0	−154.6	−0.003
		23.6	73.7	0.0	0.0	−126.0	−0.003
10	46	33.4	−68.1	0.0	0.0	−154.7	−0.014
		23.6	73.6	0.0	0.0	−126.1	−0.014
11	32	33.2	−67.6	0.0	0.0	−154.2	0.019
		23.4	73.3	0.0	0.0	−125.7	0.019
12	23	32.1	−65.9	0.1	−0.2	−154.5	−0.134
		22.3	69.3	0.1	0.4	−126.0	−0.134
13	13	27.7	−56.0	−0.5	0.7	−150.4	−0.115
		22.8	69.8	−0.5	−1.5	−121.8	−0.115

SLV−	P1L1	shear1(kN)	BM1(kNm)	shear2	BM2	Axial (kN)	Torque (kN)
1	725	8.9	−63.9	−5.5	−16.2	−125.9	−5.9
		8.9	16.2	−5.5	−21.6	−104.7	−5.9
2	710	1.0	−89.6	−6.8	−17.0	−135.0	−4.9
		1.0	−17.0	−6.8	−25.8	−113.9	−4.9
3	696	0.7	−91.8	−6.5	−16.8	−133.7	−5.0
		0.7	−18.7	−6.5	−24.9	−112.5	−5.0
4	136	9.9	−66.6	−6.6	−16.8	−131.9	−4.6
		9.9	19.1	−6.6	−25.1	−110.7	−4.6
5	121	9.5	−68.1	−6.6	−16.8	−131.7	−4.7
		9.6	17.3	−6.6	−25.0	−110.6	−4.7
6	106	7.2	−75.0	−6.6	−16.8	−132.4	−4.7
		7.2	7.6	−6.6	−25.0	−111.3	−4.7

7	91	5.6	−79.7	−6.6	−16.8	−132.7	−4.7
		5.6	0.9	−6.6	−25.0	−111.6	−4.7
8	76	6.2	−77.8	−6.6	−16.8	−132.5	−4.7
		6.2	3.4	−6.6	−25.0	−111.4	−4.7
9	61	8.7	−70.5	−6.6	−16.8	−131.8	−4.7
		8.7	13.8	−6.6	−25.0	−110.7	−4.7
10	46	9.2	−68.5	−6.6	−16.9	−132.7	−4.6
		9.2	16.4	−6.6	−25.0	−111.6	−4.6
11	32	−0.8	−95.9	−6.5	−16.8	−134.0	−5.0
		−0.8	−24.6	−6.5	−24.9	−112.9	−5.0
12	23	−1.5	−95.8	−6.7	−17.3	−135.0	−4.9
		−1.5	−27.9	−6.7	−25.2	−113.9	−4.9
13	13	8.3	−69.5	−6.2	−15.0	−126.4	−5.9
		8.3	12.3	−6.2	−24.0	−105.2	−5.9

SLV+	P1	shear1(kN)	BM1(kNm)	shear2	BM2	Axial (kN)	Torque (kN)
1	777	14.4	32.2	4.1	8.3	−62.6	7.0
2	773	16.7	62.7	3.0	6.5	−65.7	3.5
3	774	15.8	60.1	3.0	5.8	−68.5	2.5
4	242	8.1	44.6	2.1	6.6	−85.8	5.1
5	243	7.8	43.4	1.7	5.1	−87.4	3.0
6	244	11.7	48.4	1.3	4.9	−86.2	2.1
7	245	14.0	51.3	1.1	4.5	−85.5	0.9
8	246	12.9	49.8	1.4	4.7	−86.1	2.0
9	247	9.1	45.0	1.6	5.2	−87.2	3.1
10	248	9.2	46.2	2.0	6.8	−85.6	5.5
11	249	18.7	63.5	3.0	6.7	−66.0	2.7
12	250	18.7	63.2	3.1	5.8	−66.1	2.8

13	251	10.7	50.0	3.6	11.1	−75.0	4.8

SLV+

Shear force

Principle body is verified in SLV+ and SLV- for each case. In Secondary body again, the P1L1 is not verified with the condition of spacing 0.25 (m) and it is verified when the 0.16 (m) is chosen as spacing.

property of the cross section

Principle	b_w (m)	d(m)	z(m)	diameter(mm)	$A_{sw}(m^2)$	spacing(m)	A_{sw}/s
AT01-C2	0.3	1.3	1.17	8	0.000101	0.2	0.000503
AT01-C3	0.3	1	0.9	8	0.000101	0.25	0.000402
AT01-C5	0.3	1	0.9	8	0.000101	0.2	0.000503
AT02-C1	0.35	1.4	1.26	8	0.000101	0.2	0.000503
AT02-C2	0.3	1.3	1.17	8	0.000101	0.2	0.000503
AT02-C3	0.3	1	0.9	10	0.000157	0.25	0.000628
AT03-C1	0.5	1.4	1.26	8	0.000101	0.25	0.000402
AT03-C2	0.5	1.3	1.17	8	0.000101	0.2	0.000503
AT03-C3	0.4	1	0.9	7	0.000077	0.3	0.000257
AT04-3	0.3	1	0.9	8	0.000101	0.3	0.000335
T1	0.25	0.5	0.45	9	0.000127	0.25	0.000509
P1	0.25	0.5	0.45	8	0.000101	0.25	0.000402

Secondary	b_w (m)	d(m)	z(m)	diameter(mm)	$A_{sw}(m^2)$	spacing(m)	A_{sw}/s
AT1-C1	0.35	0.75	0.675	8	0.000101	0.2	0.000503
AT1-C2	0.35	1.35	1.215	8	0.000101	0.25	0.000402
AT1-C3	0.35	1.2	1.08	6	0.000057	0.2	0.000283
AT2-C1	0.35	0.75	0.675	8	0.000101	0.2	0.000503
AT2-C2	0.35	1.35	1.215	8	0.000101	0.2	0.000503
AT2-C3	0.35	1.2	1.08	6	0.000057	0.2	0.000283
TC1-C2	0.24	1.15	1.035	8	0.000101	0.7	0.000144
TC2-C2	0.34	1.15	1.035	8	0.000101	0.7	0.000144
P1L1	0.4	0.4	0.36	6	0.000057	0.25	0.000226
P1	0.25	0.5	0.45	8	0.000101	0.25	0.000402

Table 88: the property of the cross-section for the shear-force resistance

verification, Secondary body

w3	P1L1	v_{Ed1}(kN)	verification	v_{Ed2}	verification
1	725	0.156164	−1.3E−05	0.003142	0.0004
		0.122119	3.89E−05	0.003142	0.0004
2	710	0.156079	−1.3E−05	−0.00083	0.000401
		0.087803	9.16E−05	−0.00083	0.000401
3	696	0.158835	−1.7E−05	0.000108	0.000402
		0.09056	8.73E−05	0.000108	0.000402
4	136	0.168675	−3.2E−05	−3.3E−05	0.000402
		0.100399	7.22E−05	−3.3E−05	0.000402
5	121	0.173801	−4E−05	−3E−05	0.000402
		0.105525	6.44E−05	−3E−05	0.000402
6	106	0.162145	−2.2E−05	−1.7E−05	0.000402
		0.093869	8.23E−05	−1.7E−05	0.000402
7	91	0.162088	−2.2E−05	1.67E−05	0.000402
		0.093812	8.23E−05	1.67E−05	0.000402
8	76	0.160244	−2E−05	3.89E−05	0.000402
		0.091969	8.52E−05	3.89E−05	0.000402
9	61	0.164785	−2.6E−05	5.42E−05	0.000402
		0.096509	7.82E−05	5.42E−05	0.000402
10	46	0.161901	−2.2E−05	9.65E−05	0.000402
		0.093625	8.26E−05	9.65E−05	0.000402
11	32	0.160623	−2E−05	−6.7E−05	0.000402
		0.092347	8.46E−05	−6.7E−05	0.000402
12	23	0.154158	−1E−05	0.000849	0.000401
		0.085883	9.45E−05	0.000849	0.000401
13	13	0.156131	−1.3E−05	−0.00309	0.0004
		0.122085	3.9E−05	−0.00309	0.0004

w3 s=0.25

w3	P1L1	v_{Ed1}(kN)	verification	v_{Ed2}	verification
1	725	0.156164	0.000114	0.003142	0.0004
		0.122119	0.000166	0.003142	0.0004

2	710	0.156079	0.000114	−0.00083	0.000401
		0.087803	0.000219	−0.00083	0.000401
3	696	0.158835	0.00011	0.000108	0.000402
		0.09056	0.000215	0.000108	0.000402
4	136	0.168675	9.48E−05	−3.3E−05	0.000402
		0.100399	0.000199	−3.3E−05	0.000402
5	121	0.173801	8.69E−05	−3E−05	0.000402
		0.105525	0.000192	−3E−05	0.000402
6	106	0.162145	0.000105	−1.7E−05	0.000402
		0.093869	0.000209	−1.7E−05	0.000402
7	91	0.162088	0.000105	1.67E−05	0.000402
		0.093812	0.00021	1.67E−05	0.000402
8	76	0.160244	0.000108	3.89E−05	0.000402
		0.091969	0.000212	3.89E−05	0.000402
9	61	0.164785	0.000101	5.42E−05	0.000402
		0.096509	0.000205	5.42E−05	0.000402
10	46	0.161901	0.000105	9.65E−05	0.000402
		0.093625	0.00021	9.65E−05	0.000402
11	32	0.160623	0.000107	−6.7E−05	0.000402
		0.092347	0.000212	−6.7E−05	0.000402
12	23	0.154158	0.000117	0.000849	0.000401
		0.085883	0.000222	0.000849	0.000401
13	13	0.156131	0.000114	−0.00309	0.0004
		0.122085	0.000166	−0.00309	0.0004

w3 s=0.16

SLV+	P1L1	v_{Ed1}(kN)	verification	v_{Ed2}	verification
1	725	0.194957	−3.4E−05	0.042856	0.000169
		0.195096	−3.4E−05	0.042856	0.000169
2	710	0.258127	−0.00012	0.04626	0.000165
		0.258265	−0.00012	0.04626	0.000165
3	696	0.26364	−0.00013	0.045399	0.000166
		0.263779	−0.00013	0.045399	0.000166
4	136	0.203843	−4.6E−05	0.045651	0.000165

		0.203982	−4.6E−05	0.045651	0.000165
5	121	0.206524	−4.9E−05	0.04556	0.000165
		0.206663	−4.9E−05	0.04556	0.000165
6	106	0.222952	−7.1E−05	0.04558	0.000165
		0.223091	−7.1E−05	0.04558	0.000165
7	91	0.234215	−8.6E−05	0.045581	0.000165
		0.234353	−8.6E−05	0.045581	0.000165
8	76	0.229642	−8E−05	0.04559	0.000165
		0.229781	−8E−05	0.04559	0.000165
9	61	0.212345	−5.7E−05	0.045601	0.000165
		0.212484	−5.7E−05	0.045601	0.000165
10	46	0.20865	−5.2E−05	0.045754	0.000165
		0.208789	−5.2E−05	0.045754	0.000165
11	32	0.273547	−0.00014	0.045306	0.000166
		0.273685	−0.00014	0.045306	0.000166
12	23	0.269482	−0.00013	0.047368	0.000163
		0.269621	−0.00013	0.047368	0.000163
13	13	0.208451	−5.2E−05	0.037951	0.000176
		0.20859	−5.2E−05	0.037951	0.000176

SLV+. s=0.25(m)

SLV+	P1L1	v_{Ed1}(kN)	verification	v_{Ed2}	verification
1	725	0.194957	9.35E−05	0.042856	0.000296
		0.195096	9.33E−05	0.042856	0.000296
2	710	0.258127	9.26E−06	0.04626	0.000292
		0.258265	9.08E−06	0.04626	0.000292
3	696	0.26364	1.91E−06	0.045399	0.000293
		0.263779	1.72E−06	0.045399	0.000293
4	136	0.203843	8.16E−05	0.045651	0.000293
		0.203982	8.15E−05	0.045651	0.000293
5	121	0.206524	7.81E−05	0.04556	0.000293
		0.206663	7.79E−05	0.04556	0.000293
6	106	0.222952	5.62E−05	0.04558	0.000293
		0.223091	5.6E−05	0.04558	0.000293

7	91	0.234215	4.11E-05	0.045581	0.000293
		0.234353	4.1E-05	0.045581	0.000293
8	76	0.229642	4.72E-05	0.04559	0.000293
		0.229781	4.71E-05	0.04559	0.000293
9	61	0.212345	7.03E-05	0.045601	0.000293
		0.212484	7.01E-05	0.045601	0.000293
10	46	0.20865	7.52E-05	0.045754	0.000292
		0.208789	7.5E-05	0.045754	0.000292
11	32	0.273547	-1.1E-05	0.045306	0.000293
		0.273685	-1.1E-05	0.045306	0.000293
12	23	0.269482	-5.9E-06	0.047368	0.00029
		0.269621	-6.1E-06	0.047368	0.00029
13	13	0.208451	7.55E-05	0.037951	0.000303
		0.20859	7.53E-05	0.037951	0.000303

SLV+. s=0.16(m)

Table 89: the design shear stress in w3 and SLV+

design value, Secondary body

w3	P1L1	shear1(kN)	BM1(kNm)	shear2	BM2	Axial (kN)	Torque (kN)
1	725	22.5	-42.7	0.5	-0.7	-146.2	0.078
		17.6	57.0	0.5	1.5	-117.6	0.078
2	710	22.5	-43.2	-0.1	0.2	-144.8	0.085
		12.6	44.2	-0.1	-0.4	-116.3	0.085
3	696	22.9	-44.4	0.0	0.0	-142.9	0.003
		13.0	45.0	0.0	0.1	-114.4	0.003
4	136	24.3	-47.5	0.0	0.0	-145.3	0.030
		14.5	49.0	0.0	0.0	-116.8	0.030
5	121	25.0	-49.3	0.0	0.0	-145.6	-0.005
		15.2	50.9	0.0	0.0	-117.1	-0.005
6	106	23.3	-45.8	0.0	0.0	-143.4	-0.018
		13.5	46.0	0.0	0.0	-114.9	-0.018
7	91	23.3	-45.8	0.0	0.0	-143.4	-0.003

		13.5	45.9	0.0	0.0	−114.8	−0.003
8	76	23.1	−45.3	0.0	0.0	−142.8	0.005
		13.2	45.1	0.0	0.0	−114.3	0.005
9	61	23.7	−46.8	0.0	0.0	−143.6	−0.003
		13.9	46.9	0.0	0.0	−115.1	−0.003
10	46	23.3	−45.7	0.0	0.0	−143.5	−0.020
		13.5	45.9	0.0	0.0	−114.9	−0.020
11	32	23.1	−45.2	0.0	0.0	−143.0	0.017
		13.3	45.5	0.0	0.0	−114.4	0.017
12	23	22.2	−43.8	0.1	−0.2	−143.4	−0.075
		12.4	42.3	0.1	0.4	−114.9	−0.075
13	13	22.5	−44.1	−0.4	0.7	−144.8	−0.063
		17.6	55.6	−0.4	−1.5	−116.3	−0.063

SLV+	P1L1	shear1(kN)	BM1(kNm)	shear2	BM2	Axial (kN)	Torque (kN)
1	725	28.1	−8.6	6.2	15.0	−111.1	6.0
		28.1	95.3	6.2	24.0	−89.9	6.0
2	710	37.2	13.5	6.7	17.3	−118.6	4.9
		37.2	130.9	6.7	25.3	−97.5	4.9
3	696	38.0	14.2	6.5	16.8	−117.3	5.0
		38.0	133.5	6.5	24.9	−96.1	5.0
4	136	29.4	−12.7	6.6	16.9	−119.8	4.6
		29.4	97.0	6.6	25.0	−98.6	4.6
5	121	29.7	−11.4	6.6	16.8	−119.8	4.7
		29.8	98.9	6.6	25.0	−98.7	4.7
6	106	32.1	−4.7	6.6	16.8	−119.2	4.7
		32.1	108.7	6.6	25.0	−98.1	4.7
7	91	33.7	0.0	6.6	16.8	−118.9	4.7
		33.7	115.4	6.6	25.0	−97.7	4.7
8	76	33.1	−1.7	6.6	16.8	−119.1	4.7
		33.1	112.8	6.6	25.0	−97.9	4.7

9	61	30.6	−9.0	6.6	16.8	−119.7	4.7
		30.6	102.4	6.6	25.0	−98.6	4.7
10	46	30.0	−10.9	6.6	16.8	−118.9	4.6
		30.1	99.7	6.6	25.1	−97.8	4.6
11	32	39.4	18.4	6.5	16.8	−116.9	5.0
		39.4	139.5	6.5	24.9	−95.7	5.0
12	23	38.8	20.2	6.8	17.0	−116.3	4.8
		38.8	138.1	6.8	25.8	−95.2	4.8
13	13	30.0	−7.0	5.5	16.1	−110.9	5.9
		30.0	101.9	5.5	21.6	−89.7	5.9

Table 90:the corresponding design value in w3 and SLV+

5.3. Conclusion

As deep and precise discussion on result is already carried out in the regarding section, and hence in the conclusion the result of the verification is generally overviewed and some other new findings are mentioned where necessary.

In the verification of the **Serviceability Limit State** (SLS), the crack control and deflection control are examined. Consequently the members with the sufficient information, they are verified for each, crack control and deflection control in any analysis-static analysis, seismic analysis with in-plane earthquake and out-of-plane earthquake.

The **Ultimate Limit State** (ULS) is concerned with axial force, bending moment and shear force. The axial-force verification is accomplished with all the members examined. The overview of outcome is listed below (Table 91, 92 and 93). In **static analysis**, With regard to Principle body, the whole structure is verified. With regard to Secondary body, the structure is verified in terms of verification of axial force. Then, most of the columns of beam part (P1L1) are not verified in the most of the load-case combination-other than w3 and w4 in bending-moment verification. When it comes to verification of shear force, in the load case of w6, the structure is verified but other than that the members of P1L1 are not verified. However, as discussed, in ENCO (2008) it is not clearly mentioned which part of the column P1L1 is examined for the position of the reinforcement steel, and in this verification it is assumed they have the same reinforcement steel irrespective of its position. Possibly, it is relevant to this outcome, but it is impossible to go further only with the current information.

In **seismic analysis** -**out-of-plane earthquake**- the unverified part is found at the entrance part and at the bottom of the 5th arch in SLV+ and SLV- in the **bending-moment** verification.
As for the shear force verification, the whole structure is verified. Moreover, axial-force verification is also acquired.

The axial-force verification is fulfilled also in Secondary body. When it comes to bending moment, basically, the beams around the steel brace are not verified in addition to P1L1.
The shear force verification is not accomplished in P1L1 in SLV+ case.

In case of **in-plane earthquake**, the result is mostly the same as that of out-of-plane earthquake, but as mentioned in structural-analysis part, basically structure goes through less values in any force than in out-of-plane earthquake. As a result, more members are verified as seen in Table 91. 92 and 93.

In the end, it turns out that the members undergoing higher values of force-thus, in the entrance part of Principle part and in the arches around steel braces- are not verified in many cases. Moreover, especially, in Secondary body, P1L1 is turned out to be very vulnerable to bending moment and shear force. As discussed it is due to relatively small square shaped area of the cross-section 0.16m^2- and the less reinforcement and also less stirrup (in terms of number of bars and its diameter). Incidentally It is also revealed in structural analysis part that Secondary body undergo smaller value than Principle body in general. As if it corresponds to this finding, in Secondary body smaller force resistance is found especially in bending moment presumably due to less reinforcement than in Principle body.

In this chapter, the verification of the members is performed. The verification revealed that some members are vulnerable structurally and it accomplished the primal purpose of this chapter, understanding of the structure quantitatively. In the last chapter, besides the overall conclusion, the current rehabilitation project is discussed considering the results of the structural analysis and verification.

Principle	Static			
BM	w1	w2	s1	s2
	verified	verified	verified	verified

Principle	Static			
SH	w1	w2	s1	s2
	verified	verified	verified	verified

Secondary	Static							
BM	w3	w4	w5	w6	s3	s4	s5	s6
	verified	verified	P1L1	P1L1	P1L1	P1L1	P1L1	P1L1
end1			unverified	unverified	verified	verified	unverified	unverified
end2			unverified	unverified	unverified	unverified	unverified	unverified

Secondary	Static							
SH	w3	w4	w5	w6	s3	s4	s5	s6
	P1L1	P1L1	P1L1	verified	P1L1	P1L1	P1L1	P1L1
s=0.16	verified	verified	unverified		verified	verified	unverified	unverified
s=0.25	unverified	unverified	unverified		unverified	unverified	unverified	unverified

Table 91: the list of verification in static analysis Principle body and Secondary body (below)

Principle		Seismic
BM	SLV+	SLV−
	5bottom	5bottom
	13bottom	13bottom
	14bottom	14bottom
	P1	P1

Principle		Seismic
SH	SLV+	SLV−
	verified	verified

Secondary		Seismic
BM	SLV+	SLV−
	P1L1	P1L1
end1	verified	verified
end2	unverified	unverified
	2bottom	2bottom
	2middle	5 middle
	2bottom	13middle
	3middle	
	3middle	
	3bottom	
	5middle	

Secondary		Seismic
SH	SLV+	SLV−
	P1L1	verified
s=0.16	verified	
s=0.25	unverified	

Table 92: the list of verification in seismic analysis out-of-plane earthquake, Principle body and Secondary body (below)

Principle	Seismic	
BM	SLV+	SLV−
	P1	verified

Principle	Seismic	
SH	SLV+	SLV−
	verified	verified

Secondary	Seismic	
BM	SLV+	SLV−
	P1L1	P1L1
end1	verified	verified
end2	unverified	unverified

Secondary	Seismic	
SH	SLV+	SLV−
	P1L1	P1L1
s=0.16	unverified	unverified
s=0.25	unverified	unverified

Table 93: the list of verification in seismic analysis in-plane earthquake, Principle body and Secondary body (below)

6. OVERALL CONCLUSION

6.1. The report of the current rehabilitation project

Architectural rehabilitation

The site is named as "Citta' della Musica"- City of music, and it is going to be used as the commercial and business complex. This building is going to be covered with glass. Then another structure will be put inside and hence it will be transparent.

Structural rehabilitation

The pillars in Secondary body are being reinforced in three various manners: base is going to be consolidated with carbon mortar (Figure 81), the middle part with CFRP (Figure 83) and the upper part with mortar. When the result of the structural analysis and the verification is thought of, this intervention seems quite reasonable. as the structure shows the vulnerability in the middle part for bending moment and in the bottom part for shear force as discussed above.

In the Principle body, due to the less soil stiffness in lateral direction the foundation is being consolidated through two different methods: root pole -polo radice- and valved pole-polo valvolato (Figure 82). Valved pole is intervention with which the concrete is inserted into the steel pole surrounded with screed. The pole has valves literally, and the inserted concrete comes out from the valves. Hence the concrete spread laterally, and it gives the lateral strength to the foundation. On the other hand, the root pole is steel pole whose hole is filled with concrete. It also adds stiffness to the soil.

Figure 81: operation of carbon mortar

Figure 82: operation of bubble poles

Figure 83: employed CFRP for the consolidation of the beam

Figure 84: the preventative treatment for steel corrosion

6.2. Conclusion

This report started with the discussion of the history of reinforced-concrete building and its code, and the decay of the reinforced-concrete buildings in terms of material. Then, it moved to the discussion of the target structure. As for the main part, the linear analysis was carried out with static load and dynamic load. Then the verification of the member was also carried out based on the result of the structural analysis. Thanks to these processes, it resulted in revealing the structural characteristic somehow.

Principle body shows vulnerability in the entrance part and the 5^{th} arch. The 13^{th} and 14^{th} arch goes through quite significant value of bending moment and shear force.

Presumably due to the form of the structure-less height and wider plan-, Secondary body shows less value of bending moment and shear force than Principle Body. However, the columns of beam part of Secondary body (P1L1) are very vulnerable and proper intervention would be essential. It is well-known fact in general, but the effect of brace is confirmed as for both buildings. Thus, the bigger values are concentrated there.

Due to the lack of the further information and time, this report finishes at this stage and yet it can be thought of that the next step for the analysis of the structure is the verification of the member with intervention such as CFRP in addition to non-linear analysis. At any rate, the historic concrete structure is important in terms of modern historic monument and from now on presumably increasing number of the buildings is going to require the conservation or rehabilitation work, so from that viewpoint, this case study was quite intriguing and also meaningful for my own future career.

7. REFERENCES

Barbiani,E. Cantiere Venezia. Piani, progetti, realizzazioni, imprese (Building site Venice. Plans, projects, realizations, enterprises). Insula, Marsilio, Venezia (Italy), 2002

Belluco P. Valuztione della consistenza strutturale di edificio storico misto mratura e cemento armato: Il castello di Padova (the dissertation of University of Padua) 2008

Böhni, H., Corrosion in Reinforced Concrete Structures 2005

British Standards EN 1990-2002, 2002

British Standards EN1991-1-3 2003, 2003

British Standards EN1991-1-4 2005, 2005

British Standards EN 1992-1-1 2004, 2005

British Standards EN1998-1, 2004

British Standards EN1998-3, 2004

Circolare 2 febbraio 2009, n 617: Istruzioni per l'applicazione delle "Norme tecniche per le costruzioni", 2008" d icui al D.M. 2008

D.M 10 Gennaio: Prescrizioni nomali per le opere in cemento armato, G.U. n. 1907

D.M 14 Gennaio 2008: Norme tecniche per le costruzioni, pubblicato in G.U. n. 29, 2008

ENCO (Engineering Concrete SRL), Complesso "Citta' della Musica", Marghera (Venezia) Campagna di Indagini tesa alla Verifica dei Material, 2008

Lane, F. C. Venice, a Maritime Republic. 2nd ed. Baltimore John Hopkins University Press, 1973

Patassini, D. et al. Contextual Knowledge Generated by a Decision Support System for Brownfield Development – The Case of Porto Marghera. Miller, D.; Patassini. D (ed.) *Beyond Benefit Cost Analysis.* Ashgate: Adlershot [u.a.]: Ashgate, 2005, p.90

Pugliese, T. Piano strategico Città di Venezia, documento n.10 (bozza) (Strategic plan city of Venice, document no 10, draft), Comune di Venezia (Municipality of Venice), Italy, 2003

Proceeding Institution Civil Engineers (Proc. Instn Civ. Engrs), Structures and Building vol 116, 1996

Richardson, Barry A., Defects and Deterioration in Buildings 2000

Stamperia di venezia, Ente della zona industriale di Porto Marghera. 1980

Internet site reference

infoeurocde2 http://www.eurocode2.info/main.asp?page=0 [available on 21st of July, 2009]